Fire Structural Properties of Sandwich Composites

A thesis submitted in fulfilment of the requirements for the degree of PhD (Aerospace Engineering)

Aslina Anjang Ab Rahman

Master Degree in Aeronautical Maintenance and Production

School of Aerospace Mechanical and Manufacturing Engineering

College of Science Engineering and Health

RMIT University

March 2015

Declaration

I certify that except where due acknowledgement has been made, the work is that of the author alone; the work has not been submitted previously, in whole or in part, to qualify for any other academic award; the content of the thesis/project is the result of work which has been carried out since the official commencement date of the approved research program; any editorial work, paid or unpaid, carried out by a third party is acknowledged; and, ethics procedures and guidelines have been followed.

Aslina Anjang Ab Rahman

27 March 2015

Acknowledgements

The completion of this thesis could not have been possible without God willing and through help and guidance of many people.

First and foremost, I would like to express my sincere gratitude to my main supervisor, Professor Adrian Mouritz for the continuous support of my PhD study and research, for his patience, motivation, enthusiasm and encouragement. His guidance helped me in all the time of research and writing of this thesis.

I would also like to extend my sincerest appreciation to my co-supervisors, Dr Stefanie Feih and Dr Everson Kandare for the immeasurable amount of support and guidance they have provided throughout the study.

I am also indebted to Mr Robert Ryan and Mr Peter Tkatchyk, the technical staff in School of Aerospace, Mechanical and Manufacturing Engineering of RMIT who have helped me with the experimental work. My sincere gratitude also goes to Ms Lina Bubic for her co-operation during my study. A special thanks should also go to all my friends who have always been by my side for better or for worst.

Finally I would like to thank my parents, Anjang Ab Rahman and Badriah, all my siblings, my husband, Mohd Shahar and my two beautiful children, Aqilah Aisyah and Ahmad Aiman for the endless encouragement and support they have offered through the years. They have been my greatest strength which kept me focused and motivated throughout this PhD study.

Aslina Anjang Ab Rahman
School of Aerospace, Mechanical and Manufacturing Engineering
Royal Melbourne Institute of Technology (RMIT)
March 2015

This research was supported by provision of scholarship from Ministry of Education Malaysia (MOE) and Universiti Sains Malaysia (USM).

TABLE OF CONTENTS

LIST OF FIGURES

LIST OF TABLES

ABSTRACT

The main aim of this PhD project is to investigate the fire structural properties of a sandwich composite representative of the material used in naval ship structures. The sandwich composite consists of thin woven fibreglass-vinyl ester face skins and balsa wood core, and both the skins and core are combustible. Using experimental techniques and analytical models, this PhD investigates the structural response of sandwich composites during and following fire exposure. The thermal, physical and mechanical processes controlling the softening and failure of the sandwich composite under structural loading and one-sided heating by fire are determined. Two important structural loading cases of axial tension and axial compression are studied together with different radiant heat flux conditions representative of fires with different flame temperatures. To thoroughly understand the fire response of sandwich composites, this PhD determines the temperature response, softening behaviour, deformation, damage and failure mechanisms for different loading conditions, stress levels and heat flux conditions. In post-fire structural properties, reductions to the tensile and compressive properties of sandwich composites following fire exposure are investigated experimentally and analytically. The processes and mechanisms controlling the post-fire stiffness and strength properties of sandwich composites are determined.

The PhD thesis presents a comprehensive review of published research into the fire reaction and resistant properties of composites, with emphasis given to sandwich materials. The literature review critiques published research into the modelling and experimental testing of fibre reinforced polymer laminates subjected to one-sided heating and structural loading. The review also covers the fire structural response of sandwich composites, which has been studied less than laminates. Gaps and deficiencies in the understanding of the fire structural properties of sandwich composites are identified, which forms the basis for the research work performed in the PhD project.

One of the major research studies of this PhD project is tension modelling and experimental testing of sandwich composites in fire. A thermal-mechanical model is presented for calculating softening and failure of sandwich composites under combined

tension loading and one-sided unsteady-state heating conditions representative of a fire. The thermal model calculates the temperature rise of the sandwich composite when exposed to fire. The mechanical model computes the reductions to the tensile modulus and strength of the laminate face skins caused by thermal softening of the fibre reinforcement and polymer matrix and weakening of the core. The numerical accuracy of the model is assessed using experimental data obtained from fire structural tests performed on a sandwich composite consisting of thin woven glass-vinyl ester laminate skins and a thick core of balsa wood. Tests are performed at different tension stress levels and heat fluxes to rigorous valid the model. The model can determine with good accuracy the temperature rise, tensile failure stress and failure mechanism of the sandwich composite in fire. The experimental results presented in this research also provide new insights into the fire structural survivability of tension-loaded sandwich composites.

The tensile response of sandwich composites in fire is investigated further by exploring the effect of fibre orientation relative to the load direction on the softening behaviour (resin) and failure mode. The effect of changing the fibre orientation in the laminate face skins to the sandwich composite relative to the tensile load direction is studied experimentally and analytically. Experimental fire testing reveals that the tensile structural integrity of the sandwich composite decreases rapidly with increasing fibre misalignment, and this is accompanied by a transition in the failure mode. The structural softening of the composite with increasing fibre misalignment is predicted using a newly developed thermal-mechanical model.

The fire structural survivability of the sandwich composite under combined compressive loading and one-sided heating by fire is also investigated in the PhD project. This research investigates the effect of compressive stress on the softening rate, failure time and failure mode of the sandwich composite exposed to fire. The experimental results are compared against a compressive (buckling) failure model for sandwich composites in fire. Comparisons are made between the fire structural responses of the sandwich composite under compressive or tensile loads to determine the effect of load condition on the fire structural survivability.

An experimental and modelling study into the post-fire mechanical properties of the sandwich composite is performed as part of the PhD project. The effects of increasing heat flux exposure time and heat flux level on the residual tensile and compressive properties of the sandwich composite are experimentally determined. The residual properties are compared to the types and amounts of fire-induced damage. A new model for calculating the post-fire mechanical properties of the sandwich composite is formulated, and predictions are compared against experimental results to assess the numerical accuracy of the model. It was found that the model can predict the post-fire tensile and compressive properties with good accuracy.

Sandwich composites used in marine structures such as ships absorb water, which is known to alter properties such as stiffness and strength. This PhD project assesses the effect of water absorption on the fire structural response of sandwich composites. The sandwich composite was exposed to a hot-wet environment for increasing periods of time to controllably alter the amount of absorbed water. The effect of absorbed water on the thermal and mechanical responses of the sandwich composite in fire is experimentally determined. The research determines changes to the thermal response, damage, softening rate and failure mode of the sandwich material with increasing concentration of absorbed water up to and above saturation.

This PhD research work establishes a better understanding of mechanical performance and failure mechanisms of sandwich composite structures at high temperature and in fire. In addition, the research identifies the thermal, physical and mechanical processes that control the structural survivability of sandwich composites during and following fire exposure. The research provides the foundation for the development of design models and guidelines for sandwich composite structures for high fire risk applications, thus improving fire safety for ships, offshore platforms, civil infrastructures and other uses for these materials.

Chapter 1 : INTRODUCTION

1.1 BACKGROUND TO SANDWICH COMPOSITES FOR MARINE STRUCTURES

Sandwich composites generally consist of two stiff and strong face skins separated by a low density core material (Figure 1.1). The skins are often much thinner than the core, and the skins and core are bonded with an adhesive to facilitate load transfer between the materials. The most common fibres used in the laminate skins are glass, carbon and aramid. The polymer matrix to the skins holds the fibres in place, provides stress transfer between fibres, and protects the fibres from environmental degradation. Core materials come in various forms such as polymer foams, honeycombs and woods. The core supports the thin skins so that they do not deform inwardly or outwardly, and transfers stress between the skins. Sandwich composites are characterised by high stiffness and strength-to-weight ratios, fatigue and corrosion resistance, thermal and acoustic insulation, high energy absorption capability, and high flexural rigidity without substantial weight added to the structure.

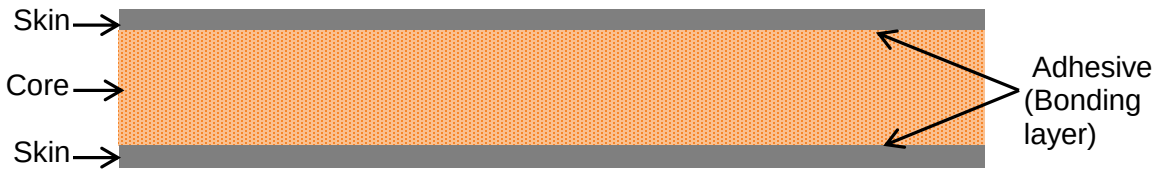

Figure 1.1: Sandwich composite construction.

Sandwich composites are used in load-bearing structures in aircraft, ships, buildings, bridges and offshore platforms. This PhD project is focussed on the fire resistant properties of sandwich composites used in naval ship structures. Currently there are a wide range of marine structures being developed using sandwich construction, as there

is a need to enhance the operational performance and reduce cost, maintenance and weight [1]. The applications of sandwich composites in ship structures include the hull, superstructure, topside structures such as masts, hangars and deckhouse, and control surfaces such as the rudder. As an example, sandwich composites consisting of fibreglass/vinyl ester face skins and balsa wood core are used in the hull of small naval ships and the masts of large warships.

The largest construction of a sandwich composite marine boat is the Skjold class vessel operated by the Royal Norwegian Navy, as shown in Figure 1.2. Skjold was commissioned in 1999 and built entirely from sandwich composites consisting of glass and carbon fibre laminate skins with polyvinyl chloride foam (PVC) core [2]. The Royal Swedish Navy built a fast patrol boat (Smyge MPC2000) from sandwich composite consisting of carbon, glass and Kevlar fibre reinforced skins and a polymer foam core.

Figure 1.2: Skjold class patrol boat. Photograph from http://www.jetsgroup.com/.

In 1992, the French Navy was the first to operate a large warship with a composite superstructure. The La Fayette class frigate makes use of balsa core with fiberglass-vinyl ester skins for deckhouse, helicopter hanger and deck structures. Additionally, the funnels and masts are made from sandwich composite, as shown in Figure 1.3.

(a)

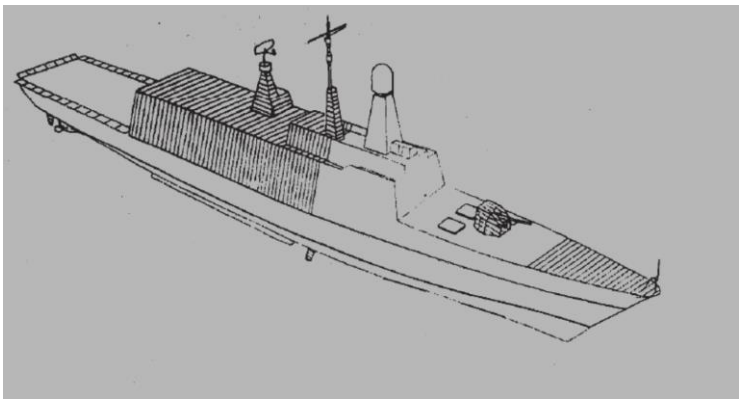

(b)

Figure 1.3: French la Fayette class frigate (a) Photograph of the frigate from Wikimedia (b) Schematic image of the frigate (hatched area representing balsa core composites)

Another important naval application of sandwich composites are mine countermeasure vessels (MCMV), that are primarily used for locating and destroying sea mines [2]. Some examples of MCMVs that utilize sandwich construction are the Flyvefisken class SF-300 (Royal Danish Navy), Oksoy and Alta class (Royal Norwegian Navy), Sandown class (Royal Navy), and Bay class (Royal Australian Navy), as shown in Figure 1.4.

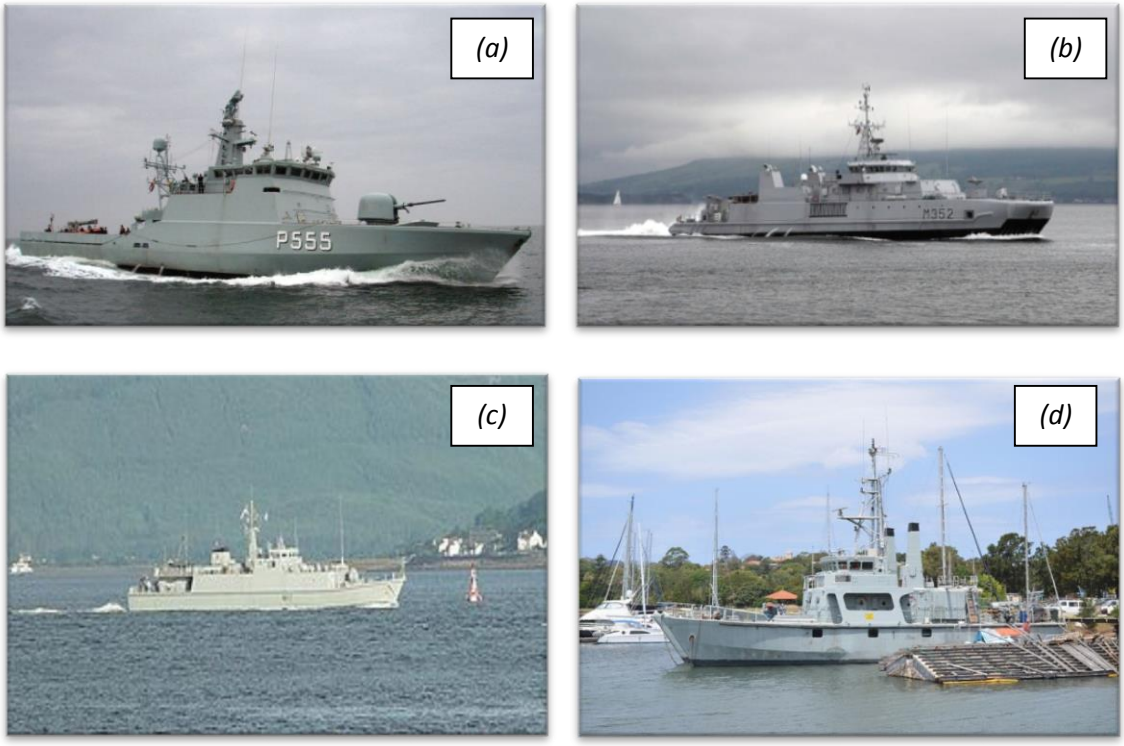

Figure 1.4: Minehunters made of sandwich composite. (a) Flyvefisken, (b) Oksoy and Alta, (c) Sandown MHS Shoreham and (d) Bay class minehunter. Photographs from Wikipedia.

Other applications of sandwich construction include ship funnels, masts, propellers and secondary structures, which have increased over the past 10-15 years. However, the growing use of sandwich construction by the marine industry has led to many technical challenges, especially with their fire performance that includes low softening temperatures and high flammability. The fire structural response of sandwich composites at elevated temperature and in fire depends on the heat-induced softening and damage to both the skins and core. Composites are reactive at high temperature due to the polymer matrix phase of the skins and the organic core, which can cause the sandwich material to decompose, ignite and burn [1]. However, distortion, creep and collapse often occur prior to flaming combustion due simply to heat-induced softening of the organic materials within sandwich composites [3-5].

A severe ship fire occurred on a Norwegian minesweeper in November 2002 that dramatically high-lighted the fire hazard of sandwich composites [6]. The fire started in

the propulsion system of KNM Orkla, which was built of sandwich composite material (Figure 1.5). The fire grew and spread rapidly (due in part to failure of the fire suppression system) and lasted for more than 24 hours. The ship was totally destroyed. This incident has concerned many navies in terms of the fire safety of sandwich composites. For this reason, there is a need to understand the fire resistance of sandwich composites under typical ship fire conditions.

Figure 1.5: Fire on the sandwich composite minesweeper KNM Orkla [6].

Studies on the fire performance of sandwich composites are focused on both the fire reaction and the fire resistance properties. Fire reaction describes the flammability and smoke toxicity of the combustible material. Some of the important fire reaction properties that affect growth of fire are heat release rate, time-to-ignition, flame spread rate, and oxygen index. Other reaction properties relate to the fire hazard, such as smoke density and gas toxicity. Fire resistance describes the burn-through resistance and mechanical integrity of a loaded material or structure during and after fire exposure. Resistance to fire also defines the ability of a material or structure to limit the spread of fire from room to room. These fire parameters can be evaluated using small, intermediate or full scale test methods. These tests are able to provide information on the mechanical integrity and burn-through resistance of the sandwich structural design for a specific fire test condition. However, the tests are expensive, complicated to perform, time consuming, and only provide information on the specific case of fire test condition. Due to this, it would be much

more efficient and cost-optimized to develop a computer model that can accurately predict the fire behaviour of sandwich structures.

1.2 AIM AND SCOPE OF PHD PROJECT

The general aim of this PhD project is to investigate the fire structural properties of a sandwich composite representative of the materials used on naval ships. Using experimental techniques and analytical models, this PhD will investigate the structural properties of sandwich composites during fire and post-fire. The thermal, physical and mechanical processes controlling the softening and failure of sandwich composites under structural loading and one-sided heating by fire will be determined. The PhD investigates the fire structural response for two important loading cases: axial tension and axial compression while the composite is simultaneously subjected to one-sided thermal loading. To understand the fire response of sandwich composites, this PhD determines their temperature response, physical response (which includes skin softening, core softening and decomposition damage), deformation behaviour (which includes both elastic and inelastic responses), and failure mechanisms for different loading conditions, stress levels, and fire (heat flux) conditions.

The PhD also aims to investigate the post-fire properties of sandwich composites. Reductions to the tensile and compressive properties of sandwich composites following fire exposure is investigated experimentally and analytically. The processes and mechanisms controlling the post-fire stiffness and strength properties of sandwich composites, such as heat-induced damage to the skins and core, are determined.

The sandwich composite investigated in this PhD is constructed with face skins of woven fibreglass-vinyl ester laminate and core of balsa wood as shown in Figure 1.6. This material was studied because it is representative of the sandwich composite used in many naval ships and other engineering structures at risk from fire.

List of research objectives:

1. To perform modelling and fire structural testing in determining the tensile and compressive properties and failure mechanisms of sandwich composite in fire.

2. To determine the post-fire mechanical properties of sandwich composites by fire structural testing and modelling.

3. To improve and validate the thermal-mechanical model with experimental fire structural testing.

4. To determine the deterioration of sandwich composite fire structural resistance due to water absorption.

These four research objectives are novel or add significantly to the current understanding of the fire structural response of sandwich composites. Objectives 1 and 4 have never previously been studied whereas limited published information is available on Objectives 2 and 3. This project is targeted towards achieving these objectives to further the science and technology of the fire properties of sandwich composite materials, particularly when used on naval ships.

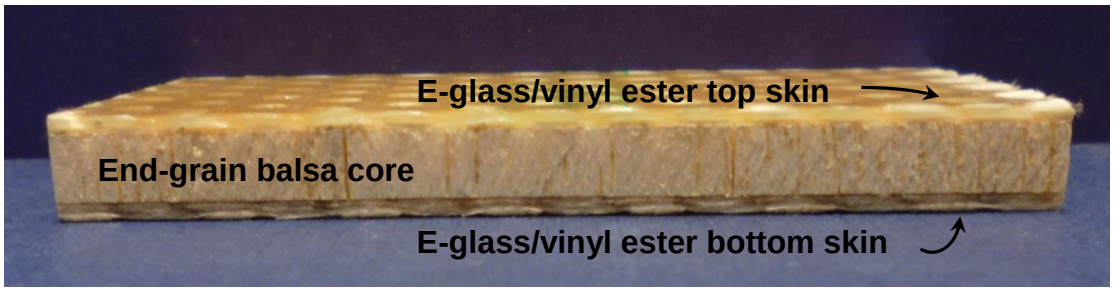

Figure 1.6: E-glass-vinyl ester/balsa core sandwich composite.

The expected outcomes of this project are as follows:

1. In-depth understanding of mechanical performance and failure mechanisms of sandwich structures at high temperature and in fire.

2. Identification of the thermal, physical and mechanical processes that control the structural survivability of sandwich composites in fire and following fire.

3. Development of design models and guidelines for sandwich composite structures for high fire risk applications, thus improving fire safety for ships, offshore platforms, civil infrastructures and other uses for these materials.

1.3 PHD THESIS OUTLINE

Chapter 2 presents a comprehensive and critical review of published research into the fire structural properties of composites, with an emphasis on sandwich materials. The literature review covers all the key aspects of the fire resistant properties of composites, including their temperature response, damage, softening and failure. Studies are reviewed into the structural response of laminates and sandwich composites both during fire and post-fire. Current progress in the modelling and experimental analysis of composites in fire is critically appraised, and scientific gaps in the field are identified. Some of these gaps form the basis for the research work performed in the PhD project.

Research is presented in Chapter 3 into the structural response and failure of a fibreglass/balsa core sandwich composite under combined tensile loading and fire attack. The sandwich material and experimental research methodology are described. The effects of elevated temperature on the stiffness and strength properties of the sandwich composite are experimentally determined. The effects of applied tensile stress level and radiant heat flux on the temperature response, damage, softening and failure of the sandwich material is experimentally assessed using a small-scale fire structural test facility. The temperature and tensile structural properties of the sandwich composite exposed to fire are analysed using a thermal-mechanical model adapted from previous work conducted on laminate materials [4]. The theoretical predictions are compared against the experimental results to assess the numerical accuracy of the model.

The tensile response of sandwich composites in fire is investigated further in Chapter 4 by exploring the effect of fibre orientation on the softening behaviour and failure mode. The effect of changing the fibre orientation in the laminate face skins to the sandwich composite relative to the tensile load direction is studied experimentally and analytically. This research provides important new insights into the contributions of fibre softening and

matrix softening/decomposition on the fire structural survivability of sandwich composites in fire.

Chapter 5 presents an analytical and experimental study into the fire structural survivability of sandwich composites under combined compressive loading and one-sided heating by fire. Research presented in this chapter investigates the effect of compressive stress on the softening rate, failure time and failure mode of the sandwich composite. The experimental results are compared against a compressive (buckling) failure model for sandwich composites in fire. Comparisons are made between the structural responses of the sandwich composite under compressive or tensile loads.

Chapter 6 presents an experimental and modelling study into the post-fire mechanical properties of the sandwich composite. The effects of increasing exposure time and radiant heat flux of the fire on the residual tensile and compressive properties are determined. Models for calculating the post-fire properties of the sandwich composite are compared against the experimental results.

Sandwich composites used in marine structures such as ships and offshore oil and gas platforms absorb water, which is known to alter properties such as stiffness and strength. Chapter 7 assesses the effect of water absorption on the fire structural response of sandwich composites. The sandwich composite was exposed to a hot-wet environment for increasing periods of time to controllably alter the amount of absorbed water. The effect of this water on the thermal and mechanical responses of the sandwich composite is experimentally determined. The research determines whether the temperature, damage, softening rate and failure mode of the sandwich material is altered with increasing amounts of absorbed water.

Chapter 8 summarises the major research findings and conclusions from the PhD project, and suggests a number of future research projects to further our understanding of the fire structural behaviour of sandwich composites.

Chapter 2 : LITERATURE REVIEW INTO THE FIRE RESISTANT PROPERTIES OF COMPOSITES

ABSTRACT

This chapter presents a comprehensive and critical review of published research into the fire structural properties of polymer matrix composites, with an emphasis on sandwich materials. The literature review covers all the key aspects of the fire resistant properties of composites, including their temperature response, damage, softening and failure. Studies are reviewed into the structural response of laminates and sandwich composites both during fire and post-fire. The review reveals that although major advances have been made in the fire structural modelling of laminates, further analysis and validation against experimental data is still required for sandwich composite. There are gaps in the literature on the fire structural properties of sandwich composite under tension, compression and other load conditions. Models and experimental data on the post-fire properties of sandwich composite are also lacking.

2.1 INTRODUCTION

Fibre reinforced composite materials have a flammable polymer matrix that can decompose and ignite at high temperature in the presence of air. Examples of composite materials commonly used in structural applications are glass-polyester; glass-vinyl ester, carbon-epoxy and carbon-thermoplastic laminates, and these (resin) soften above 100-200°C and can decompose and burn when heated above 250-350°C. The thermal decomposition and combustion of composites often results in the release of large amounts of heat, smoke and potentially toxic fumes that pose a safety hazard. Softening of composites in fire reduces their structural performance that may cause failure, which is also a hazard.

A substantial amount of research has been published on the fire reaction behaviour of composite materials. There is a wealth of experimental data on fire reaction properties for many types of composites, including their heat release rate, time-to-ignition, flame spread rate, smoke density and (to a lesser extent) smoke toxicity [6-9]. There has also been some progress on the modelling of certain fire reaction properties, such as ignition time and heat release rate [6].

While there have been important advances on fire reaction properties, less is known about the fire resistant properties of composites, particularly sandwich structures. Understanding the softening mechanisms and reduction to the mechanical properties of composite structures in fire is a critical safety issue for naval ships and some other applications (e.g. offshore oil and gas platforms, civil infrastructure). Major advances (particularly over the past five years) have been made in the modelling and testing of the structural response of composite laminates in fire. Thermal-mechanical models have been developed to predict temperature rise, softening rate, residual stiffness and strength, and failure stress/time of laminates in fire. A large amount of experimental data on the fire resistance of laminates has also been obtained, particularly for fibreglass reinforced polymer laminates. However, there has been less progress in the modelling and testing of the fire structural response of sandwich composites [1, 3, 6, 10-16]. The fire response of sandwich materials is more complicated than laminates because the temperature, damage and residual properties are controlled by the multi-material configuration of the skins and core.

This chapter presents a comprehensive review of published research into the fire structural properties of composite materials. Published research into the fire response of laminates and sandwich composites is critically appraised to identify what is known and what is still not understood. While this PhD project is focussed on sandwich composites, it is important to review work on laminates because of the insights these materials provide into the fire response of the face skins. The literature review begins with a description of complexity of the thermal, chemical, physical and failure processes which control the structural behaviour of composites in fire. The review then assesses progress in the fire

structural modelling and testing of laminates and sandwich composites. Gaps and deficiencies in the current understanding of the fire structural response of composites are identified, which forms the basis for research performed as part of this PhD project. Published research into the post-fire mechanical properties of composites is also reviewed, and again gaps are identified.

2.2 INTRODUCTION OF COMPOSITES IN FIRE

The response of composite laminates to fire is complex and depends on many parameters, including the temperature and oxygen content of the fire and the composition and thermal properties of the fibre reinforcement and polymer matrix. Fig. 2.1 shows the basic processes involved in the thermal decomposition of a laminate in fire [6]. The polymer matrix and (if present) organic fibres will soften and thermally decompose when the laminate is heated above a critical temperature. Volatile gases and smoke are released as by-products of the decomposition reaction process. The gases flow out from the decomposing composite into the flame zone where the flammable volatiles (mostly low molecular hydrocarbons) react with oxygen to cause the composite to ignite and burn. Ignition can only occur when there is a sufficient concentration of flammable decomposition gases released into the fire and the oxygen in the fire environment is above a minimum concentration (typically 10-12%). When insufficient oxygen is present, then smouldering ignition (i.e. non-flaming combustion) of the composite can occur. The combustion process at the boundary between the fire and composite involves a complex number of exothermic reactions which generate heat. The heat released by the combustion of flammable gases adds to the fuel load of the fire, causing a rise in flame temperature and flame spread rate.

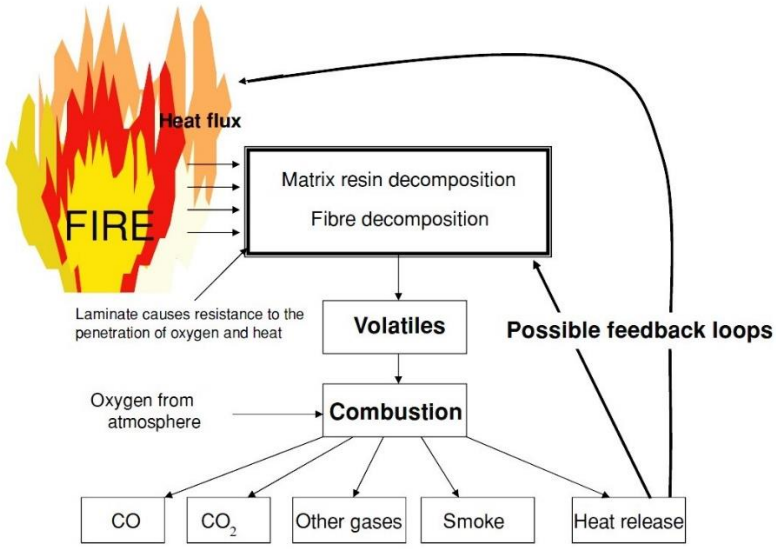

Figure 2.1: General processes of a composite in fire [6].

The general processes shown in Figure 2.1 also occur for sandwich composite materials, and the only significant difference is the contribution of the core. Organic core materials such as polymer foam or balsa wood can thermally decompose with the release of flammable volatiles that can increase the heat release rate of the composite.

Understanding the reduction to the structural properties of laminates and sandwich composites in fire requires an in-depth understanding of the thermal, chemical (decomposition), physical damage, softening and failure mechanisms [1]. Fig. 2.2 illustrates the processes involved for a hot decomposing polymer laminate exposed to one-sided radiant heating by fire [6] .Understanding the processes and their interactions is essential for analysing the structural behaviour of composites in fire. The next section provides a review on the fire reaction and fire resistance properties of composite materials.

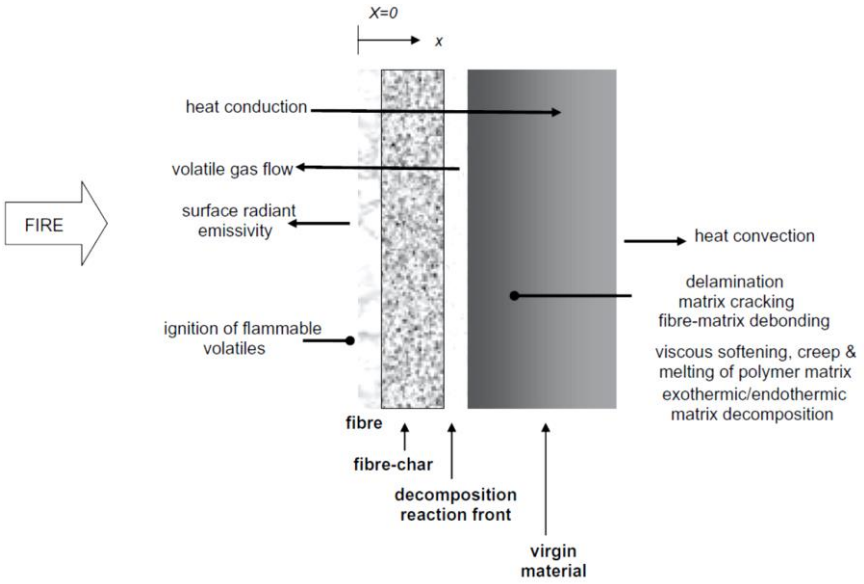

Figure 2.2: Schematic of the reaction processes of laminates exposed to fire [1].

2.3 FIRE REACTION AND FIRE RESISTANCE OF COMPOSITES

Fire reaction is a general term in fire science that defines the flammability and combustion properties of materials, including laminates and sandwich composites. Certain fire reaction properties influence the growth and spread of fire. Other fire reaction properties are critical to human survival in fire. Some of the most important fire reaction properties are time-to-ignition, heat release rate, peak heat release rate, smoke density, limiting oxygen index, and flame spread rate [17]. The fire reaction properties of many types of laminates and several types of sandwich composites have been characterised, and a wealth of reaction data for different fire (heat flux) conditions has been published [7, 17-21].

Fire resistance is different to fire reaction, which describes the physical and mechanical resistance of materials to fire attack. Fire resistance defines the softening and damage caused to materials, including the loss of mechanical properties during fire and the post-fire properties after the flame has been extinguished. Fire resistance also defines the ability of a material or structure to limit burn-through. Fire resistance is critical to the safe

use of load-bearing composites in aircraft, ships and buildings as their structures may collapse or fail due to losses in strength, stiffness and creep resistance.

Figure 2.2 shows the major thermal, chemical and physical processes that occur to composites exposed to fire. The thermal response of a composite is determined by heat conduction from the fire into the material together with surface radiation and convection effects. The internal temperature of the composite is also affected by ignition of flammable volatiles released by decomposition of the polymer matrix and organic fibres (if present), the mass flow of volatiles from the decomposition zone to the fire, and also the endothermic or exothermic heat resulting from the decomposition reactions of the matrix. Various physical changes occur when composites are exposed to fire, such as viscous softening; melting and vapourisation of the polymer matrix; softening and melting of glass fibres; oxidation of carbon fibres, growth and oxidation of char; char-glass fibre reactions; and matrix and delamination cracking [6].

All of the processes shown in Figure 2.2 can affect the structural integrity of composites in fire. Many of the processes occur simultaneously, thus make the modelling of a composite material in fire a complex problem. Understanding these processes and how they interact is crucial to modelling the fire structural response of composites.

The response of composites to fire can be generally described as follows. In the initial stage of fire, the radiant heat flux emitted by the flame is partially absorbed (with some reflected) and then conducted through the composite. The rate of heat conduction is determined by the incident heat flux (source of heat) and the thermal conductivity of the composite. Due to the relatively low thermal conductivity of most composite materials, a steep thermal gradient can occur in thick materials. The thermal gradient is often greater in sandwich composites than laminates due to the low heat conduction of the low-density core. As the composite heats-up, the kinetic energy from the heat will expand the composite specimen, and below the glass transition temperature (T_g) the amount of expansion is determined by the coefficient of the thermal expansion of the composite which can change with increasing temperature as the material undergoes phase changes.

As the composite heats-up it will eventually reach the decomposition temperature of the polymer matrix. The decomposition temperature depends on the chemical composition of the matrix and the heating rate and oxygen content of the fire. Most organic resin systems used in structural composites (e.g. polyesters, vinyl esters, epoxies) decompose over the range of 250-500^{o}C. The long molecular chains of the polymer network break-down via a complex series of chain scission reactions (endothermic reaction). The decomposition reaction process yields low molecular weight hydrocarbons, carbon monoxide and other volatiles as well as yielding a porous carbonaceous solid char. The volatiles flow towards the heated surface of the composite, and this has a convective cooling effect that partially counteracts the heat conduction process. That is, the volatiles are cooler than the decomposed material through which they flow towards the hot surface; thereby having a cooling effect. The flow of volatiles also stops air from diffusing into the decomposing composite, and therefore the decomposition process occurs in the absence of air. The polymers commonly used in engineering composites loss about 70-95% of their mass as volatiles during the decomposition process, and the residual mass is transformed into char.

Physical processes involve thermal expansion and contraction; development of thermally-induced strains; internal pressure build-up due to volatiles and vapourised moisture; formation of gas-filled pores; matrix cracking; fibre-matrix interfacial debonding; delamination damage; surface ablation; and softening, melting and fusion of fibres [1]. These physical processes influence the structural behaviour of composites in fire along with the heat flux and duration of the fire; the magnitude and type of load (tension, compression, bending, torsion etc.); and the geometry of the composite structure [1].

The approximate temperatures over which the processes described above occur in fibreglass laminate are shown in Figure 2.3 [1, 6]. A similar condition occurs for carbon fibre composites, although fibre oxidation must be considered and this commences at temperatures above ~500^{o}C [22]. The condition for sandwich composite will be different and more complex due to the core material. Cracks and other damage within the decomposing core need to be taken into account as it will change the thermal behaviour

of the sandwich composite under load. As a result, the internal temperature of the core may depend on the stress applied to the sandwich composite. The thermal behaviour of both laminates and sandwich materials is discussed into details in the next section.

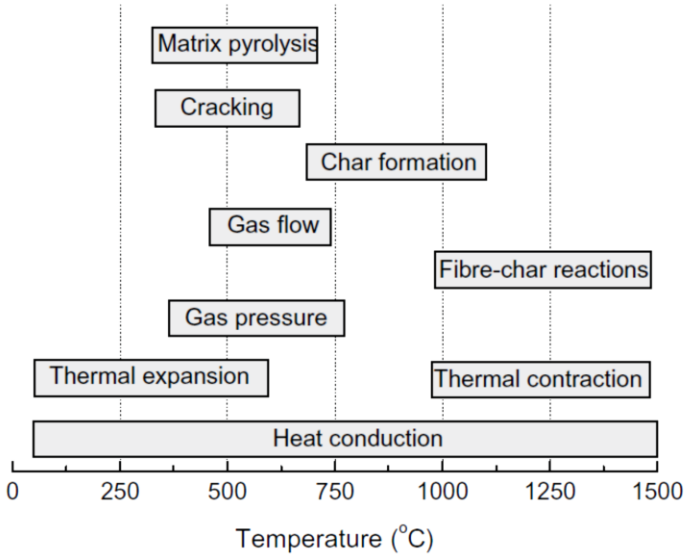

Figure 2.3: Various responses of fibreglass laminate with temperature [1].

2.4 THERMAL RESPONSE OF COMPOSITE

The initial work on thermal modelling of organic material in fire was performed for wood [23-25]. Processes of the burning wood are fundamentally similar to a burning composite. Burning woods are modelled as two-phase materials consisting of char and virgin material, as schematically illustrated in Figure 2.4. A one-dimensional (1-D) model was developed by Tinney to predict the thermal process of wood where heat transfer via conduction and radiation was based on Fourier analysis [23]. The decomposition reaction was analysed using first-order Arrhenius reaction kinetics [23]. Later in 1972, Kung [24] modelled wood pyrolysis which included transient heat conduction, internal heat convection of volatiles, decomposition of wood into volatiles and residual char, variable properties (density, specific heat and thermal conductivity), and the endothermic reaction of the decomposition process. Kansa [26] developed a model that considered the temperature-dependent thermal properties of wood, and this improved the modelling accuracy. These models have been adapted for composites in fire by Henderson and

colleagues [27-30], Sullivan and Salamon [31-33], Springer and colleagues [34-36], Dimitrienko [37, 38] and Gibson et al. [39]. The models have the capability to calculate the temperature profile distribution through a composite, but differ in terms of processes which can be analysed as summarised in Table 2.1.

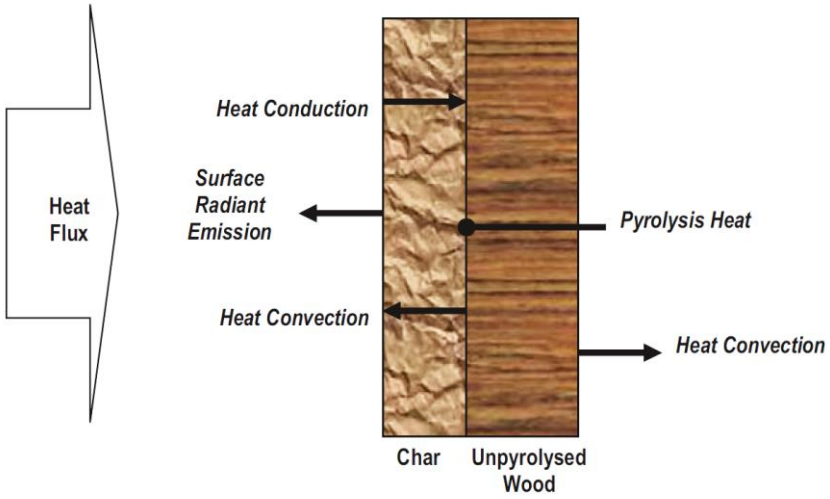

Figure 2.4: Schematic of a burning wood [6].

Table 2.1: Summary of main processes when a composite is exposed to one-sided heating by fire. The numbers shown are the references that described the models. Shaded boxes indicate the model considered in the process [1].

Processes	Reference				
	12	29	6	35	36
Heat Conduction through virgin material and char	■	■	■	■	■
Decomposition of polymer matrix and organic fibres	■	■	■	■	■
Flow of gases from the reaction zone through the char zone	■	■	■	■	■
Thermal expansion/contraction		■	■	■	
Pressure rise		■	■	■	
Formation of delamination, matrix cracks and voids					
Reactions between char and fibre reinforcement					
Ablation			■		

One of the first fire modelling studies on composites was conducted by Pering et al. [34]. Polymer composite samples were exposed to intense heat for specified time durations and the strength and mass loss were recorded. Correlations between mass loss and strength loss were observed. A model based on the 1-D heat transfer equation that includes a term for heat pyrolysis, which is determined experimentally from the material's loss rate, was formulated:

$$\rho C_p \frac{\partial T}{\partial t} = \frac{\partial}{\partial x}\left[k_x \frac{\partial T}{\partial x}\right] + \frac{\partial m}{\partial t} Q_p \qquad (2.1)$$

where $\frac{\partial m}{\partial t}$ is the mass loss rate of organic material per unit volume and Q_p is the heat of pyrolysis. The model had proven to be successful with the estimation of the mass loss of laminates in fire, but has not been assessed for sandwich composites.

The most widely used analytical model currently used to calculate the thermal response of laminates in fire was developed by Henderson et al. [27, 29] an is based on the condition illustrated in Figure 2.5. The model is based on modelling conducted by Kung [24] and Kansa [40] into the decomposition and fire response of wood. The model is a 1-D representation of the transient heating process and is expressed as:

$$\rho C_P \frac{\partial T}{\partial t} = k \frac{\partial^2 T}{\partial x^2} + \frac{\partial k}{\partial x}\frac{\partial T}{\partial X} - \dot{M}_G C_{pG} \frac{\partial T}{dk} - \frac{\partial \rho}{\partial t}(Q + h_C - h_G) \qquad (2.2)$$

where ρ, C_P and k are the density, specific heat and thermal conductivity of the material in the through-thickness direction, respectively. $\dot{M}_G$ and C_{pG} are the mass flux and the specific heat capacity of the volatile gas, respectively. Q, h_C and h_G are the heat of decomposition, enthalpy of the solid phase, and the entalphy of the volatile gas, respectively.

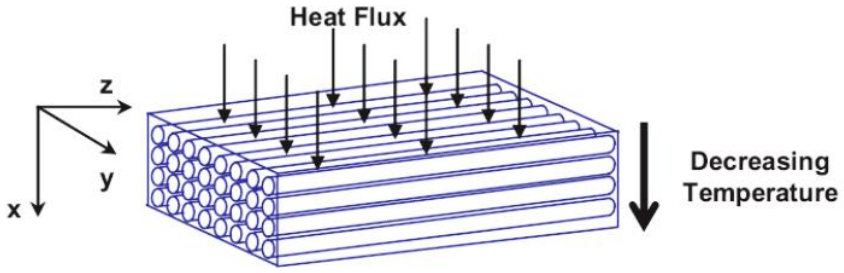

Figure 2.5: One-dimensional heat conduction through a laminate exposed to a uniform one-sided heating by fire [6].

The Henderson model considers the endothermic decomposition of matrix material, evolution of pyrolysis gases, and storage and mass transfer of these gases. The model is able to predict the temperature rise in laminates, and gives good agreement with experimental temperature data.

The Henderson equation was adapted by Gibson et al. [39] and Dodds et al. [41] to predict the fire performance of glass reinforced laminates. The model analyses three important thermal processes that occur in a composite material exposed to fire, namely conductive heat transfer; endothermic decomposition; and convective mass transfer of volatile products from the decomposing material to the hot composite surface. The 1-D equation is expressed as:

$$\rho C_P \frac{\partial T}{\partial t} = \frac{\partial}{\partial x}\left(k \frac{\partial T}{\partial x}\right) - \rho \frac{\partial M}{\partial t}(Q_P + h_C - h_G) - \dot{M}_G \frac{\partial}{dx} h_G \qquad (2.3)$$

By solving equation 2.3 for increasing temperature and time ($\frac{\partial T}{\partial t}$) through the finite difference method, the temperature can be calculated at any location and at any time in the laminate exposed to one sided-heating.

The decomposition rate ($\frac{\partial M}{\partial t}$) of the laminate expressed in the middle term of equation 2.3 is calculated using the first-order Arrhenius relationship:

$$\frac{\partial M}{\partial t} = -A\left[\frac{(m - m_f)}{m_0}\right]^n e^{(-E/RT)} \qquad (2.4)$$

where *A*, *E* and *n* are the rate constant, activation energy and order of the endothermic reaction, and *R* is the universal gas constant.

Apart from temperature prediction, the model can be used to predict the residual resin content (RRC) evolution with time using a finite difference technique. Finite element analysis can also be used to solve the model for temperature and RRC predictions [34, 42].

The thermal model can accurately predict the temperature profile and mass loss of thermoset matrix laminates [5, 34, 39, 41, 43, 44]. As examples, figures 2.6 and 2.7 show the successful prediction on the mass loss and temperature profile using the thermal model modified from Henderson model [27, 29] by Gibson et al. [39].

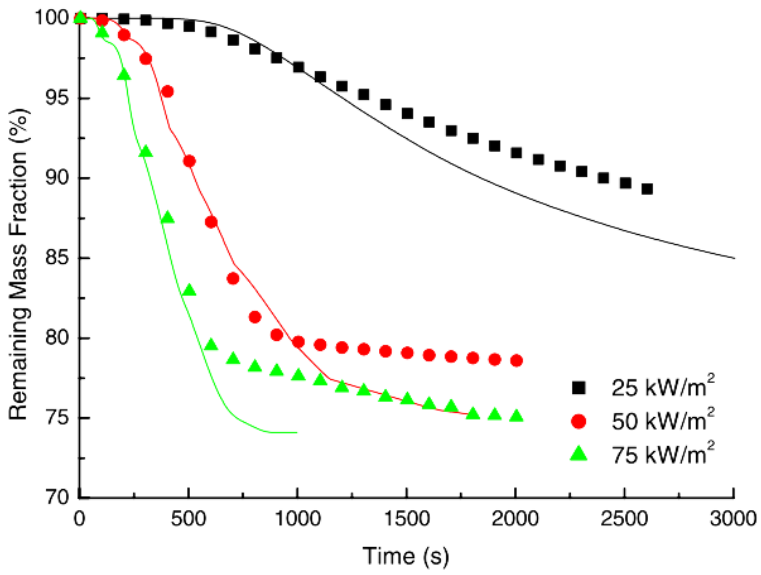

Figure 2.6: Mass loss predictions of E-glass/vinyl ester laminate for three heat fluxes [43]. The data points and curves are the measured and calculated remaining mass fraction, respectively.

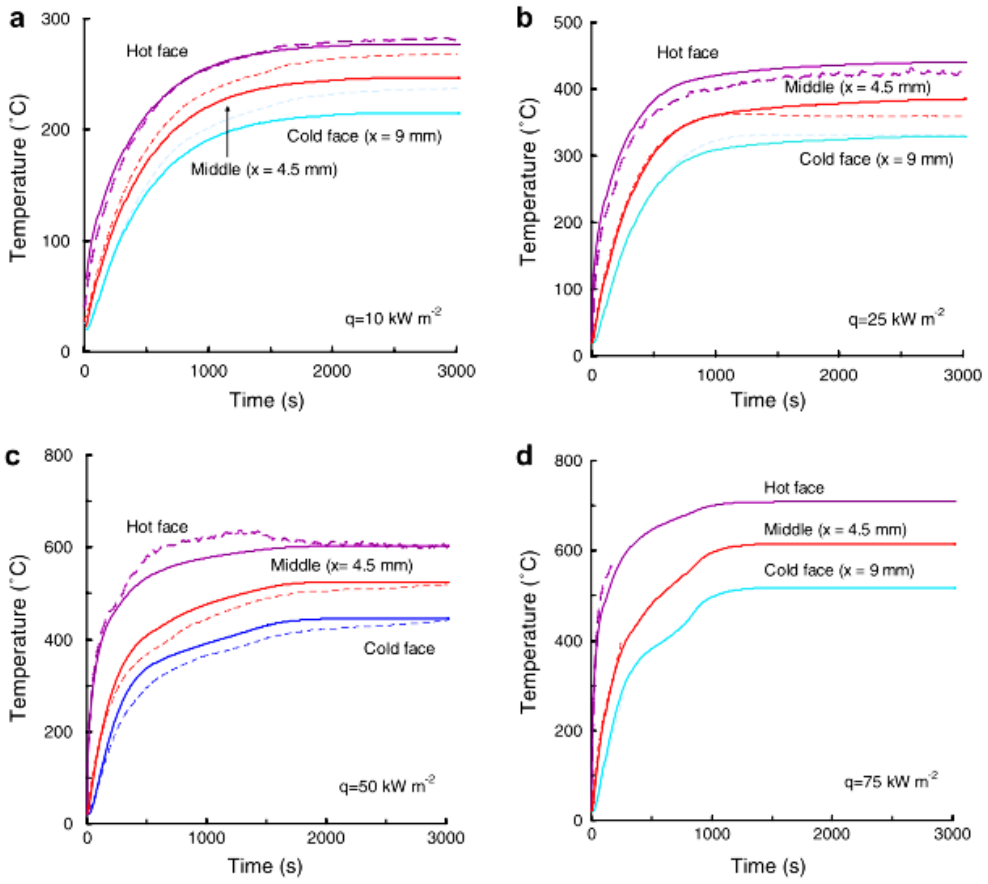

Figure 2.7: Temperature-time response of E-glass/vinyl ester laminates exposed to the heat fluxes of (a) 10kW/m², (b) 25kW/m², (c) 50kW/m² and (d) 75kW/m². The solid and dashed curves show the calculated and measured temperatures respectively [43].

Recently, the thermal model by Gibson et al. [39] was modified by Feih et al. [3] for sandwich composite materials with fibreglass laminate skins. The thermal model by Feih et al. [3] considered the temperature rise with heating time for the fibreglass face skins using Eq. 2.5a and for the core using Eq. 2.5b:

$$\rho c_{P,s}\frac{\partial T}{\partial t}=\frac{\partial}{\partial x}\left(k_s\frac{\partial T}{\partial x}\right)-\dot{M}_G\frac{\partial}{\partial x}h_{G,s}-\rho\frac{\partial M_s}{\partial t}\left(Q_{P,s}+h_{S,s}-h_{G,s}\right) \quad (2.5a)$$

$$\rho c_{P,c}\frac{\partial T}{\partial t}=\frac{\partial}{\partial x}\left(k_c\frac{\partial T}{\partial x}\right)-\dot{M}_G\frac{\partial}{\partial x}h_{G,c}-\rho\frac{\partial M_c}{\partial t}\left(Q_{P,c}+h_{S,c}-h_{G,c}\right) \quad (2.5b)$$

The subscripts *s* and *c* refer to the skins and core, respectively. The thermal properties for specific heat (c_P) and thermal conductivity (k) of the skins and core are temperature-dependent. $\dot{M}_G$ is the mass flux of volatiles. h_S and h_G are the enthalpies of the solid material and evolved gas, respectively, and Q_P is the endothermic decomposition energy.

Similar to model by Gibson et al. [39], the decomposition reaction rates of the skins and core are expressed in the last term of Eq. 2.5 by ($\frac{\partial M}{\partial t}$). When the skins and core decompose via a single-stage reaction process then the mass loss rate is calculated using the first-order Arrhenius relationship:

$$\frac{\partial M}{\partial t} = -AM_o\left(\frac{M - M_f}{M_o}\right)e^{(-E_a/RT)} \qquad (2.6)$$

The thermal model makes two main assumptions about the thermal behaviour of sandwich composites in fire. Firstly, the model is a one-dimensional equation that only analyses conductive heat transfer and mass transport of decomposition gases in the through-thickness (x) direction. Secondly, it is assumed that heat-induced delaminations, skin-core interfacial cracking and other types of damage to the sandwich composite do not change the mass flux of gases. Figure 2.8 shows temperature-time profiles at different locations within a sandwich composite [3]. The temperatures were measured using thermocouples at different locations in the composite. The agreement between the measured and calculated temperatures are very good.

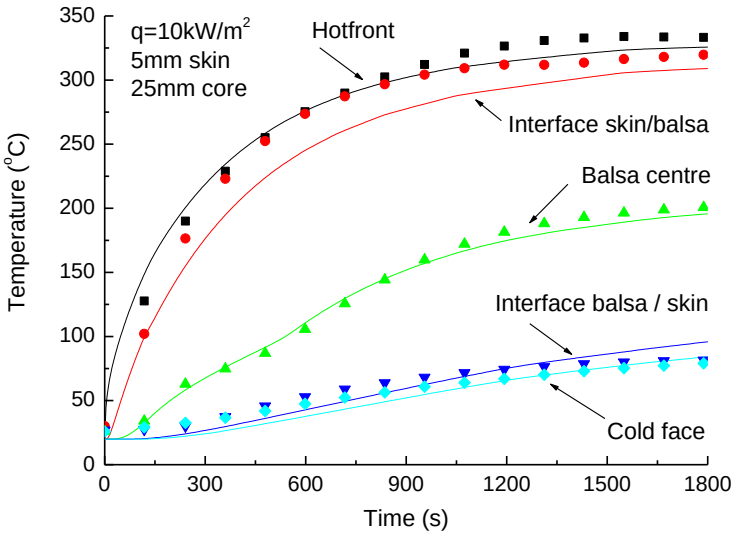

Figure 2.8: Comparison of calculated (curve) and measured (data points) temperature profiles at different locations in a sandwich composite. The composite consisted of glass-vinyl ester laminate face skins and balsa core, and it was exposed to the heat flux of 10 kW/m² [3].

In summary, thermal models have been developed for predicting the fire response of laminates. The model developed by Henderson et al. [27] can predict with good accuracy the temperature rise in fibreglass laminates. More complex thermal models have been formulated that consider other effects on the internal temperature, such as internal pressure, strain and moisture [30, 31, 35, 38, 39]. However, the accuracy of many of these models have only been assessed for one or a few types of laminates exposed to fire. In building and bridge application using E-glass fibre, Bai and Keller [45-47] has validated their thermomechanical response model by combining temperature-dependent material property models based on kinetic theory.

There is also a progress in thermal modelling of sandwich composite that has been validated by experimental fire testing [3, 12, 48]. Thermal model modified by Feih et al. [3] assumed that cracks, delaminations and skin-core debonding that might occurred during the decomposition process will have no significant effect on temperature profile. Despite the assumptions, the modified thermal model is able to predict the temperature at any location in sandwich composite materials with good accuracy. Thermal model by Looyeh et al. [12] accurately predict the temperature profile of a sandwich composite

constructed from combustible face skins with a non-combustible core. Reasonable thermal response prediction also has been obtained by Luo et al. [48] using finite element model that considered delamination in sandwich composite structure.

New thermal models are needed which consider fire-induced damage, such as delamination and matrix cracking. The main challenge in advanced thermal modelling is to develop a unified damage model that concurrently analyses all types of damage on a composite laminate exposed to fire.

2.5 COMPOSITES IN FIRE UNDER TENSILE LOADING

Several models have been developed to calculate tensile softening and failure of polymer laminates in fire [3, 5, 49]. Modelling the tensile response in fire is different and more complicated than compression modelling, which is described in the next section. In analysing the tensile response, both matrix and fibre softening effects need to be analysed and incorporated into the fire structural model. The first step into the fire structural modelling under tensile loading is to calculate the through-thickness temperature profile of the laminate exposed to one-sided heating. The thermal model was described in Section 2.2. In the second analytical step, mechanical models are used to calculate reductions in tensile stiffness and strength of the laminate. The thermal-mechanical model developed by Feih et al. [5] can be used to calculate the temperature rise, decomposition, and softening and failure of E-glass laminates under tension.

The through-thickness temperature profile is used to then compute the reduction to the tensile properties through the laminate. The model assumes that the mechanical properties of the laminate will decrease via a single-stage (rigid-to-glassy) glass transition of the polymer matrix with increasing temperature. The tensile strength of most polymer laminate skins decrease with increasing temperature as depicted in Figure 2.9. The elastic and matrix-dominated properties show this temperature-dependence, which has been measured for many laminate materials [5, 50, 51]. The strength remains at the room

temperature strength value ($\sigma_{m(0)}$) until it reaches a critical softening temperature (T_{cr}). Above (T_{cr}), the strength decreases progressively with increasing temperature to a minimum value, ($\sigma_{m(R)}$) when the matrix has fully softened. Below $\sigma_{m(R)}$, strength decreases very gradually due to further viscous softening and finally pyrolysis of the matrix, which typically occurs above 250-500^{0}C. As can be seen in Figure 2.9, the curve is almost symmetric around T'$_g$, which is the mechanical glass transition temperature where the strength has dropped by 50%.

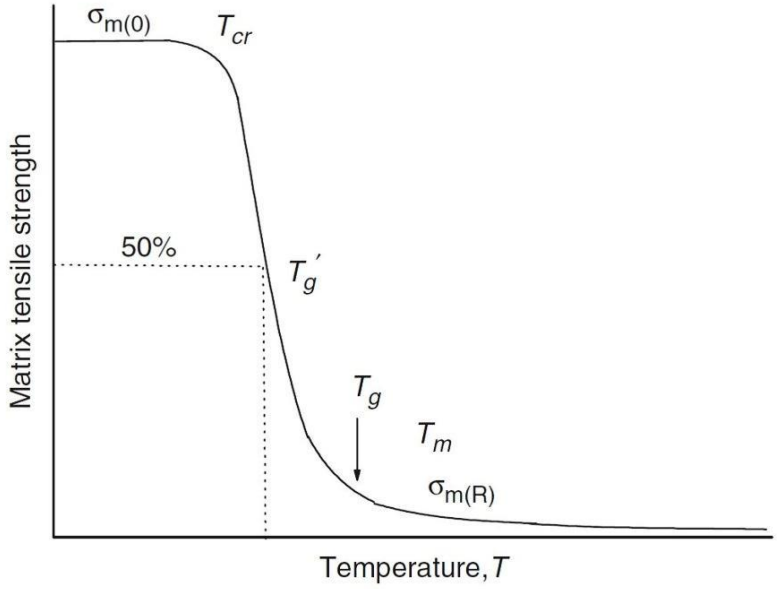

Figure 2.9: Typical relationship between temperature and tensile strength for a polymer laminates [5].

A mathematical function is needed to analyse the near-symmetric behaviour around T'$_g$. The hyperbolic tanh function can relate the strength with temperature [5, 50]. The tensile properties are related to the temperature via this function according to [50]:

$$\sigma(T) = \left(\frac{\sigma_{m(0)}+\sigma_{m(R)}}{2} - \frac{\sigma_{m(0)}+\sigma_{m(R)}}{2} tanh\left(k_m\left(T - T'_g\right)\right)\right) R_{rc}(T)^n \qquad (2.7)$$

The equation considers the effect of both viscous softening and decomposition of the polymer matrix. *T* is the temperature calculated using Equation (2.2) and k_m is an empirical constant describing the temperature range across which softening occurs. $R_{rc}(T)$ is a scaling function to account for mass loss during decomposition of the polymer matrix and can be calculated using Equation (2.3). The exponent *n* is a constant dependent on the relationship of mass loss with mechanical property. When *n=0* it is assumed that

decomposition has no effect on the mechanical property. When *n=1* it is assumed a linear relationship exists between mass loss and mechanical property. Feih et al. [5] have shown taking *n=3* gives good estimation for a vinyl ester matrix laminate.

Figure 2.10 shows the reduction to the tensile strength of an E-glass/vinyl ester composite with increasing temperature measured by Feih et al. [5]. The minimum strength is reached at about 150^0C and then remains constant up to 300^0C. Feih et al. [5] have shown that the tensile strength variation with temperature (such as shown in Figure 2.10) can be fitted using the rule of mixtures expression:

$$\sigma_{(i)}(T,t) = \Phi_{LT}(T)V_f\sigma_{fb(i)}(T,t) + \left(1 - V_f\right)\sigma_{m(i)}(T) \quad \text{with } T<T'_g \qquad (2.8)$$

where:

v_f is the volume fraction of load-bearing fibres

$\sigma_{fb(i)}$ is the fibre bundle strength

$\sigma_{m(i)}$ is the matrix strength

Φ_{LT} is the load transfer factor, and when the value is 1; Equation (2.8) yields the standard rule-of-mixtures.

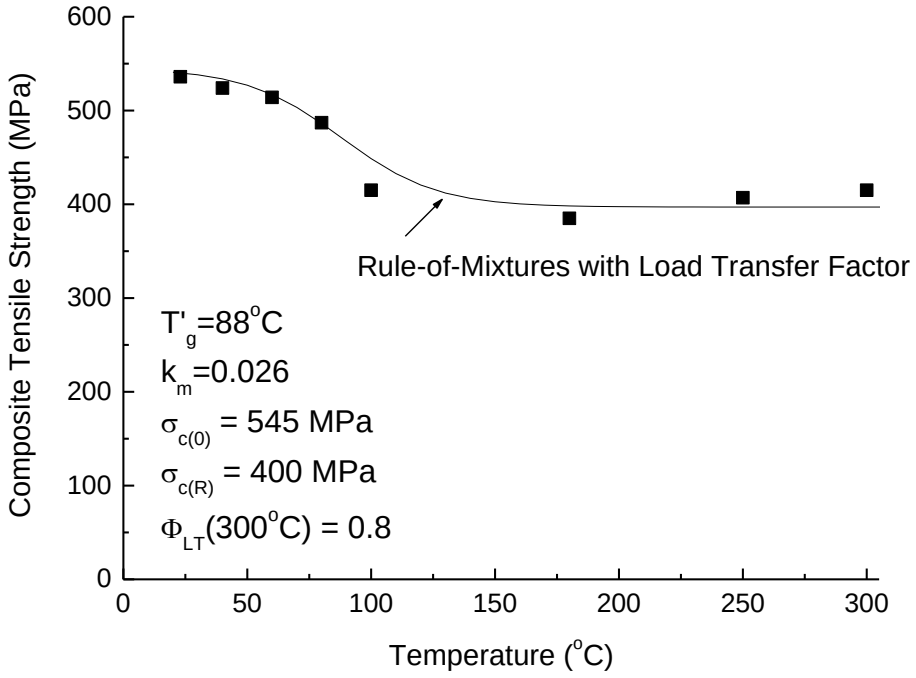

Figure 2.10: Effect of temperature on the tensile strength of E-glass/vinyl ester composite [5].

In modelling the high temperature strength of laminates, both softening of polymer matrix and fibre reinforcement must be considered. Feih et al. [5] report that the matrix strength can be calculated using Equation 2.7. When using this equation it is assumed that the reduction in matrix strength is not time-dependent (i.e. no creep and visco-elastic deformation). The measured fibre strength loss is both time and temperature dependent. Figure 2.11 shows the effect of temperature and heating time on the normalised tensile strength of E-glass bundles [5]. The tensile strength of the fibre bundles decreases with increasing temperature and heating time. A phenomenological model using tanh function was developed by Feih et al. to mathematically describe the profile of E-glass fibre strength reduction shown in the Figure 2.11. The function relates the fibre bundle strength σ_{fb}, to the temperature T and heating time t via:

$$\sigma_{fb}(t,T) = \sigma_{fb(0)} - \sigma_{loss}(T)tanh\left|k_{fb}(T)t\right| \quad (2.9)$$

where:

$\sigma_{fb(0)}$ is the room temperature tensile strength of the fibre bundle

$\sigma_{loss}(T)$ is the steady-state strength of the fibre bundle at a fixed temperature

$k_{fb}(T)$ is the rate of strength loss as a function of temperature, and is calculated using,

$$k_{fb}(T) = k_1 e^{k2T} \quad (2.10)$$

where k_1 and k_2 are curve fit constant that have to be determined by elevated temperature strength test on fibre bundles.

The strength loss function, $\sigma_{loss}(T)$ occurs in a symmetric trend at about $T_{50\%}$ at which the fibre bundle loses 50% of its tensile strength for long-term heat exposure. The strength loss is derived from:

$$\sigma_{loss}(T) = \frac{\sigma_{fb(0)}}{2} + \frac{\sigma_{fb(0)}.tanh\left|p_{fb}(T-T_{50\%})\right|}{2} \quad (2.11)$$

with $T_{50\%}$ and p_{fb} being curve-fit constants. From the experimental data as depicted in Figure 2.11, it will be possible to determine the values for $k_{fb}(T)$, $T_{50\%}$ and p_{fb}.

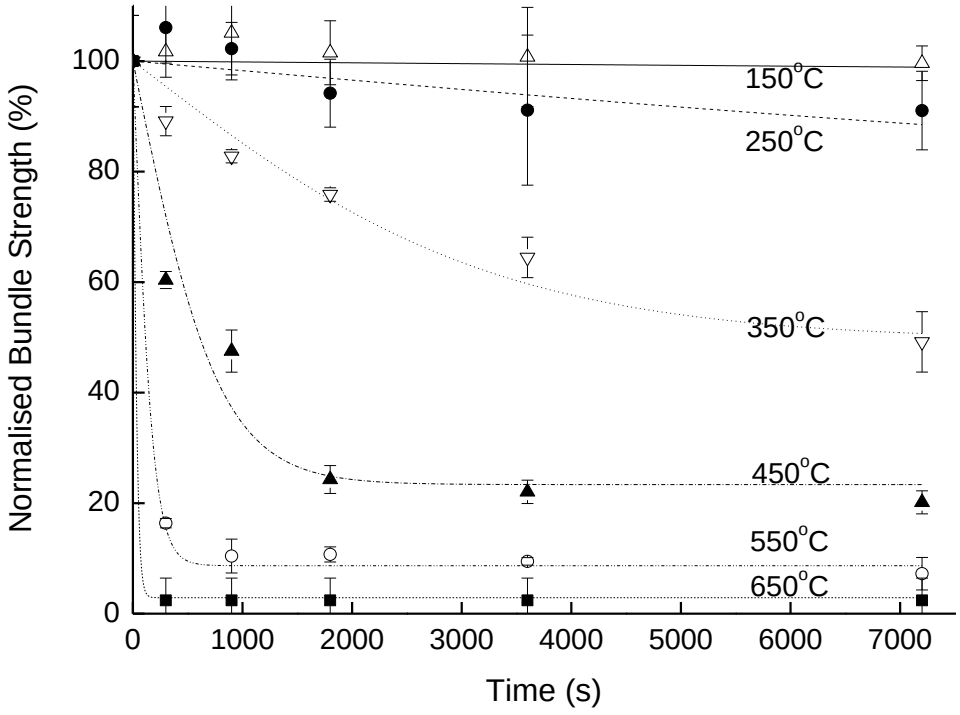

Figure 2.11: E-glass fibre bundles strength degradation with increasing temperature and heating time. The normalised strength is the elevated strength normalised to the original strength at room temperature [5].

Feih et al. [5] showed that the reduction to the tensile strength of the polymer matrix due to softening and decomposition at different locations through a fibreglass laminate exposed to fire is calculated based on the temperature profile. The loss in strength of the glass fibre reinforcement at different locations is calculated as a function of temperature and time using

$$\sigma_{fb(j+1)}\left(T_{av(j+1)}(x_i), t_{eff,j+1}(x_i) + \Delta T\right) = \sigma_{fb(0)} - \sigma_{loss}(T_{av(j+1)}(x_i) tanh\left|k\left(T_{av(j+1)}(x_i), t_{eff,j+1}(x_i) + \Delta t\right)\right| \quad (2.12)$$

Equation (2.12) is valid for silica-based fibres.

Rule-of-mixtures in Equation (2.8) is then used to calculate the reduction to the tensile strength of the polymer matrix and glass fibres with increasing temperature and

increments of time at each location in the laminate. Feih et al. [5] report that the load transfer factor (Φ_{LT}), which defines the stress transfer efficiency between the fibres and polymer matrix is assumed to reach a minimum value upon complete softening of the matrix. The value is determined by elevated temperature tests as shown in Figure 2.10. Once the residual strength at different locations in the through-thickness direction is calculated, the residual strength can be determined at each time interval by integrating the property values using Simpson integration:

$$\sigma_{av} = \frac{1}{t}\int_{-x/2}^{+x/2} \sigma\left(T_{av}(x), t_{eff}(x)\right) dx \qquad \text{with:} \tag{2.13}$$

$$\int_{-x/2}^{+x/2} \sigma\left(T(x), t_{eff}(x)\right) dx = \frac{h}{3m}\Big[\sigma\left(T_{av}(x_0), t_{eff}(x_0)\right) + 4\sigma\left(T(x_1), t_{eff}(x_1)\right) + 2\sigma\left(T(x_2), t_{eff}(x_2)\right) + \cdots + 2\sigma\left(T(x_{k-2}), t_{eff}(x_{k-2})\right) + 4\sigma\left(T(x_{k-1}), t_{eff}(x_{k-1})\right) + \sigma\left(T(x_k), t_{eff}(x_k)\right)\Big] \tag{2.14}$$

m defines the number of locations in the through-thickness direction where the local residual strength is calculated, and *h* is the laminate thickness. The procedure for calculating the tensile strength of an E-glass/vinyl ester composite exposed to a radiant one-sided heating is summarised in the flowchart in Figure 2.12.

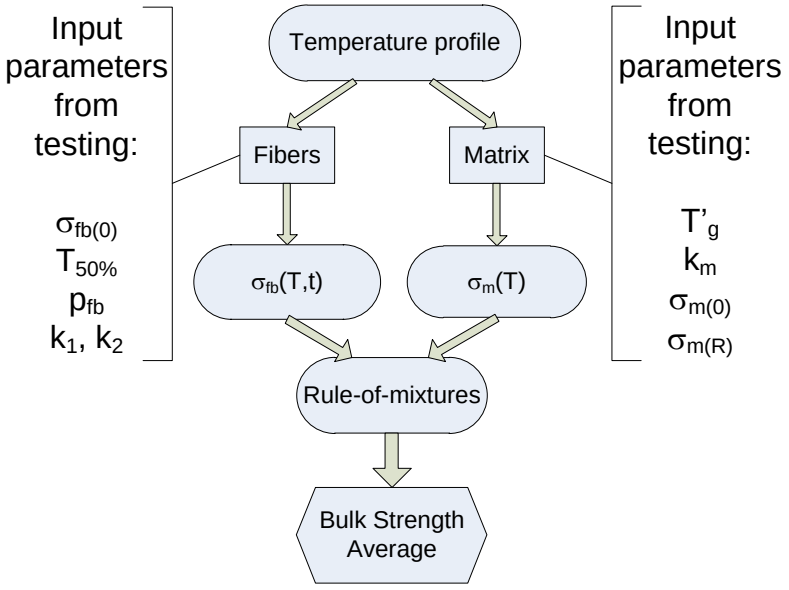

Figure 2.12: Schematic flow chart of analytical algorithm to calculate the tensile strength of a fibreglass laminate in fire [5].

The average strength model developed by Feih et al. [5, 50] can predict the failure stresses and times of E-glass laminates with good accuracy, as shown in Figure 2.13. This figure shows the effect of applied tensile stress on the failure times of a glass-vinyl ester laminate exposed to heat fluxes of 10, 25, 50 and 75 kW/m^2. The measured times are shown by the data points and the curves were calculated by Feih et al. using the model. Thermal softening of the matrix reduces slightly the tensile strength when initially exposed to fire, but eventually has no significant effect once the matrix has completely softened and decomposed. Fibre softening mostly controlled the tensile failure of the laminate. While this study has shown that the model gives a good estimation of tensile strength and failure time of E-glass/vinyl ester composite, further analysis and validation against experimental data is required. For example, the tension model by Feih et al. [5] does not analyse all the damage processes which control the mechanical properties and failure such as thermal strain, pore formation, delamination and fibre-matrix debonding. A model to analyse the tensile response of sandwich composites exposed to fire is also required.

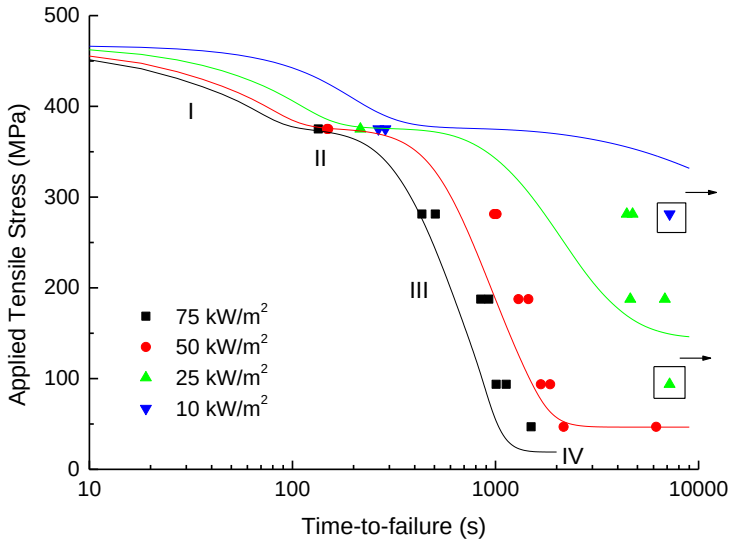

Figure 2.13: Comparison of failure times calculated using average strength model for a glass-vinyl ester laminate exposed to different heat fluxes [5].

Another model by Gibson et al. [50] has shown that the thermal model coupled to laminate theory can give reasonable predictions for mechanical behaviour under load. The thermal model coupled to this laminate theory is from previous analysis that predicts the evolution of temperature and resin decomposition with time through-the-thickness of the laminate. The model is based on laminate theory analysis and the predictions for tensile behaviour are conservative, due to the non-linearity of stress-strain behaviour computed using the model as shown in Figure 2.14 (a). Figure 2.14 (b) also shows the failure curve calculated using the average strength model of a glass/polyester laminate.

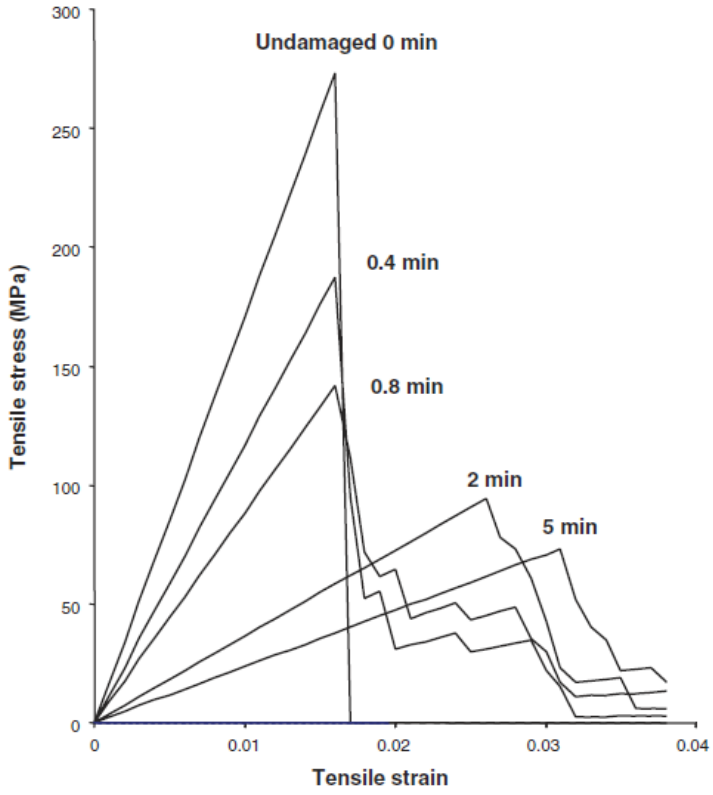

(a)

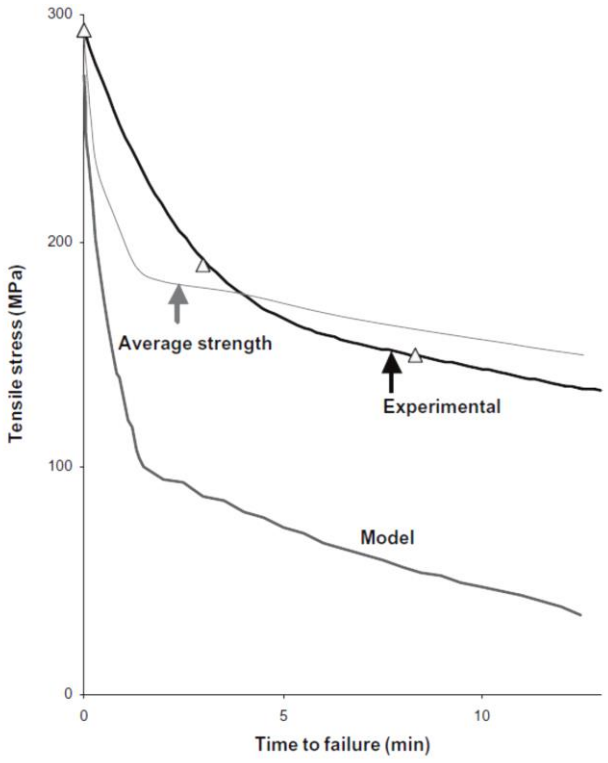

(b)

Figure 2.14: (a) Predicted glass/polyester laminate stress vs strain curves at various times. (b)Time-to-failure prediction for glass/polyester laminate using laminate theory analysis and addition using average strength model [50].

2.6 COMPOSITES IN FIRE UNDER COMPRESSIVE LOADING

Major progress has been made in the development of finite element and analytical models to analyse the compressive structural integrity of composites in fire [10, 12, 14, 42-44, 49, 50, 52-58]. Modelling the fire structural response of composites under compression loading is less complicated than tension because the fibre reinforcement is not significant in controlling softening and failure. The thermal model used in compression is the same as for the tension structural model from Feih et al. [5]. Similar to tension modelling, the initial step in analysing the compression properties is the calculation of the temperature distribution through the composite with increasing time using the thermal model. By using the through-thickness temperature distribution, the reduction to the mechanical properties can be calculated. Currently, the reduction to the mechanical properties with increasing

temperature must be measured experimentally under iso-thermal conditions. Similar to the tension model, the compression model also assumes that the mechanical properties of the laminate decrease via a single-stage (rigid-to-rubbery) glass transition of the polymer matrix with increasing temperature. The compression strength of most polymer laminates decreases with increasing temperature as depicted in Figure 2.15.

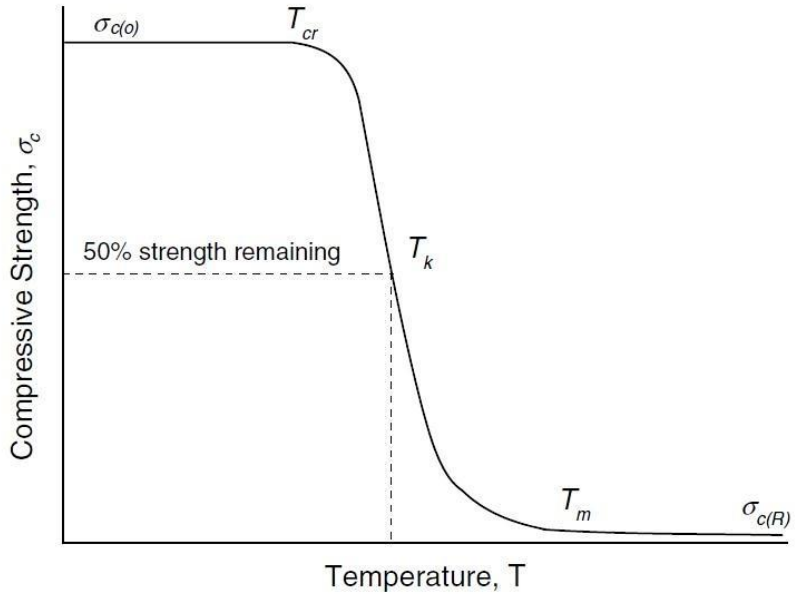

Figure 2.15: Typical relationship between temperature and compressive strength.

Several curve-fitting techniques can be used to empirically relate the compressive properties with temperature using experimental data, including polynomial [59] and tanh functions [4, 43, 50]. The polynomial equation used to relate temperature and compressive strength is expressed as [59]:

$$\mathrm{P(T)}=\left[1-\xi_1^*\left(\frac{T-T_\infty}{T_g-T}\right)-\xi_2^*\left(\frac{T-T_\infty}{T_g-T}\right)^2-\xi_3^*\left(\frac{T-T_\infty}{T_g-T}\right)^3\right].P_0 \qquad (2.15)$$

and the tanh equation is [50]:

$$P(T)=\left(\frac{P_0+P_R}{2}-\frac{P_0-P_R}{2}\,tanh\left(k_m\left(T-T'_g\right)\right)\right)R^n(T) \qquad (2.16)$$

Both equations are valid when the composite softens in a single-stage process. Figure 2.16 shows the effect of increasing temperature on the compressive strength of an E-

glass/vinyl ester laminate [4]. Many other laminates experience a similar reduction in compressive strength with increasing temperature [3, 4, 43, 56].

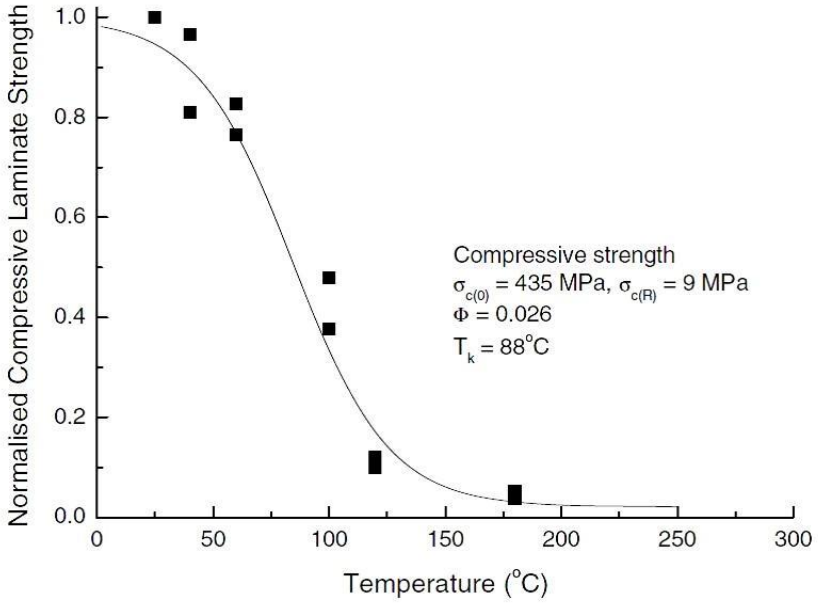

Figure 2.16: Effect of the temperature on the compressive strength of a glass-vinyl ester laminate. The elevated temperature strength has been normalised to the strength at room temperature [4].

Different mechanical models have been developed to analyse the reduction to the compression properties and failure of laminates under combined compression loading and one-sided heating [4, 10, 42-44, 50, 53, 54, 58-61]. The two most used and rigorously validated models are the average strength model [4, 5, 43, 50] and visco-elastic softening model [58]. Gibson et al. [50] developed an average strength model that is based on ply-by-ply analysis to compute the compressive softening that occurs progressively in the through-thickness direction of laminates exposed to fire. Figure 2.17 shows the comparison between predicted time-to-failure values calculated using the average strength model and experimental failure time data.

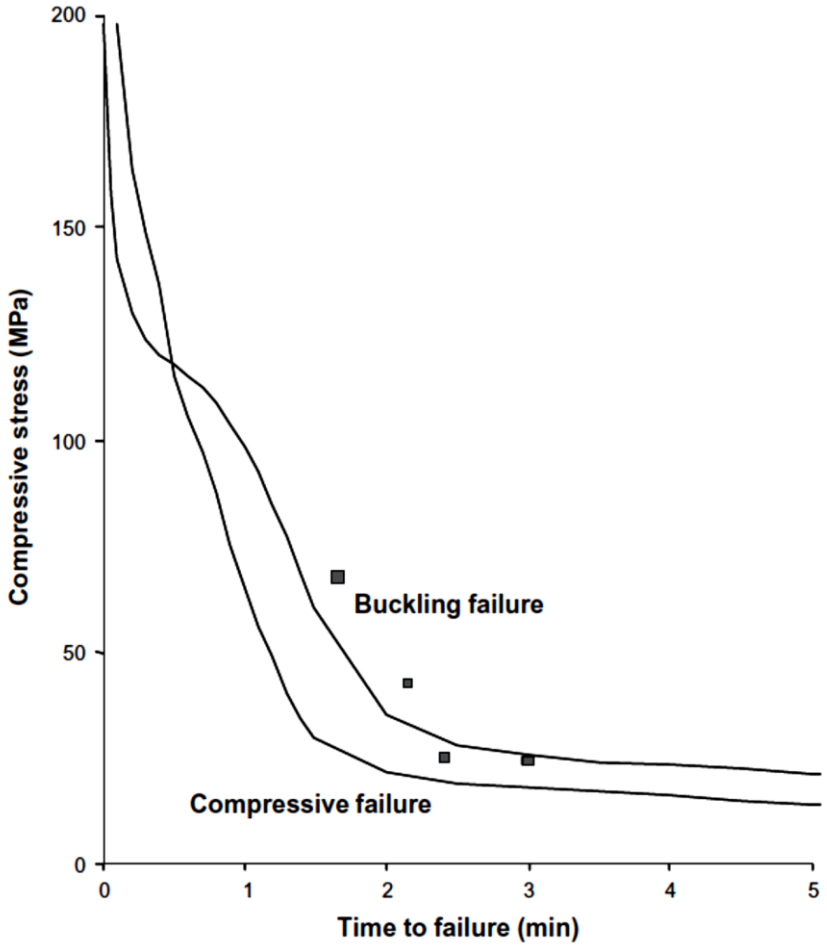

Figure 2.17: Comparison of failure times calculated using average strength model for a glass-polyester laminate under combined compression loading and one-sided heating of heat flux 75 kW/m^2 [50].

Feih et al. [4, 43] used average stress analysis in which the properties of each ply are effectively 'smeared' over the load-bearing area of the composites to analyse softening in fire. The average strength model calculates the residual compression strength and time-to-failure of laminates and sandwich composites. The model gives reasonable predictions for the compression behaviour under load. Equation 2.16 is used to calculate the residual compression strength at different locations through the composite materials. Local compressive strength values are then averaged over the load-bearing area using Simpson integration in order to determine the reduction to the bulk compression strength of the composite at any time during a fire event. The compression model assumes weakening of the skins to sandwich composites is caused solely by matrix softening. The

accuracy of the model has been evaluated for fibreglass laminates and sandwich composites with fibreglass laminate skins [3, 43]. The compression model is able to predict with reasonable accuracy the failure time for a woven glass/vinyl ester laminate and sandwich composites at different heat flux condition as shown in Figures 2.18 and 2.19, respectively.

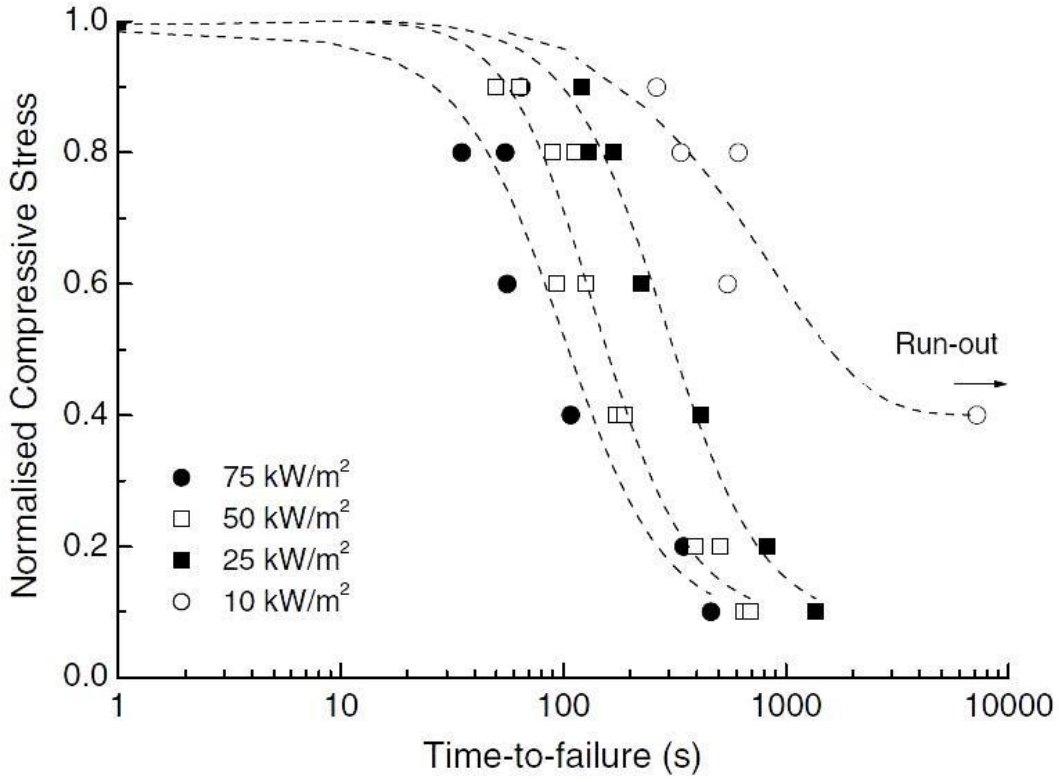

Figure 2.18: Calculated (curves) and measured (data points) failure times for a glass-vinyl ester laminate under combined compressive loading and one-sided heating at different heat fluxes [4].

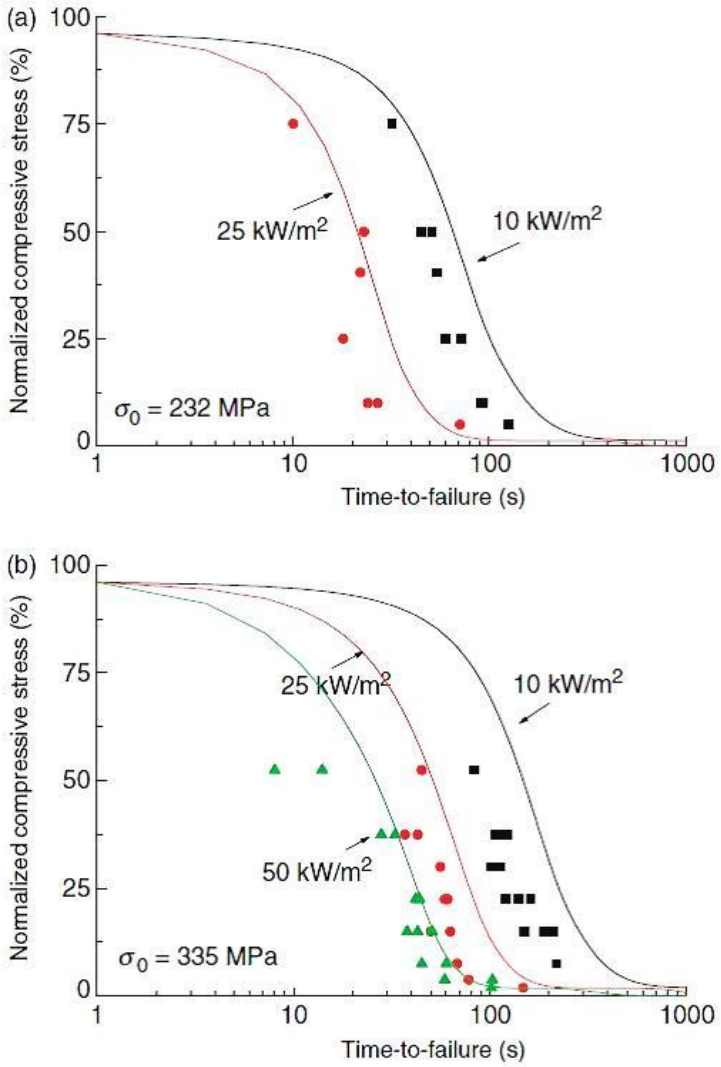

Figure 2.19: Time-to-failure for a sandwich composites under combined compression and one-sided heating at different thermal fluxes (a) 2mm thickness skins and (b) 5mm thickness skins (solid curve: prediction, data points: experimental) [3].

The thermal-mechanical model developed by Feih et al. [3] is able to calculate with reasonable accuracy the failure times of E-glass/vinyl ester and balsa core sandwich composite. As shown in Figure 2.19, the model predicts that the time-to-failure increases with the skin thickness and when the applied compressive stress or heat flux are reduced [3]. However, the model was not able to accurately predict the failure time for all heat flux conditions due to the complexity of failure process of the face skins. The model is accurate

when all plies in the front skin fail at the same time due to microbuckling, which occurs under high heat flux and high stress conditions.

Some other mechanical models has been developed to analyse the reduction of compression properties based on Euler buckling theory [59] and visco-elastic softening [54, 58] for laminates, and on buckling [59, 62, 63] and skin wrinkling [55] models for sandwich composites. For example, Bausano and colleagues [58] modelled the compressive response for fiberglass laminate, and found reasonable agreement between experimental and theoretical results. Boyd et al. [54] developed a model based on visco-elastic creep of the polymer matrix and microbuckling (kinking) of the fibres. They found good agreement between their experimental failure time result and model, as shown in Figure 2.20. Boyd and colleagues concluded that matrix viscoelasticity controls the delayed failure in the glass transition temperature region. At higher temperature, failure is controlled by thermal softening as the effect of viscoelastic creep is less significant than temperature-controlled strength loss.

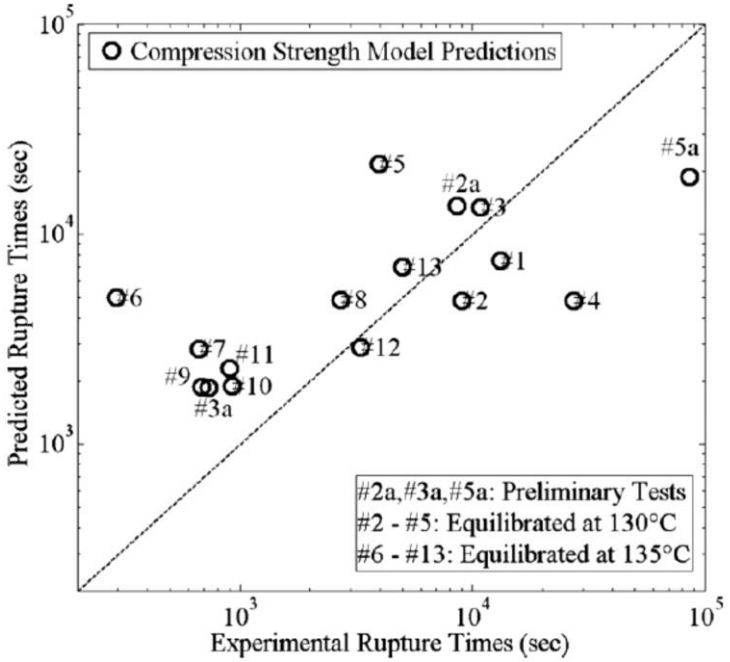

Figure 2.20: Predicted rupture times vs experimental rupture times of E-glass/vinyl ester laminates [54].

Gu and Asaro [10, 11, 53-55] developed mechanical models to analyse the failure mechanisms of sandwich composite under thermal gradients caused by fire. Global buckling, skin wrinkling and core failure are some compressive failure modes considered due to combine compressive load and thermal gradient. The mechanical models developed by Gu and Asaro have not been validated using experimental testing data. Lua et al. [51] developed a finite element model to analyse the compressive response of sandwich composites exposed to fire and predicted the decomposition, stiffness degradation, and delamination at skin/core interface. It has found that compressive load and stiffness degradation causes local buckling of the skin in the sandwich composite.

Despite the extensive amount of research towards the development of thermal-mechanical models for calculating the fire structural response and failure of composites under compression load, much remains to be done. As the models assume that the weakening of the composite is solely due to matrix softening, and that other softening processes such as pore formation and delamination are not considered. Further analysis and validation is needed to incorporate damage and failure processes into thermal-compressive mechanical models. The accuracy of newly developed model also needs to be determined against experimental data for a wide variety of composite materials.

2.7 POST-FIRE MECHANICAL PROPERTIES OF COMPOSITES

Another factor limiting the use of polymer composites by the marine industry is the reduction in strength and stiffness experienced by the structure following fire. After a fire is extinguished, it is important to analyse the post-fire properties in order to assess the residual integrity and safety of the structure. Experimental fire studies by Pering et al. [34] determined the residual tensile and shear properties of graphite/epoxy laminates after short-term exposure to a propane gas burner at temperatures up to 980^0C. Sorathia et al. [64] measured the post-fire flexural properties for a wide variety of laminates. Mouritz and Mathys [65-67] showed that the residual mechanical properties of composite following fire can be significantly reduced due to decomposition and damage of the polymer matrix.

A simple bi-material layer model has been proposed by Mouritz and colleagues [40, 66-71] to calculate the post-fire mechanical properties of burnt laminates. Mouritz and Mathys [66, 67] suggested that when a burnt composite is loaded in uniaxial tension at room temperature, the residual tensile properties can be approximated using a rule-of-mixtures model. In the model, the post-fire properties are determined by combining the tensile properties of the unburnt and char regions using a rule-of-mixture formulation to give the bulk post-fire strength and stiffness of the fire-damaged composite. Figure 2.21 shows a schematic of fire damage in a laminate which forms the basis of the model. The post-fire tensile stiffness of an evenly burnt composite can be estimated using:

$$S_t = \left(\frac{d-d_c}{d}\right) S_0 + \frac{d_c}{d} S_c \quad (2.17)$$

Where d_c is the char thickness, d is the original thickness of the composite, and S_c and S_o are the tensile stiffness values of the char and unburnt laminate, respectively. The first term on right hand side of the equation 2.17 represents the tensile stiffness of the unburnt region and the second term is the stiffness of the burnt region. The same approach is used to calculate the post-fire tensile failure strength:

$$\sigma_t = \left(\frac{d-d_c}{d}\right) \sigma_{t_{(0)}} + \left(\frac{d_c}{d}\right) \sigma_{t_{(c)}} \quad (2.18)$$

where: $\sigma_{t(0)}$ and $\sigma_{t(c)}$ are the tensile failure stress values for the unburnt laminate and char, respectively.

Similar to post-fire tension, Mouritz and Mathys [66, 67] developed analytical expressions to calculate post-fire compression strength, bending (four-point) load and Euler buckling load respectively as per below equations:

$$\sigma_c = \left(\frac{d-d_c}{d}\right) \sigma_{c_{(0)}} + \left(\frac{d_c}{d}\right) \sigma_{c_{(c)}} \quad (2.19)$$

$$P_f = \frac{8\sigma_{f(0)} b}{3L_f} \left[[(d-d_n)^2] + \frac{(d_n-d_c)^3}{(d-d_n)} + \frac{E_{f(c)}}{E_{f(0)}} . \frac{[d_n^3-(d_n-d_c)^3]}{(d-d_n)} \right] \quad (2.20)$$

$$P_f = \frac{C\pi^2 E_c b (d-d_c)^3}{12_c^2} \quad (2.21)$$

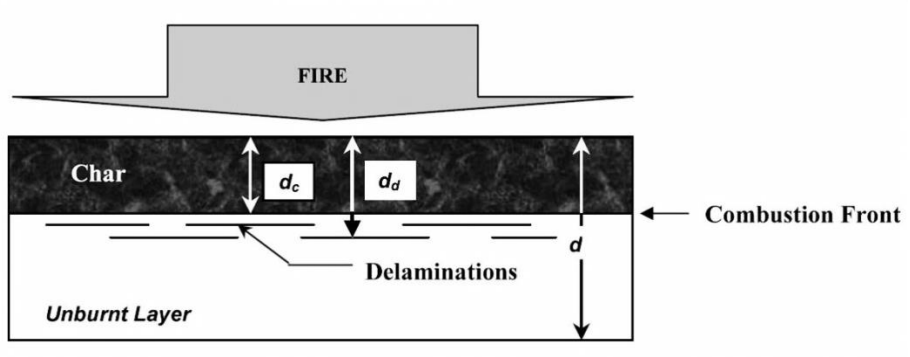

Figure 2.21: Schematic of a damaged composite laminates.

The post-fire models have been validated for several types of laminates [8, 40, 66-69, 71-74]. Figure 2.22 shows one example of successful validation of the post-fire tensile strength and stiffness of a woven glass/polyester laminate. The post-fire properties decrease with increasing heating time, and the agreement between the calculated and measured post-fire properties is good. The reduction is due to the thermal degradation of the polymer matrix that forms a weak char region.

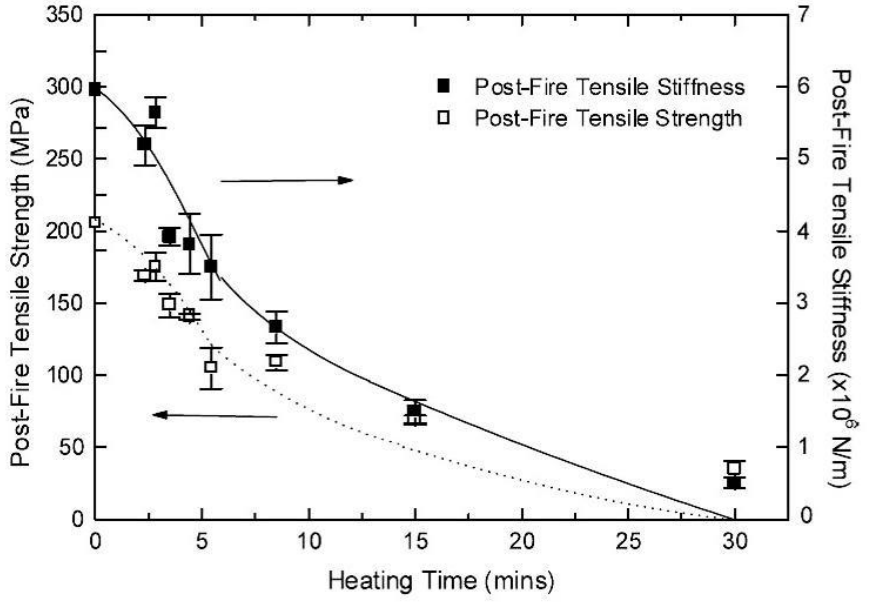

Figure 2.22: The effect of heating time on the post-fire tension properties of woven glass/polyester composite. The data points and curves represent the measured and calculated properties, respectively [68].

Figure 2.23 shows reductions to the post-fire tension, compression and flexural strengths of a woven glass-vinyl ester laminate following increasing exposure time to the heat flux of 50 kW/m^2. As expected, the strengths decrease with increasing time. The agreement between the post-fire models and the experiment data is reasonable. Similar observations have been found for the post-fire stiffness properties.

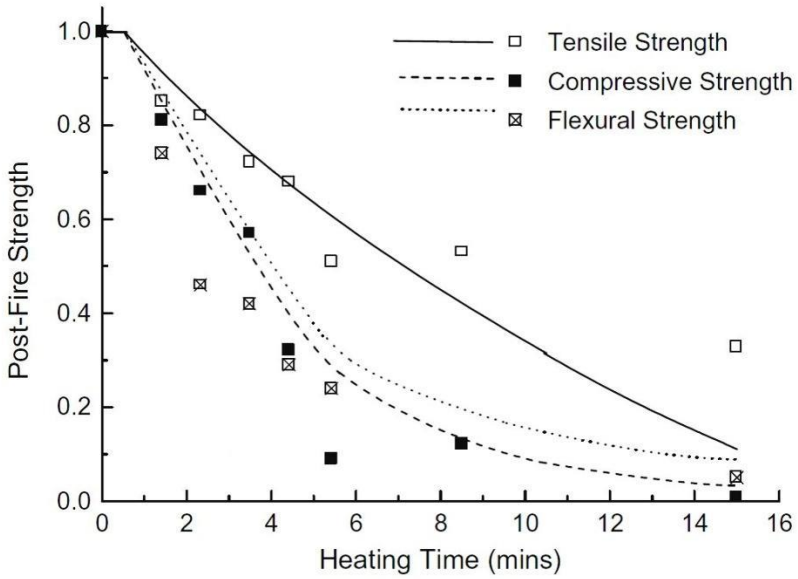

Figure 2.23: Comparison of theoretical (curves) and measured (data points) reductions to the post-fire tension, compression and bending strength of a glass-polyester laminate [1].

The two-layer model was developed further by Gardiner and Mouritz [40] to calculate the post-fire compression properties of sandwich composites. The effects of increasing heat flux and heating time on sandwich composites with glass-vinyl ester skins and PVC foam core and phenolic laminate skins with phenolic foam core were investigated. Figure 2.24 shows the effect of heating time on the post-fire compression stiffness and failure load of these sandwich composites following exposure to the heat flux of 50 kW/m^2. When the sandwich composites were exposed to a high heat flux they ignited and the PVC core was severely damaged (depleted) compared to the phenolic-core sandwich material, which degraded to solid char. The arrow in Figure 2.24 indicates the heating time at which ignition occurs in the sandwich material. The compressive properties are degraded significantly before ignition, which indicates that substantial thermal damage occurs prior to ignition. The curves for the post-fire stiffness properties of the sandwich composite in

Figure 2.24(a) are lines-of-best fit. In figure 2.24(b), a buckling model was used to calculate the theoretical post-fire compressive failure load, and good agreement was found with the measured loads.

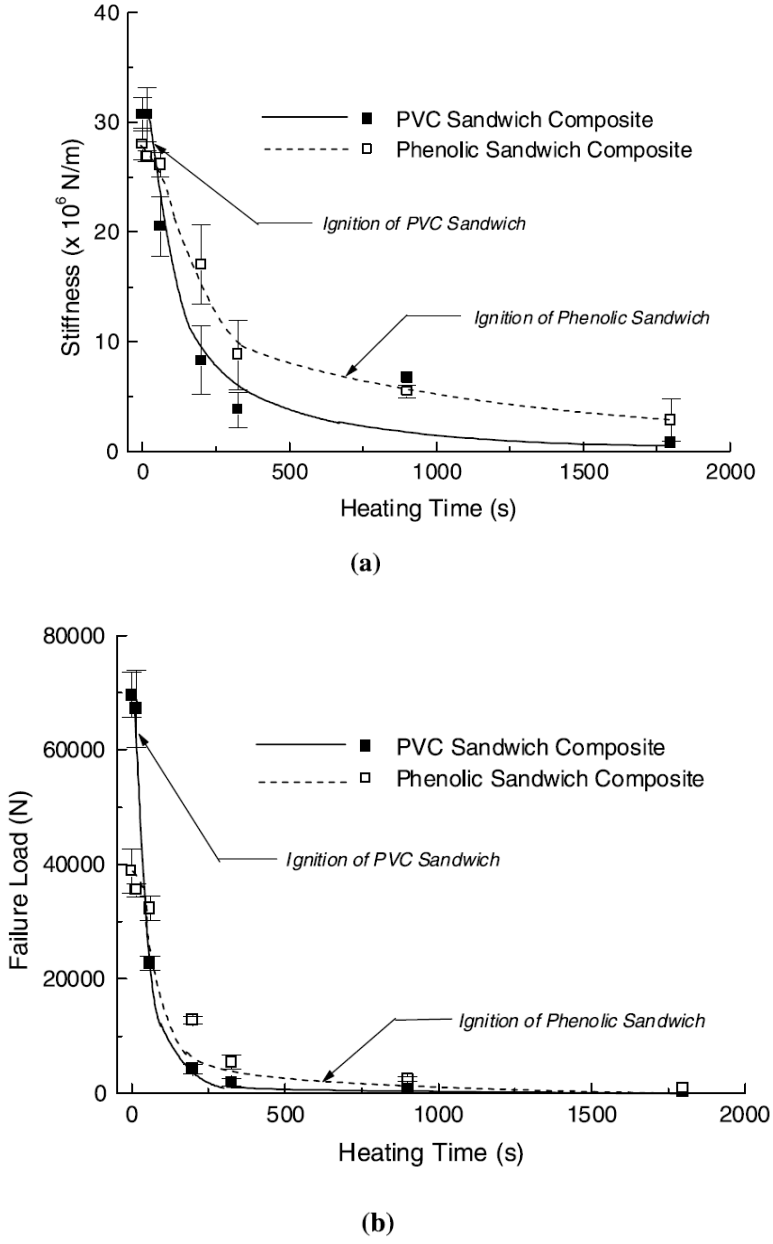

Figure 2.24: Effect of heating time on the post-fire compression (a) stiffness and (b) failure load of two sandwich composites [40].

Post-fire property modelling and testing has advanced significantly in recent years, although gaps remain. Sandwich composites have been tested and validated using the simple and effective model in predicting the post-fire compressive properties. However, models to calculate the post-fire tension and bending properties of sandwich materials have not been developed. Also, experimental data on the post-fire tensile properties is lacking.

2.8 CONCLUSION

A large amount of research has been performed on the fire structural modelling of polymer laminates; however there is a need to advance the analysis for sandwich composites. Thermal models have been developed to calculate the temperatures in sandwich composite exposed to one-sided heating by fire. The models are able to calculate with good accuracy the temperature rise in composites containing non-reactive fibres such as fiberglass. The capability of thermal model to analyse the temperature of composites containing reactive fibres such as carbon and Kevlar still needs to be addressed, as oxidation and decomposition of fibres influence the temperature profile. Improvement to thermal modelling is also required to consider the effect of fire-induced damage, such as delamination cracking and skin-core debonding which affects heat conduction.

There has been good progress in the development and validation of models to predict amount of decomposition and char formation. There has also been some progress in modelling the formation and growth of delamination cracks and gas-filled pores; however most of the models restrict the analysis to one single type of damage. There is a need to develop a unified damage model that can concurrently analyse all possible types of damage.

Several mechanical models have been developed to predict the structural response of composites when exposed to one-sided heating by fire. The models has been validated for fiberglass laminates and sandwich composite under compression loading. A model has also been developed for the tensile response of laminates in fire. However, models

to analyse the fire tensile response of sandwich composites are not available. On top of this, models to analyse the fire structural properties for other load conditions such as shear, torsion and fatigue have not been developed.

Another important issue remains the development of more accurate and robust models in solving highly non-linear behaviour. A mechanistic-based model is needed to accurately analyse the mechanisms and processes controlling temperature distribution, damage and softening failure of sandwich composite. This mechanistic-based model will improve the reliability of previous models which rely too much on empirical data.

Chapter 3 : TENSILE PROPERTIES AND FAILURE OF SANDWICH COMPOSITES IN FIRE - MODELLING AND EXPERIMENTAL TESTING

ABSTRACT

This chapter presents original research into the tension modelling and experimental testing of sandwich composites in fire. A thermal-mechanical model is presented for calculating softening and failure of flammable sandwich composites under combined tension loading and one-sided unsteady-state heating conditions representative of a fire. The thermal model calculates the temperature rise of the sandwich composite when exposed to fire. The mechanical model computes the reduction to the tensile modulus and strength of the laminate face skins caused by thermal softening of the fibre reinforcement and polymer matrix and weakening of the core.

The numerical accuracy of the model is assessed using experimental data obtained from fire structural tests performed on a sandwich composite consisting of thin woven glass-vinyl ester laminate skins and a thick core of balsa wood. Tests were performed at different tension stress levels and heat fluxes to rigorous valid the model. The model can determine the temperature rise, tensile failure stress, and failure mechanism of the sandwich composite in fire. The experimental results presented in this chapter also provide new insights into the structural survivability of tension-loaded sandwich composites in fire.

The research presented in this chapter has been published in:
A. Anjang, V.S. Chevali, E. Kandare, A.P. Mouritz, S. Feih, Tension modelling and testing of sandwich composites in fire, *Composite Structures, 2014;113:437-445.*

3.1 INTRODUCTION

Until recently, models to analyse the fire structural integrity of sandwich composites were not available. Instead, the conventional approach to assess the structural behaviour was to perform fire tests on sandwich composite components that are representative of the structural application, such as bulkhead or superstructure panels for ships [11, 75]. Large-scale fire tests provide information on the mechanical integrity and burn-through resistance of the structural design. However, these tests are technically difficult, time-consuming, expensive, and only provide information relevant to the fire test condition. It is not possible to extrapolate the information obtained for a specific test to predict the structural behaviour of sandwich composites in other fire scenarios, including ship-board fires.

As described in the previous chapter, thermal-mechanical models have been developed to predict the temperature, decomposition, softening and compression failure of fibre-polymer sandwich structures in fire [3, 10, 12-14, 42, 55, 63]. Fire research on sandwich materials has focused solely on compression failure because of their use in structures supporting compression loads [3, 10, 14, 15, 42, 63]. The fire structural performance of sandwich composites under tension loading has not been investigated. Feih and co-workers [4, 5, 22, 56, 76] assessed the fire resistance of glass and carbon fibre laminates under tension loading, and found that the softening rate (resin and fibre), survival time and failure mode is different to compression loading. Because of the current and emerging uses of sandwich composites in structural applications subjected to tension loads, an assessment of their fire resistance is required.

This chapter presents a new thermal-mechanical model to predict the temperature rise, softening rate, failure time and failure mechanisms of sandwich composites under combined tension loading and one-sided heating by fire. This model is an extension of the analysis performed by Feih et al. [5] to predict the tension failure of fibreglass laminates in fire. The model is only valid for sandwich composites with fibreglass laminate skins, although the general modelling approach can be adapted for other types of face skin materials. The model is validated using data from small-scale fire structural tests

performed on a sandwich composite consisting of fibreglass/vinyl ester laminate face skins and balsa core. This material is representative of the sandwich composite used in naval ship structures [2].

3.2 THERMAL MODEL FOR SANDWICH COMPOSITE

3.2.1 Thermal-Mechanical Model

The model to calculate tensile softening and failure of sandwich composites in fire involves thermal and mechanical analysis of the laminate face skins and core. Thermal analysis, which is the first step in the model, calculates the temperature profile through-the-thickness of a sandwich composite when heated from one-side by fire, as illustrated schematically in Figure 3.1. The thermal model is described in Section 3.2.2. In the second analytical step, mechanical models are used to calculate reductions to the tensile stiffness and strength of the face skins and core due to heat transfer through the sandwich composite from the fire-exposed surface to the opposing (colder) surface. By calculating the residual tensile stiffness and strength at different locations through the hot sandwich composite, and then averaging these values across each skin and core, it is possible to calculate the residual tensile properties and predict the failure mechanism. The mechanical model is out-lined in Section 3.2.3.

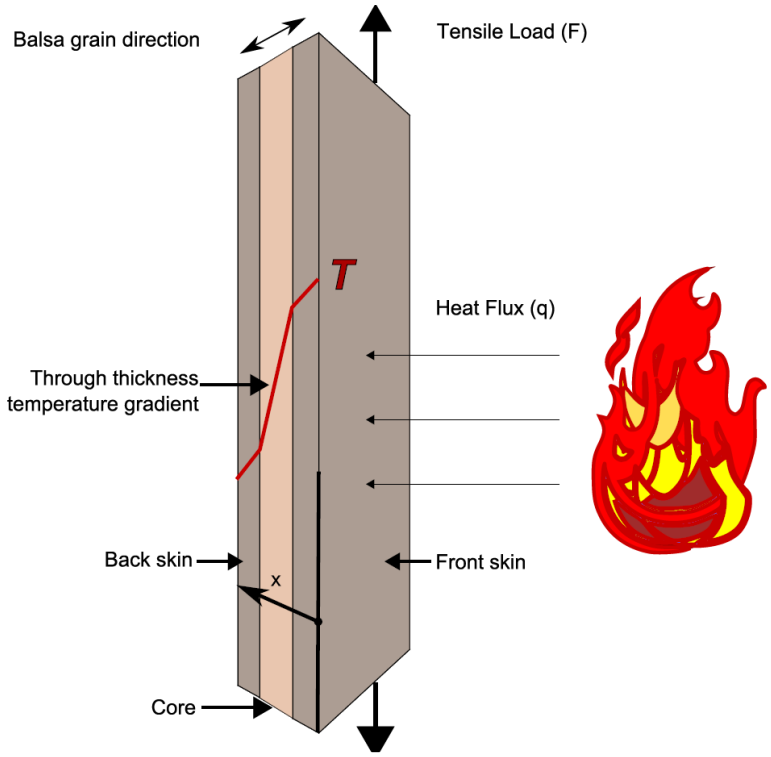

Figure 3.1: Representation of a sandwich composite subjected to combined tension loading and one-sided heating by fire.

The thermal and mechanical analysis is coupled in such a way that the mechanical properties are considered as temperature-dependent, but not vice-versa. It is assumed with the model that the internal temperatures are independent of skin, core or interface failure events, which (as discussed later) can affect the temperature.

3.2.2 Thermal Model for Sandwich Composite

Thermal analysis of the sandwich composite is performed using a modified version of the models developed by Henderson et al. [27] and Gibson et al. [39] for single-skin laminates in fire, which are described in chapter 2. To briefly recap, the model can predict the temperature rise in a hot laminate in which the polymer matrix undergoes thermal decomposition. The model can also predict the amount of resin decomposition. The thermal model was modified by Feih et al. [3] for sandwich composites consisting of combustible laminate face skins and a flammable core material.

The thermal model analyses the three important thermal processes that occur in a sandwich material exposed to fire; namely heat conduction through the heated face skin into the core and then into the back skin; heat generation or absorption by decomposition reactions of the polymer matrix to the skins and the organic core; and convective cooling due to mass transfer of decomposition gases from the skins and core towards the hot surface of the sandwich composite.

The temperature rise with heating time ($\partial T / \partial t$) in the front skin (exposed directly to the fire), underlying core and back skin are calculated using the equations [3]:

Front and back skins:

$$\rho c_{P,s} \frac{\partial T}{\partial t} = \frac{\partial}{\partial x}\left(k_s \frac{\partial T}{\partial x} \right) - \dot{M}_G \frac{\partial}{\partial x} h_{G,s} - \rho \frac{\partial M_s}{\partial t}\left(Q_{P,s} + h_{S,s} - h_{G,s} \right) \quad (3.1a)$$

Core:

$$\rho c_{P,c} \frac{\partial T}{\partial t} = \frac{\partial}{\partial x}\left(k_c \frac{\partial T}{\partial x} \right) - \dot{M}_G \frac{\partial}{\partial x} h_{G,c} - \rho \frac{\partial M_c}{\partial t}\left(Q_{P,c} + h_{S,c} - h_{G,c} \right) \quad (3.1b)$$

The subscripts *s* and *c* refer to the skins and core, respectively. The thermal properties for specific heat capacity (c_P) and thermal conductivity (k) of the skins and core are temperature-dependent. $\dot{M}_G$ is the mass flux of volatiles. h_S and h_G are the enthalpies of the solid material and evolved gas, respectively, and Q_P is the endothermic decomposition energy. h_{solid} (h_S) and h_{gas} (h_G) are the enthalpies of the solid material and decomposition gas, respectively, and respectively are defined as:

$$h_{solid} = \int_{T_\infty}^{T} C_{p(solid)} dT \quad (3.2)$$

$$h_{gas} = \int_{T_\infty}^{T} C_{p(gas)} dT \quad (3.3)$$

k_x, $C_{p(solid)}$, $C_{p(gas)}$ and E_a must be experimentally determined for the skins and core.

The thermal model is validated in this study using a sandwich composite consisting of woven E-glass/vinyl ester laminate skins and balsa wood core. Lattimer et al. [77]

experimentally determined the thermal conductivity of these materials up to about 600°C, and are defined as a function of temperature using:

skin
$$k_{x(s)} = 4.405x10^{-5}T + 0.312 \quad \text{below the matrix decomposition temperature} \quad (3.4a)$$
$$k_{x(s)} = 2.83x10^{-4}T + 0.095 \quad \text{above the matrix decomposition temperature} \quad (3.4b)$$

core
$$k_{x(c)} = 9.211x10^{8}T^{2.503} + 0.06 \quad \text{below the balsa decomposition temperature} \quad (3.5a)$$
$$k_{x(c)} = 2.223x10^{6}T^{2.503} + 0.0008 \quad \text{above the balsa decomposition temperature} \quad (3.5b)$$

Lattimer et al. [77] also determined the empirical relationship between specific heat capacity and temperature for the skins and core:

skin
$$C_{p(s)} = 0.0452T + 1080 \quad \text{below the matrix decomposition temperature} \quad (3.6a)$$
$$C_{p(s)} = 0.259T + 1041 \quad \text{above the matrix decomposition temperature} \quad (3.6b)$$

core
$$C_{p(c)} = 0.68T + 1420 \quad \text{below the balsa decomposition temperature} \quad (3.7a)$$
$$C_{p(c)} = 1.33T + 3194 \quad \text{above the balsa decomposition temperature} \quad (3.7b)$$

The specific heat capacities of the gases evolved from the polymer matrix to the skins and the balsa core are dependent on the temperature according to [77]:

skin $\quad C_{pg(s)} = -91.151 + 4.400T - 1.7279x10^{-3}T^{2} \quad (3.8a)$

core $\quad C_{pg(c)} = 299.8 + 5.4037T - 1.60x10^{-3}T^{2} \quad (3.8b)$

The first term on the right-hand side of Eq. (3.1) relates to heat conduction through the skins and core. The second term defines the convection cooling effect from decomposition gases flowing through the skins and core towards the fire. The last term is the endothermic decomposition term that defines the decomposition reaction rate of the face skins or core, which is assumed to be endothermic. By solving Eq. (3.1) for

increasing temperature and time ($\partial T / \partial t$) through the finite difference method, it is possible to calculate the temperature at any time and location in the sandwich composite. The decomposition reaction rate of the skins and core is expressed in the last term of Eq. (3.1) by the mass loss rate ($\partial M / \partial t$). When the skins and core decompose via a single-stage reaction process then $\partial M / \partial t$ is calculated using the first-order Arrhenius relationship:

$$\frac{\partial M}{\partial t} = -AM_o\left(\frac{M - M_f}{M_o}\right)e^{(-E_a/RT)} \qquad (3.9)$$

where A and E_a are the rate constant and activation energy of the endothermic reaction, respectively. R is the universal gas constant. M, M_f and M_o represent the instantaneous mass during decomposition, final mass, and the original mass, respectively. (M_f = 0 for the balsa core). The change to the densities of the face skins and core during decomposition are calculated using this expression. The density of the skins (ρ_s) is calculated using rule-of-mixtures, in which the glass fibres are assumed to be thermally inert.

The thermal boundary condition applied to the hot skin is assumed to be a constant thermal flux. The model can consider any thermal boundary condition for the cold face. In this study the surface of the back skin is assumed to be partially insulated.

The thermal model makes two important assumptions about the thermal behaviour of sandwich composites in fire. Firstly, the model is a one-dimensional equation that only analyses conductive heat transfer and mass transport of decomposition gases in the through-thickness (x) direction (as indicated in Figure 3.1). Multi-directional heat conduction in the lateral and transverse directions are not considered. Secondly, it is assumed that heat-induced delaminations, skin-core interfacial cracking and other types of damage to the sandwich composite due to decomposition and failure processes do not accelerate the mass flux of gases, although this assumption will be revisited later in this chapter.

3.2.3 Tension Mechanical Model for Sandwich Composite

Mechanical models are used to calculate reductions in tension stiffness and strength of the skins and core as the temperature rises in the through-thickness direction of the sandwich composite, which is determined using the thermal model. The current models account for the unsymmetrical stiffness loss to the front skin, balsa core and back skin as thermal softening and decomposition occurs non-uniformly through the sandwich composite due to the non-uniform temperature gradient. This affects the stress distribution within the sandwich material assuming that the skins and core experience the same tensile strain under the applied load.

Assuming the two face skins and core experience the same strain under tension loading, then the following stress distributions for the three material constituents are derived:

$$\sigma_{s1} = \frac{E_{s1}F}{A_s\left(E_{s1}+E_{s2}\right)+A_cE_c},\ \sigma_{s2} = \frac{E_{s2}F}{A_s\left(E_{s1}+E_{s2}\right)+A_cE_c} \text{ and } \sigma_c = \frac{E_cF}{A_s\left(E_{s1}+E_{s2}\right)+A_cE_c} \tag{3.10}$$

where '*s1*', '*s2*' and '*c*' denote the front (heated) skin, back skin and core, respectively. A_s and A_c are the load-bearing areas of a single skin and core, respectively. *F* is the applied tension load and E is the elastic modulus.

Tension Stiffness Modelling

Losses to the tensile stiffness need to be evaluated for the skins and core to calculate the stress distribution through-the-thickness of the sandwich composite. The stiffness loss of the face skins (E_{s1}, E_{s2}) is due mostly to plastic straightening of the crimped load-bearing (0°) tows in the woven glass fabric caused by thermal softening of the polymer matrix. The tows in the woven fabric are wavy due to the interlaced weave of the warp and weft yarns. The tows will attempt to straighten in the tensile load direction, although this is dependent on plastic deformation of the polymer matrix. The yield stress of the polymer decreases with increasing temperature thereby allowing plastic tow straightening.

The Young's modulus of the skins is related to the temperature via the phenomenological expression [4]:

$$E_s(T) = \frac{E_{s0} + E_{sR}}{2} - \frac{E_{s0} - E_{sR}}{2} \tanh\left(k_m\left(T - T_k\right)\right) \qquad (3.11)$$

where E_{s0} is the original Young's modulus of the skin at room temperature. E_{sR} is the skin modulus when the polymer matrix has fully softened at elevated temperature. k_m and T_k are parameters related to the softening behaviour of the skin, which are fitted to experimental Young's modulus-temperature data. Upon complete softening of the polymer matrix, the tension modulus is typically 50-70% lower than the original stiffness.

Goodrich et al. [78] investigated the high temperature properties and softening behaviour of balsa wood. Balsa is the core material used in this study to validate the thermal-mechanical model. Goodrich and colleagues found experimentally the elastic modulus of balsa is related to the temperature via the empirically-derived linear equation:

$$E_c(T) = E_{c0} - (\phi_E . T) \qquad \text{for } T < 280°C \qquad (3.12)$$

E_{c0} is the elastic modulus of the core at room temperature. Φ_E is a material constant that defines the modulus softening rate, and this must be determined experimentally by elevated temperature tests. This equation is only valid between room temperature and the decomposition temperature of the core material, which for balsa is about 280°C [78]. Above the decomposition temperature, the modulus of balsa is negligible. Balsa is an anisotropic material in which the elastic properties are different in the grain and anti-grain directions. Therefore, the elastic properties of the balsa must be determined for the tension load direction applied to the sandwich composite. In this work, the balsa grains are aligned transverse to the load direction (as indicated in Figure 3.1).

To calculate the bulk elastic softening of the sandwich composite, the reduction to the tensile modulus of the face skins and core is calculated at many locations through-the-

thickness of the sandwich material based on the local temperature at each location (which is calculated using Eq. (3.1)). The average modulus of each skin and the core is then calculated separately by integrating local modulus values over their respective load-bearing area:

$$E_{s,c,av} = \frac{1}{t_1 - t_0} \int_{t_0}^{t_1} E_x(x) dx \qquad (3.13)$$

where the local modulus (E_x) of the skins or core is calculated with Simpson integration (which in this study involved 51 points evenly spaced in the through-thickness direction of the sandwich composite).

Tension Strength Modelling

This section describes the model to calculate the tension strength of the sandwich composite in fire. Reductions to the strength properties of the skins and core are modelled separately. Modelling the high temperature strength of the skins must consider softening of both the polymer matrix and fibre reinforcement, which occurs over different temperature and time regimes. As discussed in Chapter 2, Feih et al. [5] developed a rule-of-mixtures model to calculate the tension strength of a single-skin fibreglass laminate in fire. The model is based on the temperature-dependent matrix strength $\sigma_m(T)$ and temperature and time-dependent fibre strength properties $\sigma_{fb}(T,t)$ via the expression:

$$\sigma(T,t) = \Phi_{LT}(T) V_f \sigma_{fb}(T,t) + (1 - V_f)\sigma_m(T) \quad \text{with} \quad \Phi_{LT}(T) \leq 1 \qquad (3.14)$$

V_f is the volume fraction of load-bearing fibres. Φ_{LT} is the temperature-dependent load transfer factor which defines the efficiency of stress transfer between the fibre reinforcement and matrix phase. The value of Φ_{LT} is unity at room temperature and in that case Eq. (3.14) yields the standard rule-of-mixtures for laminates. Load transfer between the fibres and matrix is reduced once the polymer starts to soften, and is assumed to reach a minimum value upon complete softening. The minimum value of Φ_{LT} is determined by elevated temperature testing of the laminate skins under tension loading.

The matrix strength may be considered as temperature-dependent only for fast heating times when visco-elastic-plastic deformation can be ignored. The matrix strength is dependent on the temperature according to [5]:

$$\sigma_m(T) = \frac{\sigma_{m(0)} + \sigma_{m(R)}}{2} - \frac{\sigma_{m(0)} - \sigma_{m(R)}}{2} \tanh\left(k_m\left(T - T_k\right)\right) \quad (3.15)$$

The fitting parameters k_m and T_k are generally similar to those fitted in Eq. (3.11).

The fibre strength is dependent on the temperature and loading time according to [5]:

$$\sigma_{fb}(T,t) = \sigma_{fb(0)} - \sigma_{\text{loss}}(T) \tanh\left\lfloor k_{fb}(T)t \right\rfloor \quad (3.16)$$

where $\sigma_{fb(0)}$ is the fibre strength at 20°C, $\sigma_{loss}(T)$ describes the steady-state strength reduction at a given heat exposure temperature, and $k_{fb}(T)$ describes the reduction rate in fibre strength as a function of temperature. $k_{fb}(T)$ is determined from the curve-fit temperature function:

$$k_{fb}(T) = k_1 e^{k_2 T} \quad (3.17)$$

where k_1 and k_2 are curve fit constants. $T_{50\%}$ is the temperature at which the fibres lose 50% of their tensile strength for long-term heat exposure. The fibre strength loss is determined using:

$$\sigma_{\text{loss}}(T) = \frac{\sigma_{fb(0)}}{2} + \frac{\sigma_{fb(0)} \tanh\left\lfloor p_{fb}(T - T_{50\%}) \right\rfloor}{2} \quad (3.18)$$

with $T_{50\%}$ and p_{fb} being curve-fit constants.

The reduction to the tension strength of the balsa core is linearly related to the temperature according to [78]:

$$\sigma_c(T) = \sigma_{c0} - (\phi_\sigma . T) \qquad \text{for } T < 280°C \tag{3.19}$$

$\sigma_{c(0)}$ is the core strength at room temperature and Φ_σ defines the linear strength loss rate up to the decomposition temperature of balsa. Above this temperature, the tensile strength of balsa is negligible.

The average tension strength of the sandwich composite is then calculated by integrating the strength values of the two face skins and the core over their respective load-bearing area:

$$\sigma_{s,c,av} = \frac{1}{t_1 - t_0} \int_{t_0}^{t_1} \sigma_x(x) dx \tag{3.20}$$

where the local tensile strength (σ_x) of the skins or core is calculated with Simpson integration.

The averaging approach for tension modulus and strength of skins and core neglects progressive failure events. However, the model considers that failure of one material will influence failure of the other parts; upon first failure of either skin or core then the applied load is redistributed and increases in the other materials. If the applied load is sufficiently low to be carried by the remaining materials, separate failure events may occur.

3.3 MATERIALS AND FIRE STRUCTURAL TESTING

3.3.1 Sandwich Composite

The thermal-mechanical model was validated and its accuracy assessed using experimental data for a sandwich composite with flammable face skins and core. The laminate face skins to the sandwich composite were manufactured from E-glass plain woven fabric (800 g/m^2, Colan Industries) and vinyl ester resin (Derakane 411-350). The resin did not contain flame retardant fillers or additives, and had a glass transition temperature (T_g) of 120°C. The T_g value was measured by Feih et al. [5] using differential scanning calorimetry (DSC). The skins had a fibre volume fraction of 0.44 measured from burn-off test. The core material was Baltek® SB structural end-grain balsa (ρ_c = 150 kg/m^3). The balsa was supplied as flat sheets composed of rectangular blocks bonded with a thin film of adhesive. The rectangular blocks of balsa comes in different arrangements as shown in Figure 3.2. The sizes of the blocks ranged from 50 by 25 mm to 100 by 70 mm, and were bonded together with an adhesive into flat sheets with a thickness of 6 mm. The balsa grains were aligned in the through-thickness direction of the sandwich composite, which is normal to the direction of tension loading (as indicated in Figure 3.3).

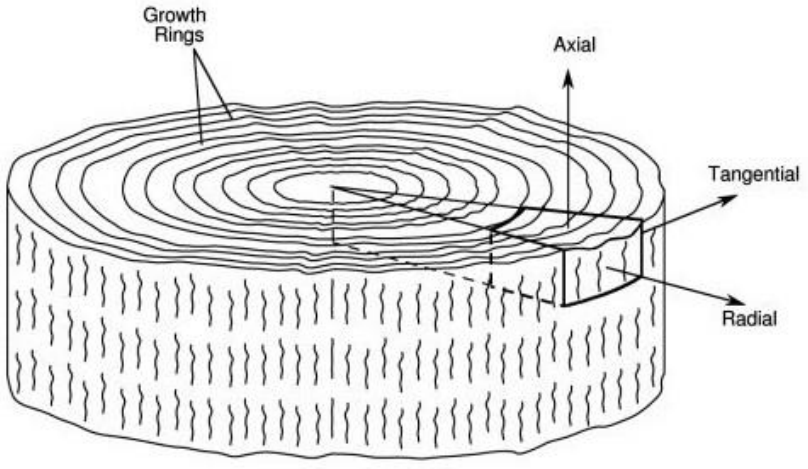

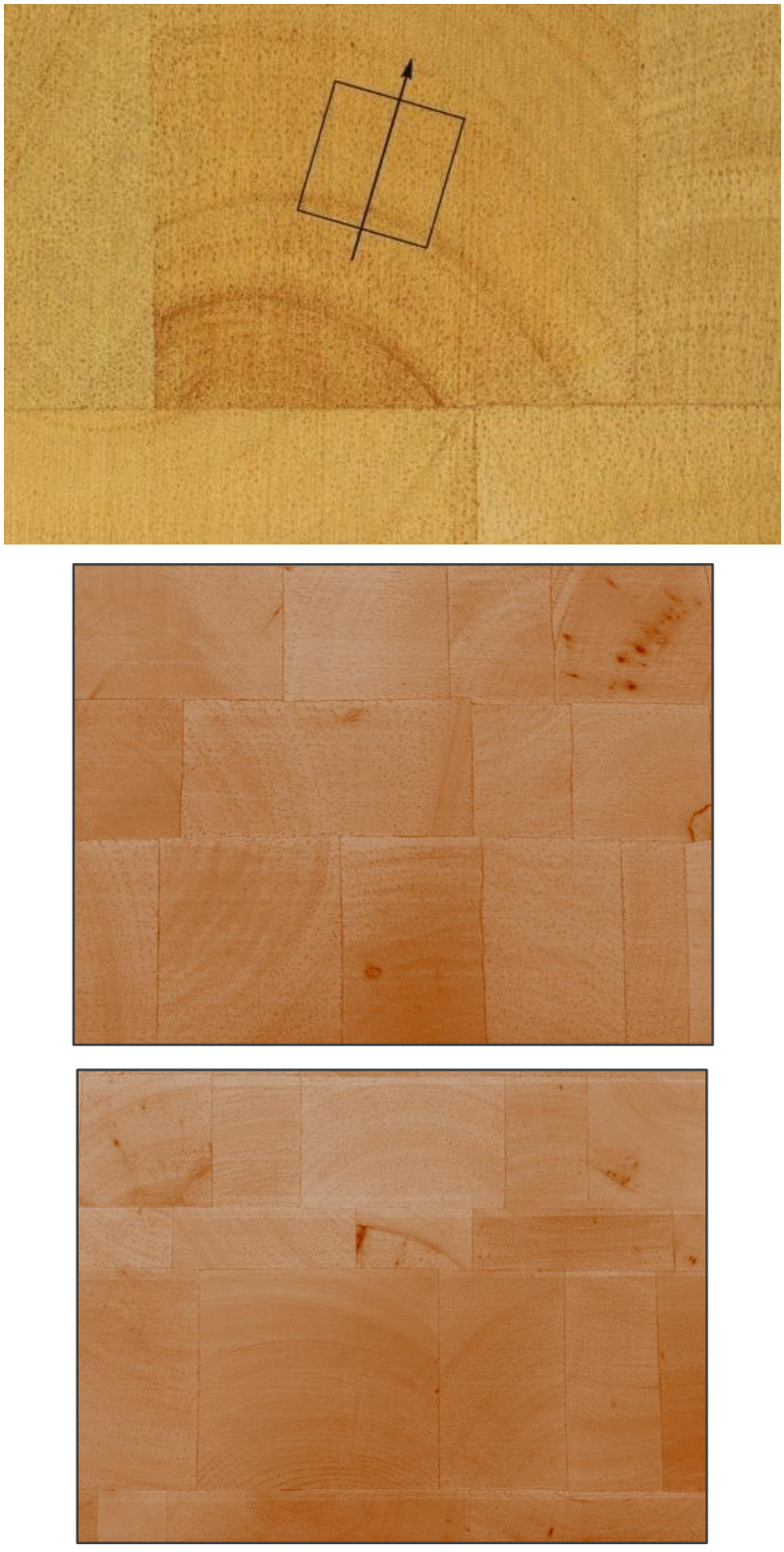

Figure 3.2: Arrangement of balsa blocks bonded into sheets. The direction of the balsa grains was along the radial direction, as indicated [79].

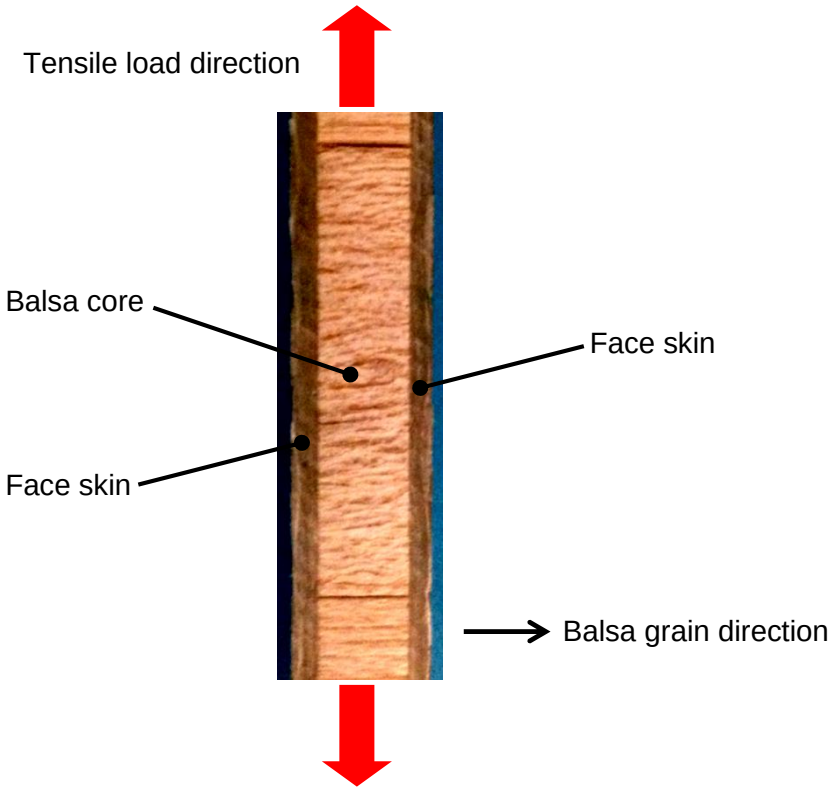

Figure 3.3: Through-thickness balsa grain alignment in sandwich composite (normal to the direction of tensile load).

Previous work by Feih et al. [3, 5], fabricated the composite specimens using the vacuum-bag resin infusion process. In this research, stages to manufacture the sandwich composite are shown sequentially as Figure 3.4. Firstly, the surfaces to the balsa core were sealed with a thin layer of vinyl ester (Fig 3.4a). Sealing was necessary to minimise excessive resin absorption from the uncured skins. One of the laminate skins was laid-up on the core (Fig 3.4b) and the core with end blocks of laminate were consolidated with the laid-up skin (Fig 3.4c). The panel was then consolidated under the pressure applied using a vacuum bag (Fig 3.4f). After the face skin had cured at room temperature for at least one day, the second skin was laid-up and also consolidated and cured under the vacuum bag (repeated similar to process in Fig. 3.4b to 3.4f). The completed sandwich composite was then post-cured in the oven for two hours at 80^{o}C.

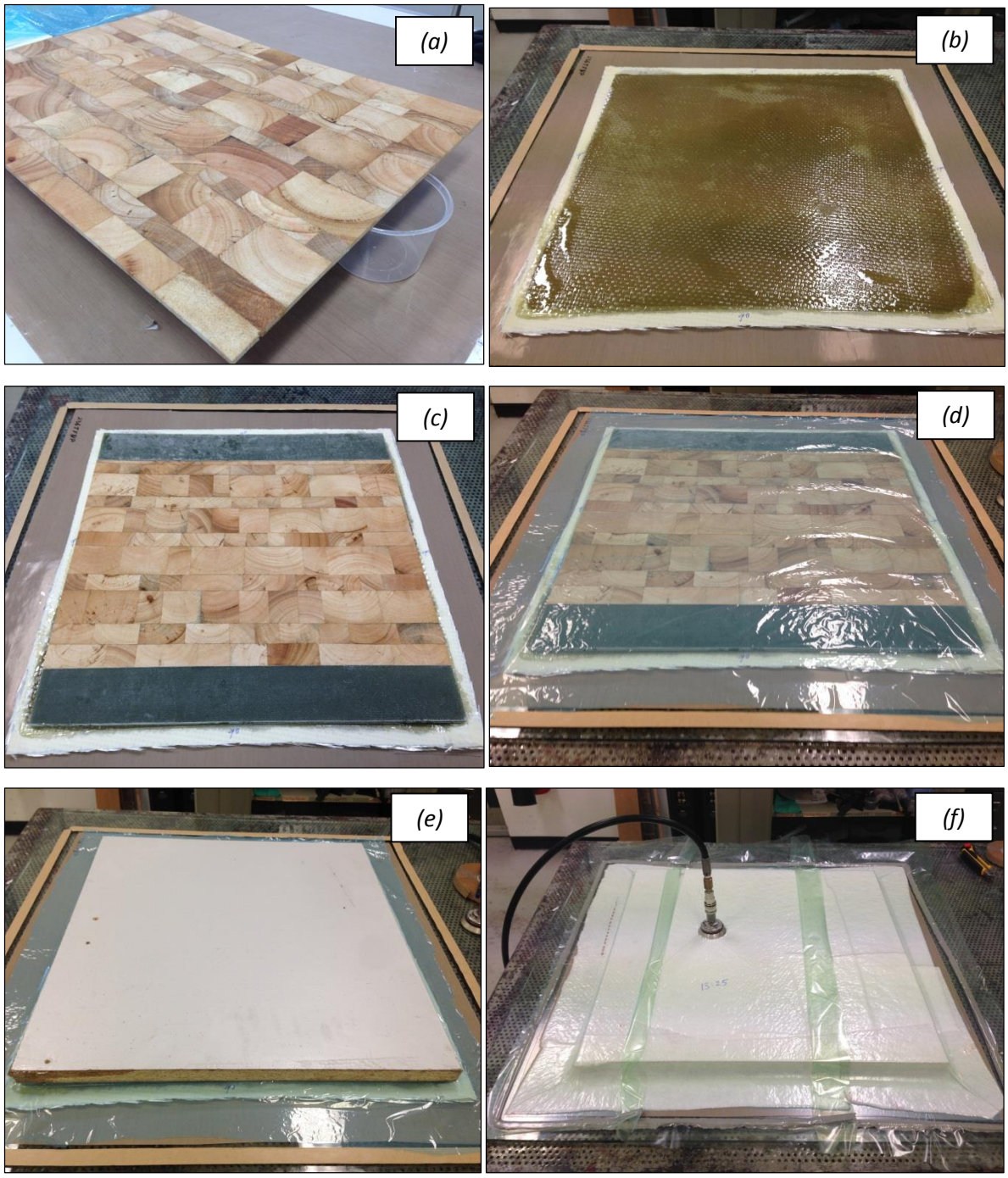

Figure 3.4: Sandwich composite manufacturing process. (a) Sealing of the core. (b) First skin wet lay-up. (c) Cured balsa with laminate inserts placed onto the first skin. (d) Release film placement. (e) Caul plate placement. (f) Complete vacuum-bag installation.

The geometry and dimensions of the sandwich specimens used for fire structural testing is shown in Figure 3.5. The specimens were cut from a larger panel using a CNC router. The middle section of the specimen consists of the sandwich composite with 1.7 mm thick laminate skins and 6 mm thick balsa core. Solid laminate was used to replace the balsa core over a length of 80 mm at both ends of the specimen to avoid core crushing in the pressure grips of the tensile loading machine (Fig 3.5b). Laminate tabs were bonded to the specimen ends to achieve a uniform strain distribution across the solid core/balsa interface. Tensile test was then performed axially on the sandwich composite specimen at room temperature to determine the ultimate strength using a 250 kN MTS mechanical test machine. The sandwich specimen failed due to fibre rupture at the gauge section with 230 MPa ultimate tensile stress.

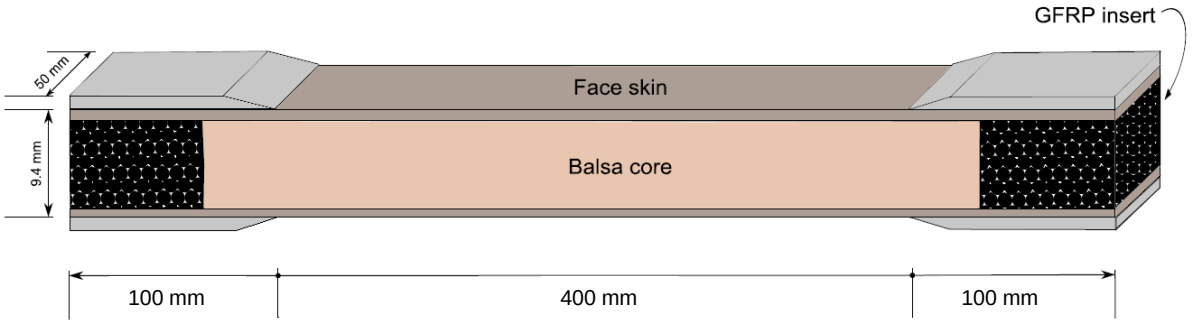

(a)

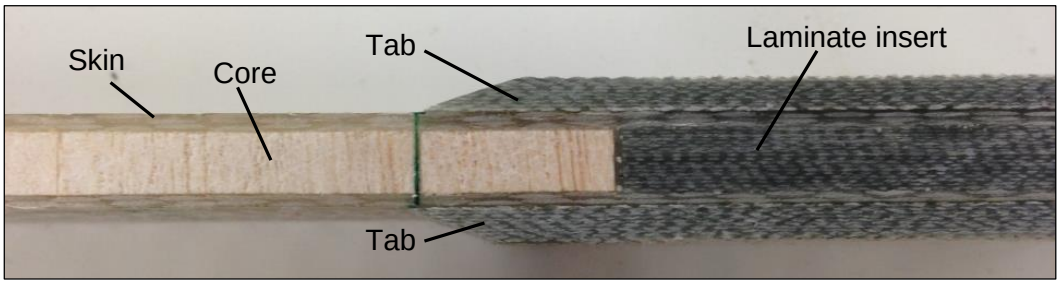

(b)

Figure 3.5: (a) Geometry and dimensions of the fire structural test specimen. (b) Close-up view of laminate core and end tabs which was inserted into the grips of the loading machine to avoid crushing of the balsa core.

3.3.2 Fire Structural Tests

Small-scale fire structural tests were performed on the sandwich composite to obtain experimental data on the failure times and failure modes to validate the model. The test involved pre-loading the sandwich specimen in tension while simultaneously heating one side using a radiant heater. In the test, a constant tension stress between 10% and 90% of the ultimate strength at room temperature (which was 230 MPa) was applied to the sandwich specimen using a 250 kN MTS mechanical test machine, as shown in Figure 3.6. The machine was thermally protected with insulation and it was fitted with an exhaust hood to remove fumes and smoke released by the sandwich composite. During testing, the ends of the sandwich specimen were constrained by rigid clamping within the wedge grips to the loading machine.

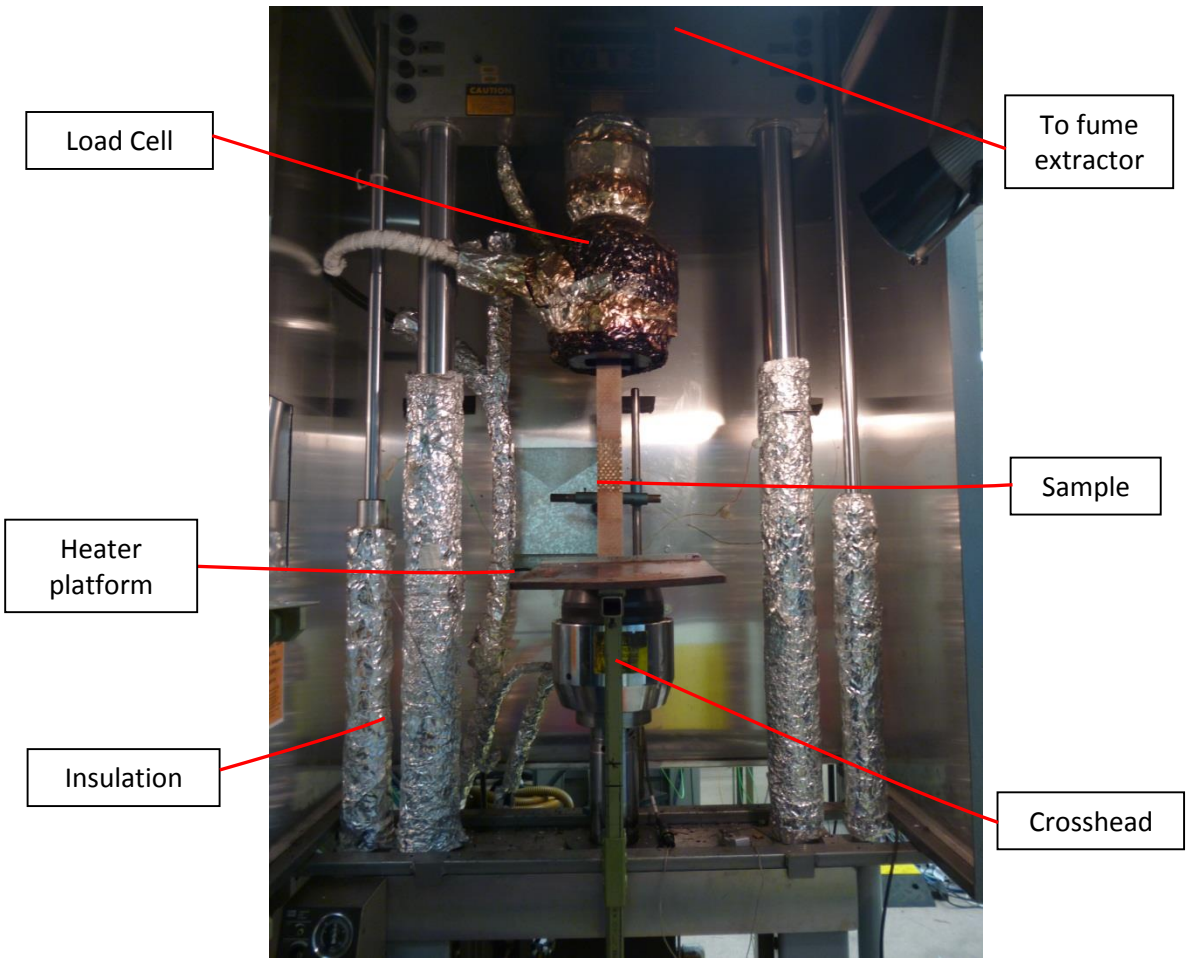

Figure 3.6: MTS 250kN machine used for fire structural testing of the sandwich composite.

While under load, the front skin was exposed directly to an electric heater that radiated constant heat fluxes of 25, 35 or 50 kW/m^2. The radiant heater used in the tests is shown in Figure 3.7. This is the same type of heater used in cone calorimeters. The heater was circular with an external diameter of 150 mm. The heat flux was controlled within 1 kW/m^2 by adjusting the electrical current into the heating element. The heater and sandwich specimen were spaced 25 mm apart and aligned parallel in the load direction as shown in Figure 3.8. The specimen was centrally heated over a length of 100 mm, while outside of this region the material was thermally insulated with a ceramic fibre mat as shown in Figure 3.9. The surface temperatures of the two face skins were recorded continuously using K-thermocouples (with standard limit of error about 0.75%) during testing. The specimens were free to thermally expand during heat exposure (constant load). The elongation of the sandwich composite was monitored continuously during testing by the change in the separation between the cross-heads of the loading machine. Fire-under-load tests were performed until the specimen failed, and the heating time taken for the specimen to rupture, called the time-to-failure, was measured. Two specimens for each loading condition and heat flux were tested in the fire structural test. Due to the design of the fire structural test facility is was not possible to accurately measure the strains induced to the sandwich composite specimens. The heated surface of the specimen was masked by the heater and the back surface was masked by the smoke hood, making it impossible to measure the strains. The axial displacement were measured through the test, but it was not possible to translate this into strain

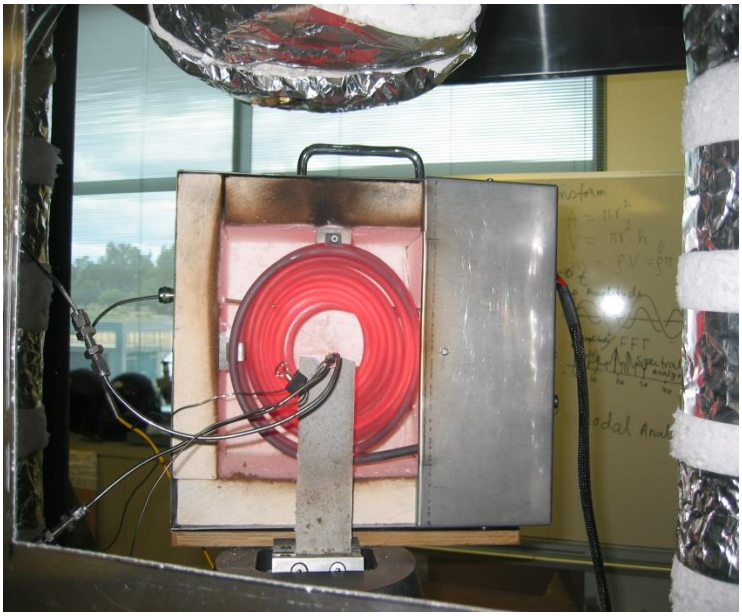

Figure 3.7: Cone heater used to generate the radiant heat flux applied to the sandwich composite. The circular heating element is enclosed within an insulated box.

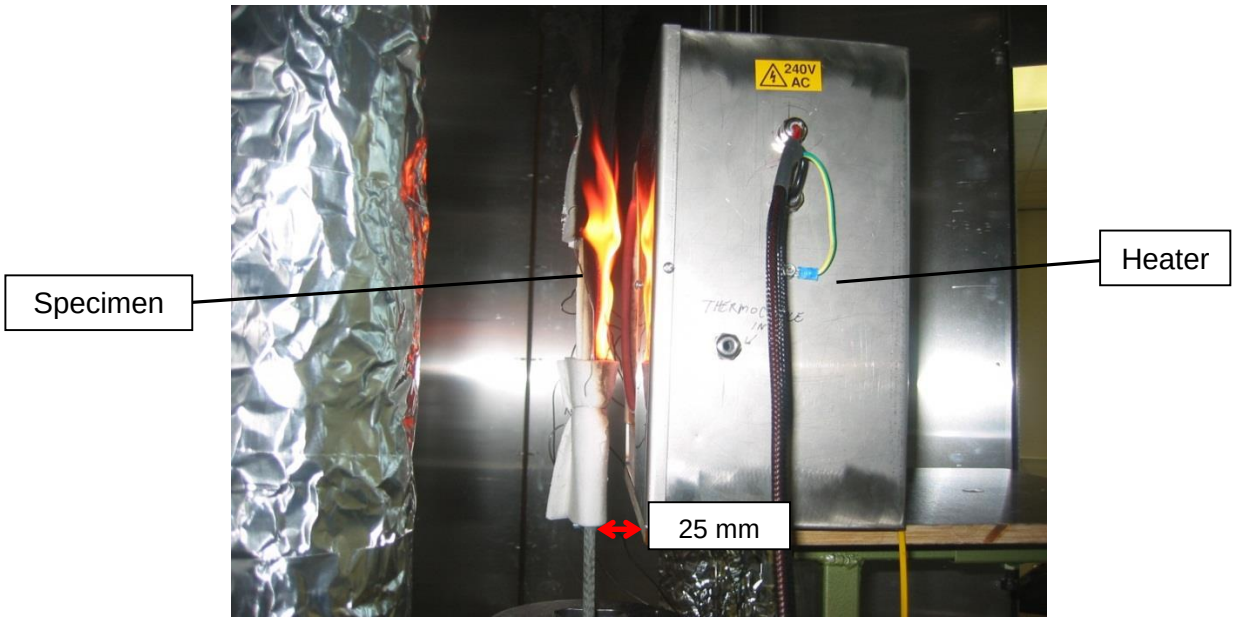

Figure 3.8: Side-view of a fire structural test with the composite sample and heater on the left hand and right hand sides, respectively.

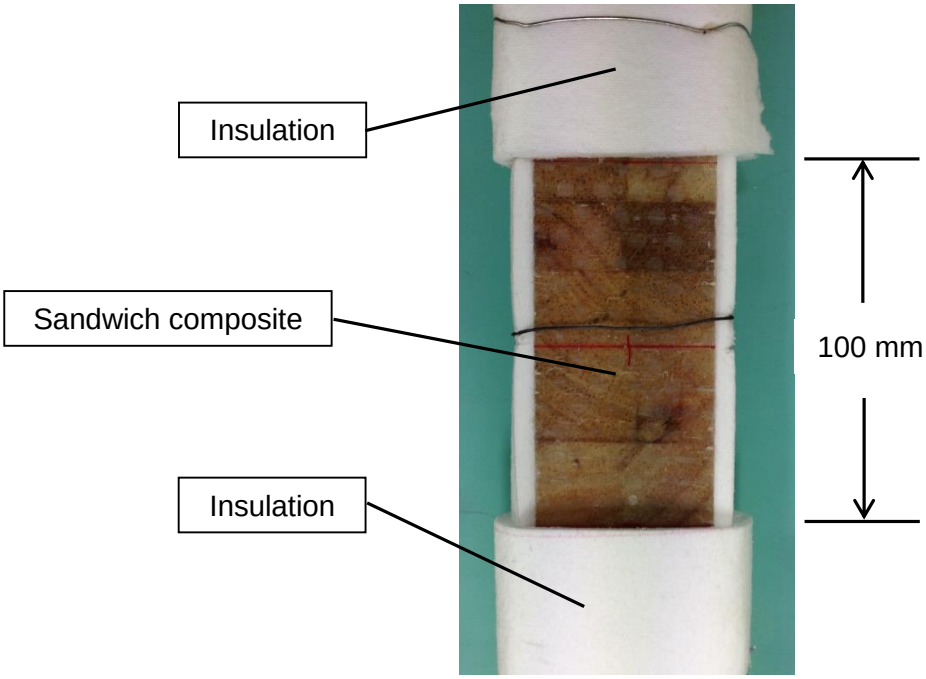

Figure 3.9: Central region of the sandwich composite specimen that was exposed directly to the heat flux.

3.3.3 Elevated Temperature Tests

The tensile properties of the laminate face skins and balsa core materials were measured at elevated temperature. This property data is needed to solve the mechanical component of the model described earlier to analyse the fire structural response of sandwich composites. The elevated temperature tests were performed using a 100kN MTS testing machine with a heating cartridge as shown in Figure 3.10. Samples measuring 150 mm long by 25 mm wide were tensile tested at different temperatures between room temperature and 300^{o}C. Two samples were tested at each temperature. While at elevated temperature, the sample was loaded at a constant extension rate of 1 mm/min until failure. A 100 mm extensometer was attached to the sample to measure the strain, and from this the tensile modulus was determined. The failure stress was determined from the maximum breaking force applied to the sample.

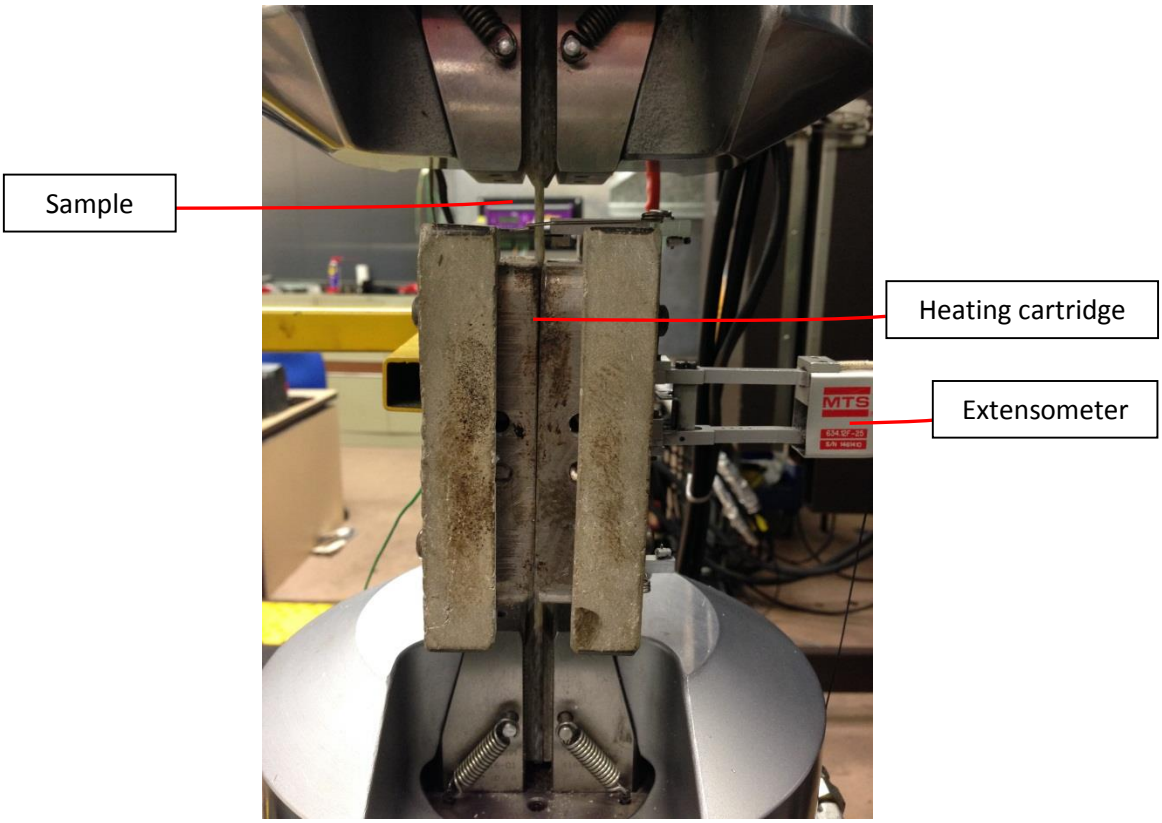

Figure 3.10: Elevated temperature test on 100 kN MTS with heating cartridge.

3.4 RESULTS AND DISCUSSION

3.4.1 Thermal Response of Sandwich Composite in Fire

3.4.1.1 Thermal Response of Unloaded Sandwich Composite

The accuracy of the thermal model (described in Section 3.2.2) in the calculation of temperatures at the surfaces and within the sandwich composite was assessed using temperature data obtained from fire structural tests performed at the heat fluxes of 25, 35 and 50 kW/m^2. Thermocouples were located on the hot and cold surfaces as well as the mid-thickness point of the sandwich composite to experimentally measure the temperatures. Figure 3.11 presents two sets of temperature-time profiles measured at three locations in the sandwich composite when exposed to the heat flux of 25 kW/m^2. These profiles were measured when the sandwich composite was unloaded. The repeatability of the measured temperatures is reasonably good. The variance in the

measured temperatures at the three locations was typically less than 20°C based on two measurements. Variations in the temperatures are expected due to the stochastic nature of some of the processes controlling heat transfer through the material, such as delamination cracking and skin-core interfacial debonding.

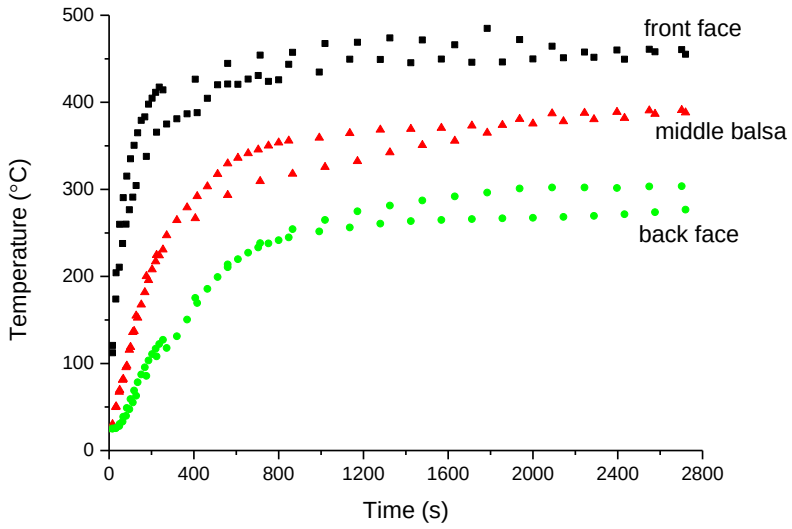

Figure 3.11: Two sets of measured temperature-time profiles for the sandwich composite exposed to the heat flux of 25 kW/m^2. The sandwich composite was not under load when the temperatures were measured.

Figure 3.11 shows that the temperature at the front face skin of the sandwich composite exposed directly to the heat flux increased rapidly with time over the initial 500-800 second heating period. Beyond this period the front surface reached a quasi-steady state maximum temperature. The maximum temperatures at the front surface reached about 400, 530 and 630°C when exposed to the heat fluxes of 25, 35 and 50 kW/m^2, respectively. Regardless of the heat flux, there was a steep thermal gradient through-the-thickness of the sandwich composite. The temperature of the front skin was typically around 200°C hotter than the back skin, and this was due to the high thermal insulating properties of both the skins and, in particular, the balsa core.

Figure 3.12 compares the measured and calculated temperature-time profiles for the sandwich composite when exposed to the heat fluxes of 25, 35 and 50 kW/m^2. The data

points and solid lines show respectively the measured and calculated temperature profiles at the heated (front) face skin, middle of the balsa core, and unheated (back) skin of the composite. Temperature profiles were measured at the different test heat flux levels through the sandwich composites and were determined for the unloaded condition. The temperature profiles were calculated with the thermal model (Eqn. 3.1) using thermal and physical property data for the laminate skins and core given in Table 3.1.

Figure 3.12 shows that the thermal model was capable of approximating the measured temperature profiles for the different heat fluxes. Ignition and flaming combustion of the sandwich composite did not occur at the heat fluxes of 25 and 35 kW/m^2, and therefore the temperature rise was due to heat conduction from the heater into the material which was opposed by endothermic decomposition of the polymer matrix to the face skins and the balsa core (which had a cooling effect) and by out-flow of decomposition gases such as CO, CO_2, H_2O and low molecular weight hydrocarbon compounds (which also had a cooling effect). At the highest heat flux of 50 kW/m^2 the balsa core (but not the face skins) ignited during testing (at the time indicated in Figure 3.12c). Ignition caused the core temperature to rise rapidly (rather than reach a steady-state temperature) due to combustion of flammable gas released during decomposition of the balsa. This internal ignition was incorporated into the thermal analysis via an increase to the external heat flux at the onset of ignition.

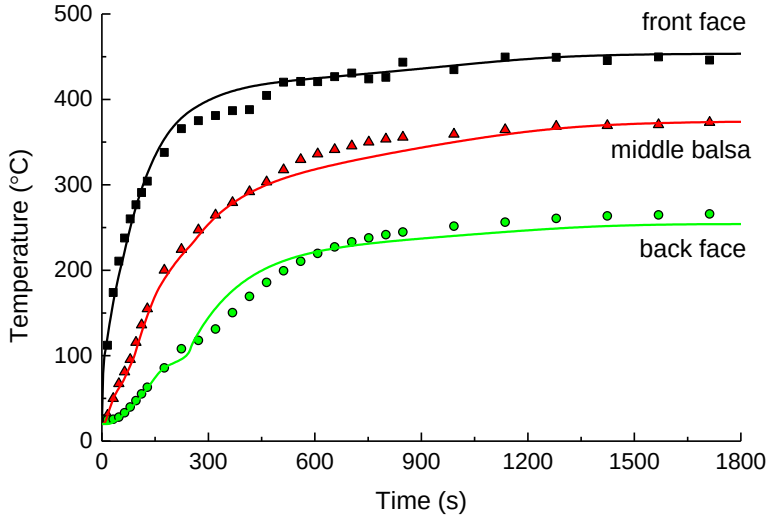
front face
middle balsa
back face
Temperature (°C)
Time (s)
0
100
200
300
400
500
0
300
600
900
1200
1500
1800

(a)

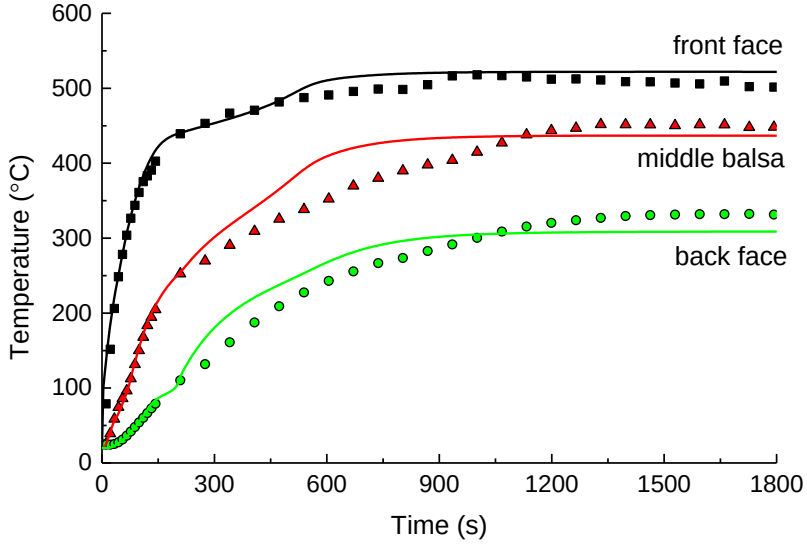
front face
middle balsa
back face
Temperature (°C)
Time (s)
0
100
200
300
400
500
600
0
300
600
900
1200
1500
1800

(b)

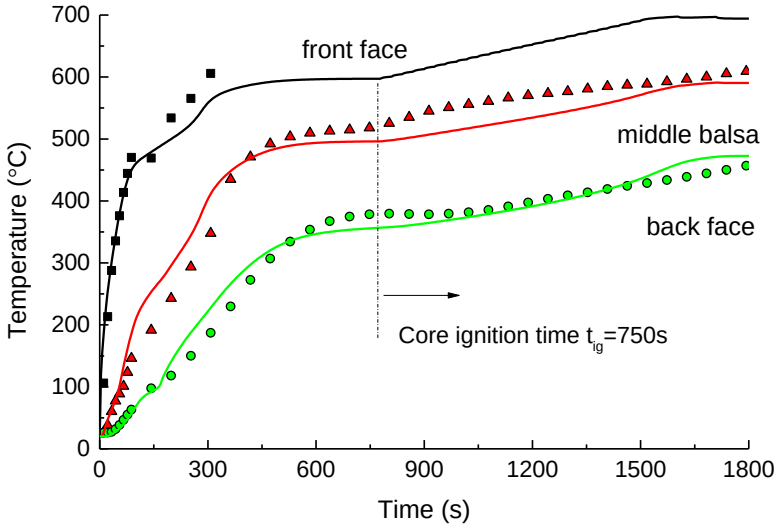

(c)

Figure 3.12: Temperature-time profiles at the front (heated) face skin, middle of the balsa core and back face skin of the sandwich composite (without tension pre-load) exposed to the heat flux of (a) 25, (b) 35 and (c) 50 kW/m^2. The curves and data points are the calculated and measured temperatures, respectively.

Table 3.1: Parameters for thermal model

Property	Skin	Core	Source
Rate constant [1/s]	5.6 x 10^{13}	6.7 x 10^{7}	[3]
Activation energy [J/mol]	212705	116488	[3]
Heat of decomposition [J/kg]	378800	556000	[3]
Specific heat of glass/vinyl ester [J/(kg K)] (140ºC)	890+2.4T-0.003T^2	1420 + 0.68T	[3]
Specific heat of char [J/(kg K)]	890+2.4T-0.003T^2	3194 + 1.33T	[3]
Specific heat of gas [J/(kg K)]	2387	1009	[3]
Thermal conductivity of virgin [W/(m K)] (60-300ºC)	0.2	0.2	[3]
Thermal conductivity of char [W/(m K)] (300-500ºC)	0.4	0.008 + 2.22e^{-6} x T$^{1.89}$	[3]
Density [kg/m^3]	1921	150	[3]
Remaining Resin Mass Fraction [%]	3	15	[3]
Fibre volume fraction	0.44	-	Burn-off test
Moisture content [wt%]	2	8	[3]

3.4.1.2 Thermal Response of Tensile Loaded Sandwich Composite

Measurements of the temperature-time profiles of the sandwich composite while under tension loading revealed that the thermal response was stress-dependent. It was discovered that the temperatures of the core and back face skin were dependent on the applied tension stress. (The front face temperature is affected to a lesser extent as this temperature is determined by the applied heat flux and surface thermal boundary condition). For example, Figure 3.13 shows the effect of tension stress on the temperature-time response measured at the back surface of the sandwich composite. The applied stress is expressed as a percentage of the ultimate strength of the sandwich composite at room temperature. Figure 3.13a shows the applied stress level had little influence on the back face temperature at the lowest heat flux of 25 kW/m^2 for heating times under ~2000 s. Above this time the temperature increased with the applied stress. Similarly, for the heat flux 35 kW/m^2 (figure 3.13b) the temperature initially rises at the same rate for the different applied stress levels until a heating time of about 600 s, at which point the balsa core ignited. Following ignition, the heating rate of the composite increased rapidly with the applied stress. This accelerated heating effect is attributed mostly to heat generated by the balsa core during combustion of hydrocarbon gases produced by the decomposition reaction process. The balsa core becomes heavily cracked as it thermally decomposes. Goodrich et al. [78] found that this cracking process starts at temperatures above ~250°C. These cracks are expected to accelerate the egress rate of flammable gases as indicated in Figures 3.14 and 3.15. Figure 3.15 summarizes the thermal processes in the hot decomposing sandwich composite which includes egress and ignition of flammable volatiles released by the core. It is expected that both the number of cracks and the amount of crack opening in the balsa increased with the applied stress, thereby aiding the gas flow. Cracks in the balsa core are able to open up further once the front or back skin failed. For this reason, higher loads led to significantly higher core and back face temperatures.

The dependence of internal temperature on applied tensile stress for sandwich composites exposed to fire has not been previously reported, and it adds to the complexity of thermal modelling these materials under combined mechanical loading and one-sided

heating. The thermal model presented in section 3.2.2 is unable to accurately calculate the temperature rise for the sandwich composite with increasing applied tensile stress. A model that incorporates this phenomenon needs to be developed, but was not performed as part of this PhD project. Such a model requires full coupling of the mechanical model and the failure modes with the thermal model, and is worthy of further research.

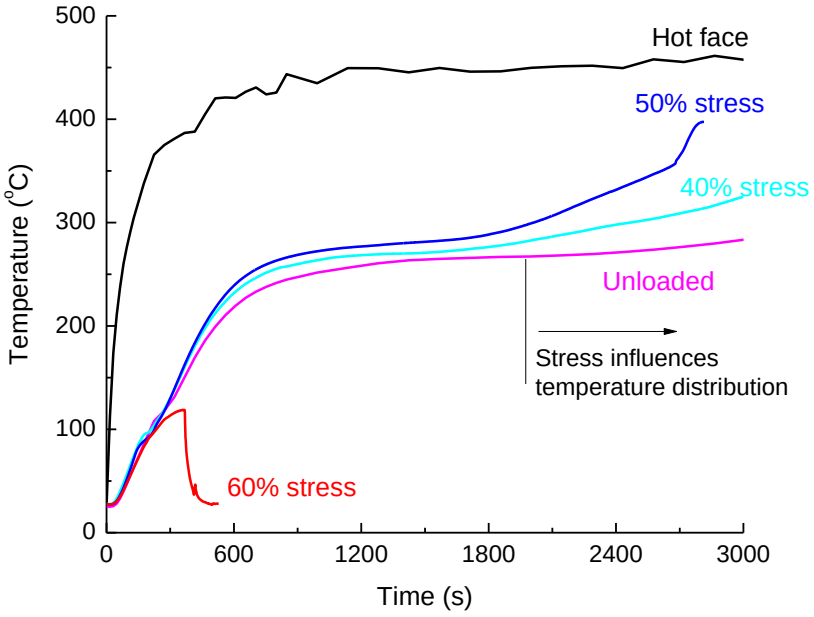

(a)

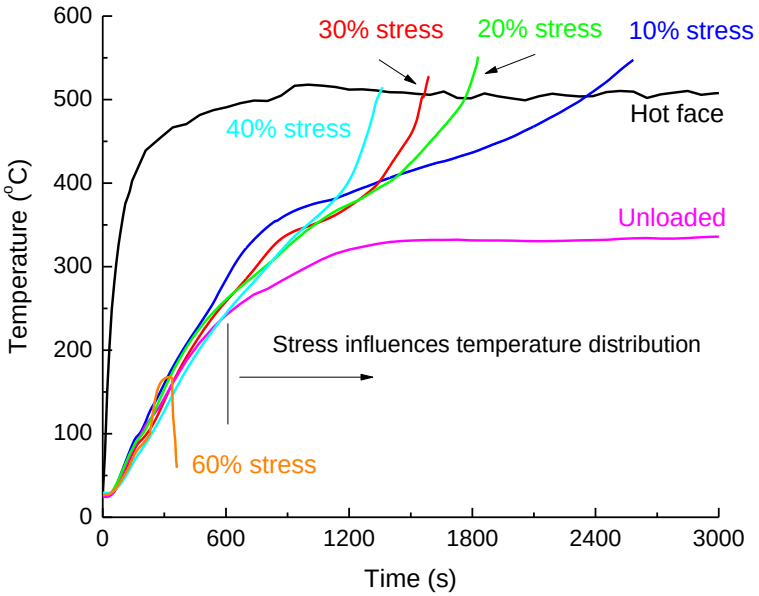

(b)

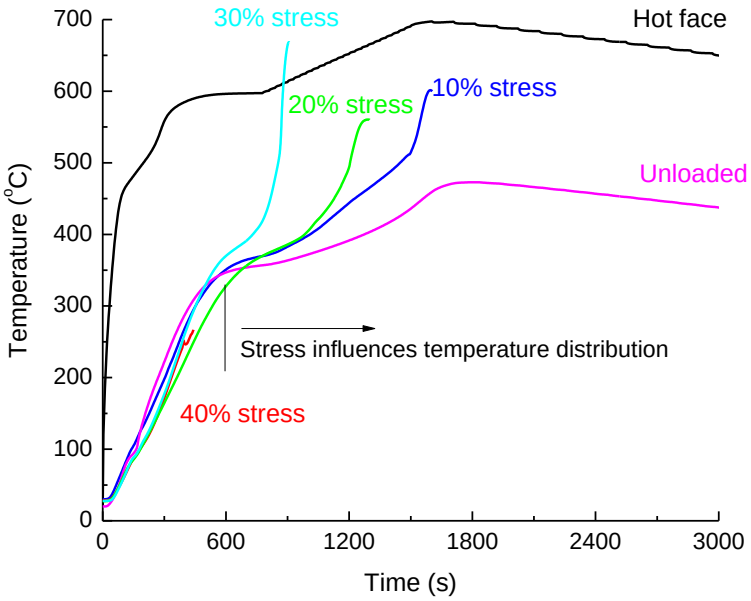

(c)

Figure 3.13: Effect of applied tensile load on the back face temperature of the sandwich composite exposed to the heat flux of (a) 25 kW/m² (b) 35 kW/m² (c) 50 kW/m². The load values are expressed as a percentage of the ultimate tensile strength of the composite.

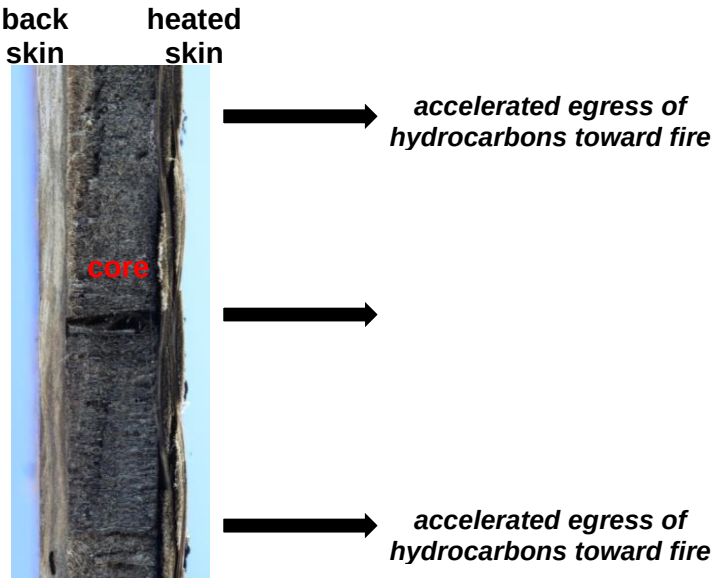

Figure 3.14: Egress of flammable gases from the decomposing balsa core which increases the combustion temperature. Gases flow more rapidly along cracks in the core.

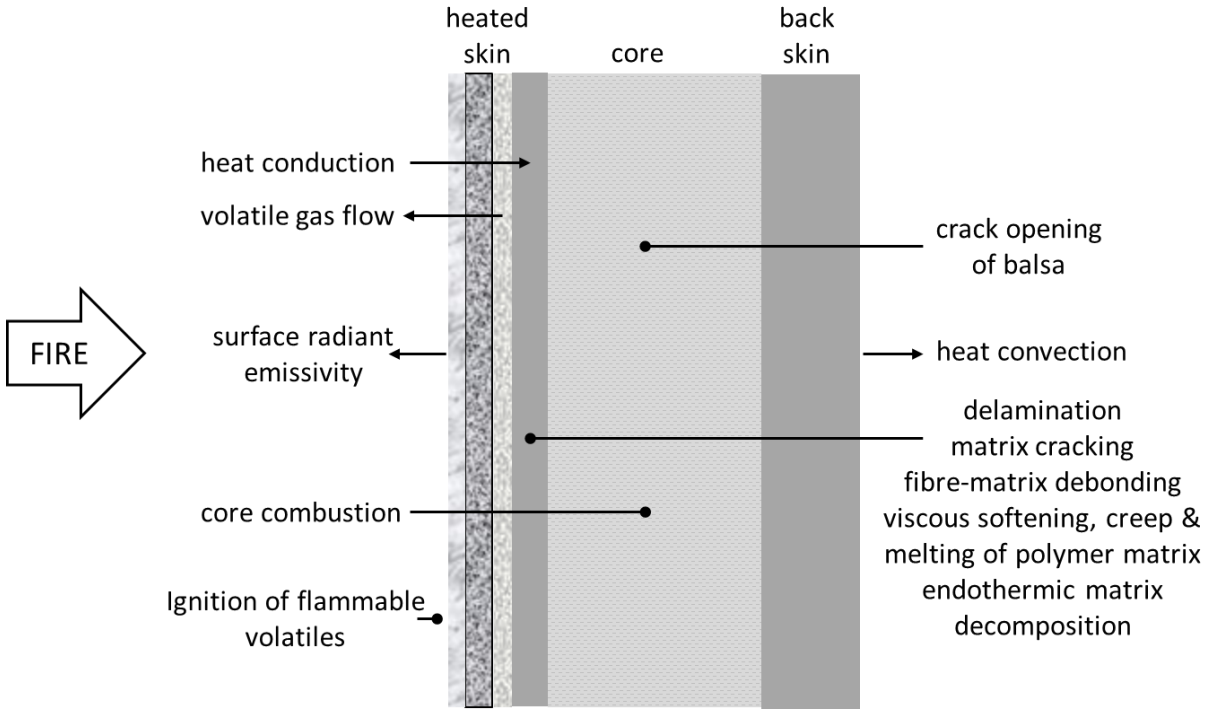

Figure 3.15: Egress and ignition of flammable volatiles for sandwich composite.

3.4.2 High Temperature Properties of Sandwich Composite

The tension strength and elastic modulus as a function of temperature is applied directly to the mechanical model for sandwich composites, as described in Section 3.2.3. Figure 3.16 shows the loss in tensile strength and stiffness due to resin softening for the laminate used for the face skins to the sandwich composite. The stiffness loss is attributed to the straightening of woven fibres as the matrix softens. Strength loss is attributed to the reduction in the stress transfer efficiency between load-bearing fibres as the resin softens. The figure also shows the fitted data curves as described in Equations (3.11) and (3.15).

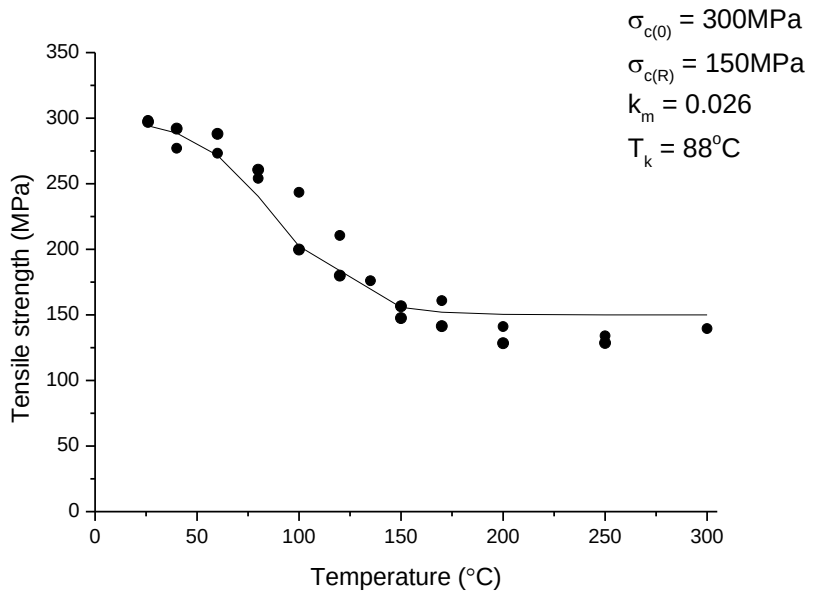

(a)

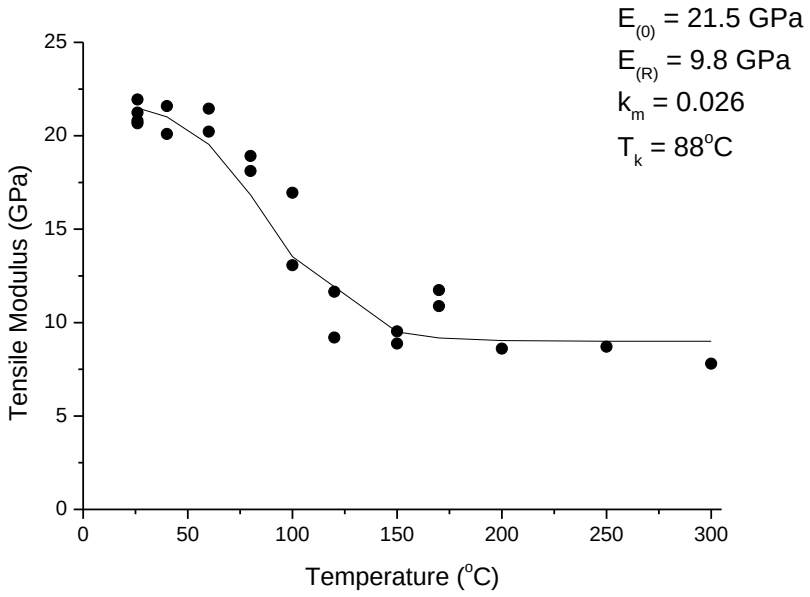

(b)

Figure 3.16: Effect of increasing temperature on the measured (a) tensile strength and (b) tensile modulus of the laminate used for the face skins to the sandwich composite.

The strength and stiffness loss of the end-grain balsa core with increasing temperature is shown in Figure 3.17. Due to the variation of density in balsa core, the room temperature properties are scattered and the failure occurred either in the adhesive bond-line between the balsa blocks or in a low density region of the wood. A steady decline in strength and stiffness with increasing temperature occurred for the balsa core.

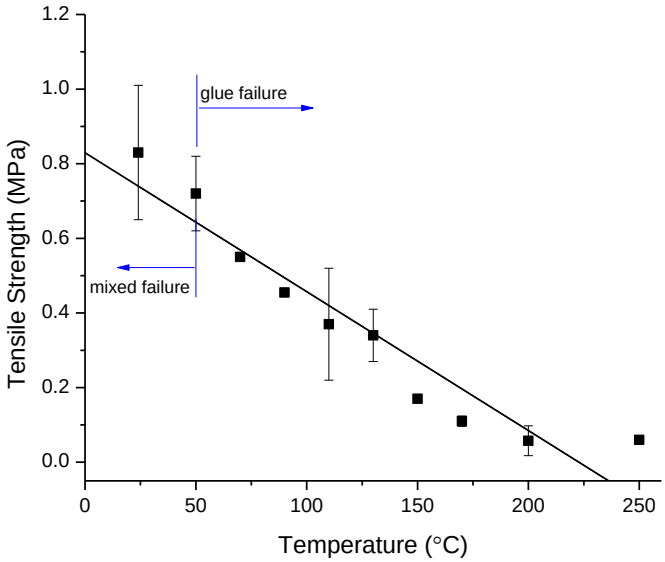

(a)

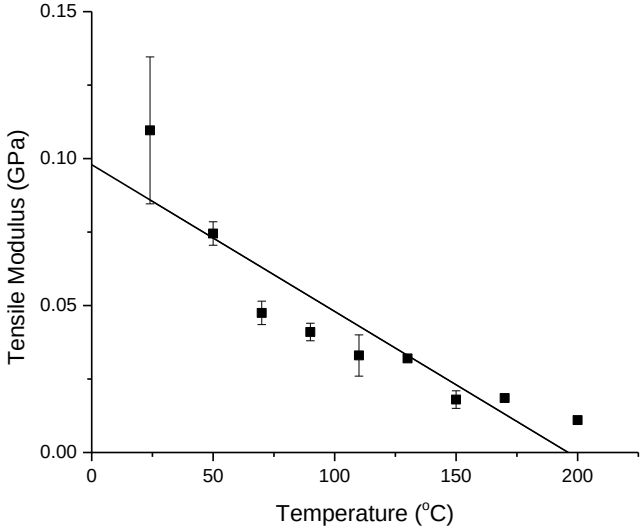

(b)

Figure 3.17: Effect of increasing temperature on the (a) tensile strength and (b) tensile modulus of the balsa core. The error bars indicate one standard deviation.

When modeling the fire structural response of materials it is important to consider the change in the stress-strain response at elevated temperature. Figure 3.18 shows tensile stress-strain curves for the laminate skin measured at temperatures between 20^{o}C and 300^{o}C. As expected, the stiffness and maximum stress decreased and failure strain increased with increasing temperature. However at 60^{o}C, the modulus remain unchanged or slightly higher due to the formation of cross-linking. The curves become increasingly non-linear with increasing temperature, and this is attributed to plastic softening of the polymer matrix close to and above the glass transition temperature. Figure 3.19 shows the tensile stress-strain curves for the balsa core at elevated temperature. As expected, the failure stress and stiffness decreased with increasing temperature.

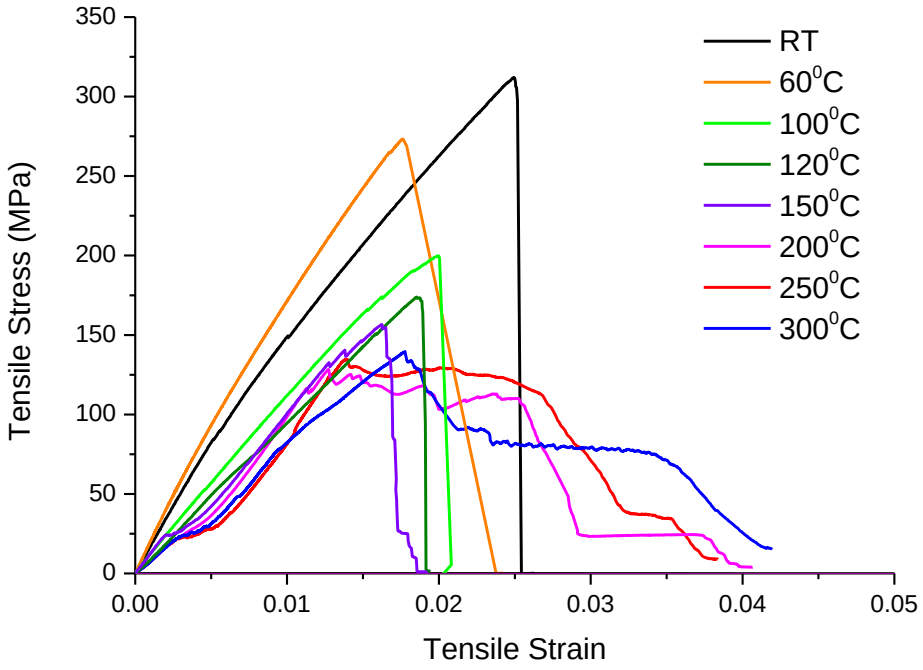

Figure 3.18: Tensile stress vs strain curves for the face skin laminates at different temperatures.

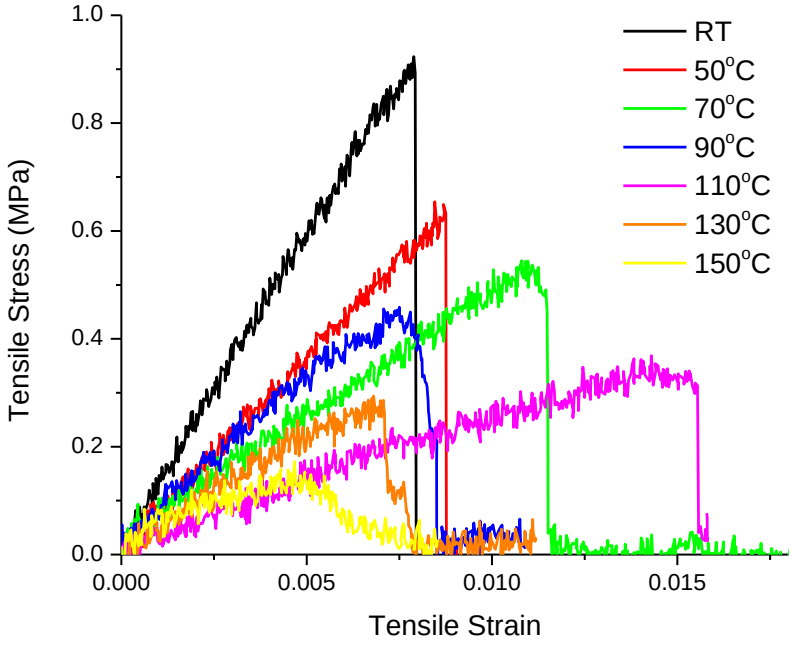

Figure 3.19: Tensile stress vs strain curves for the balsa core at different temperatures.

3.4.3 Tensile Response of Sandwich Composite in Fire

Fire structural testing was performed on the sandwich composite at different applied tensile stress and heat flux levels to obtain experimental data and information to validate the thermal-mechanical model. Figure 3.20 shows the axial displacement-heating time curves measured for the sandwich composite over the course of fire structural tests performed at different load levels and heat fluxes. When the sandwich composite is subjected to a constant tension load, it initially deforms rapidly due mostly to thermal expansion and softening of the front face skin. The deformation rate then slows to a quasi-steady state condition until the displacement rate increases extremely rapidly as the sandwich composite undergoes catastrophic failure. As expected, the displacement increased with time and percentage of applied load. Due to the design of the fire structural test facility is was not possible to accurately measure the strains induced to the sandwich composite specimens. The heated surface of the specimen was masked by the heater and the back surface was masked by the smoke hood, making it impossible to measure

the strains. The axial displacement were measured through the test, but it was not possible to translate this into strain.

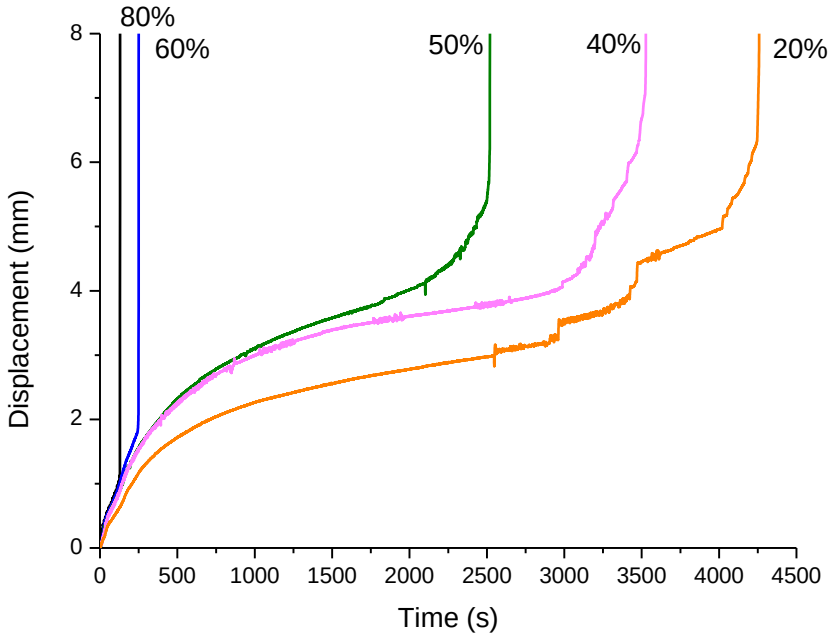

(a)

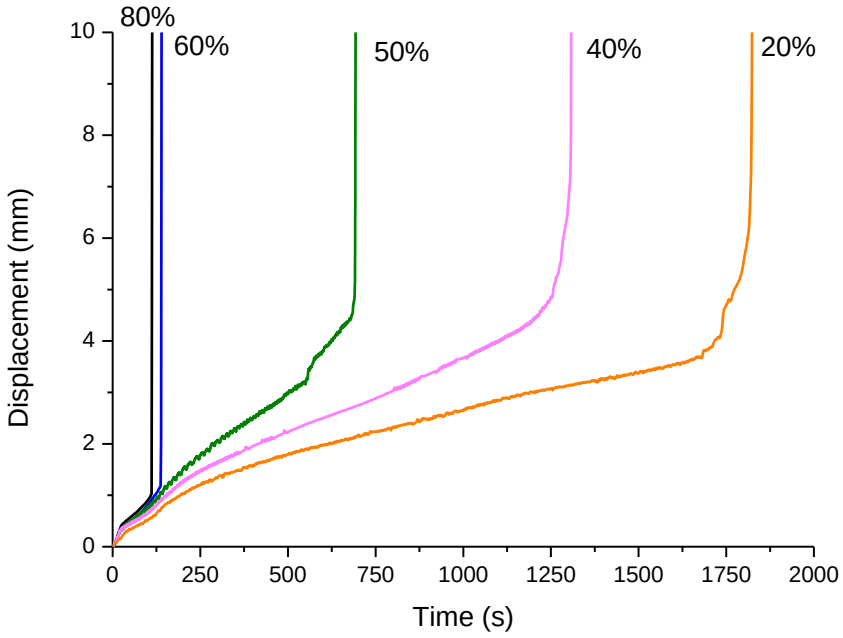

(b)

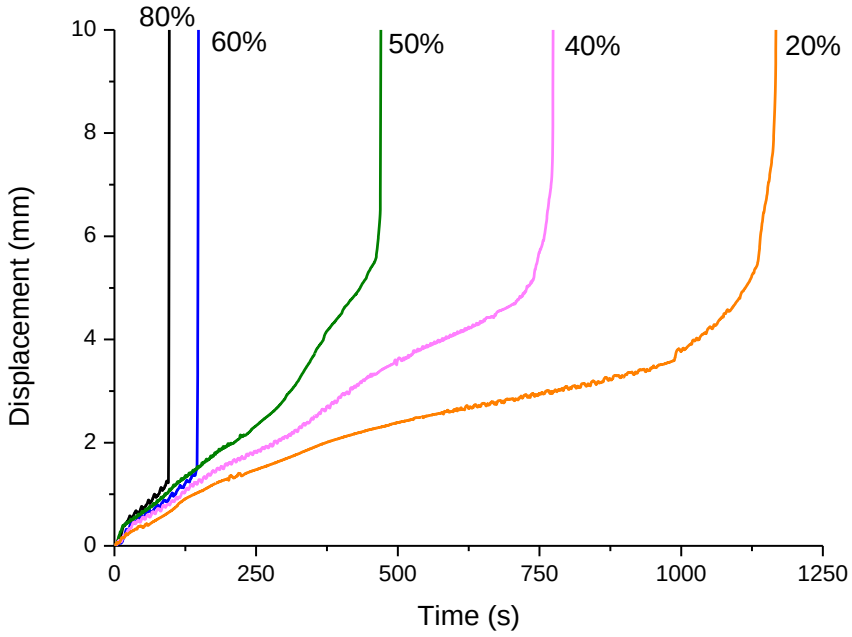

(c)

Figure 3.20: Experimental axial displacement-heating time curves for the sandwich composite when tested at the heat flux of (a) 25, (b) 35 and (c) 50kW/m^2 and different percentage load levels.

Figure 3.21 shows the effect of applied tension stress on the failure time of the sandwich composite measured by fire structural testing at different heat fluxes. Separate failure times are given for the front and back face skins. Included in the figure are photographs of the failed sandwich composite specimens. As expected, the failure time increased with decreasing heat flux and/or applied stress. A similar trend occurs for single-skin laminates under combined tension loading and one-sided heating [5, 22]. In all cases, the sandwich specimens failed by tensile rupture, and the tensile failure modes are described in greater detail later in this chapter. The extent of fire-induced damage, indicated by charring and decomposition of the specimens, increased with decreasing stress due to the longer exposure time to the heat flux before failure. At low loads the polymer matrix to the front skin has completely decomposed and vapourised, exposing the fibreglass reinforcement.

Figure 3.22 shows a close-up view of the typical appearance of the failed sandwich composite, in which the skins have charred and experience extensive fibre fracture.

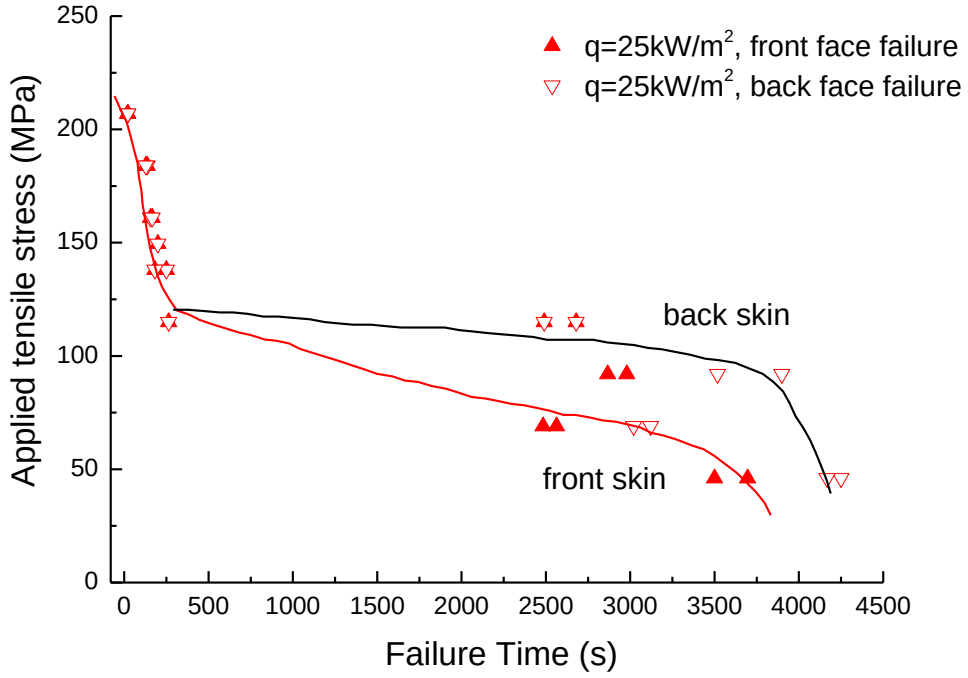

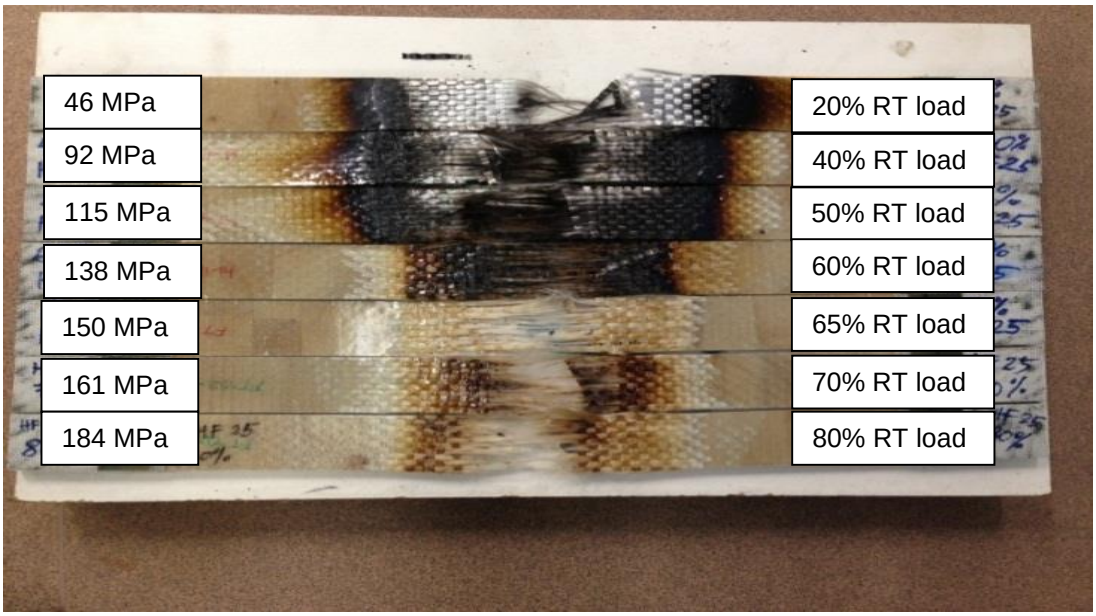

(a)

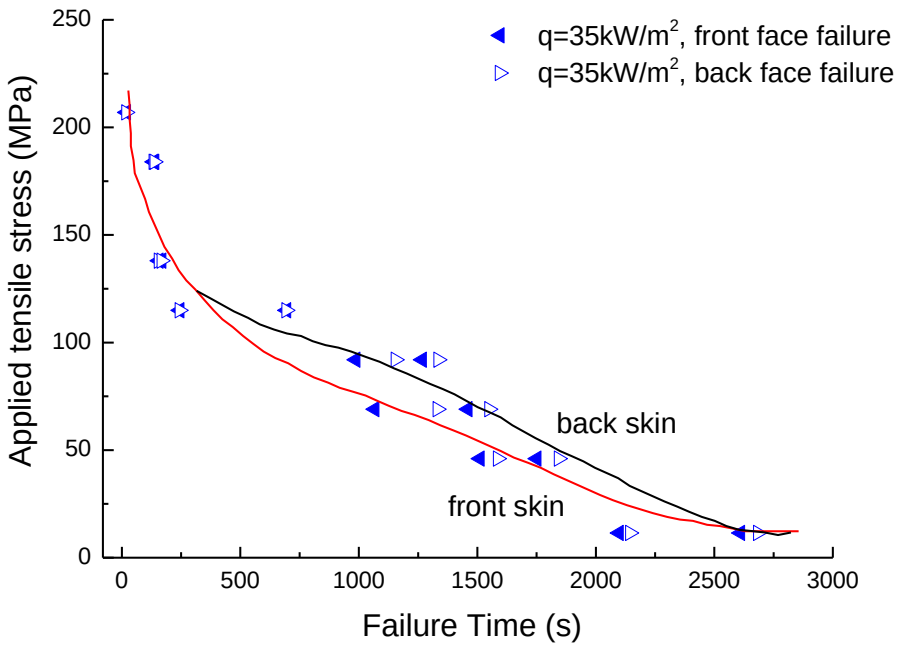
q=35kW/m2, front face failure
q=35kW/m2, back face failure
Applied tensile stress (MPa)
Failure Time (s)
back skin
front skin
0
50
100
150
200
250
0
500
1000
1500
2000
2500
3000

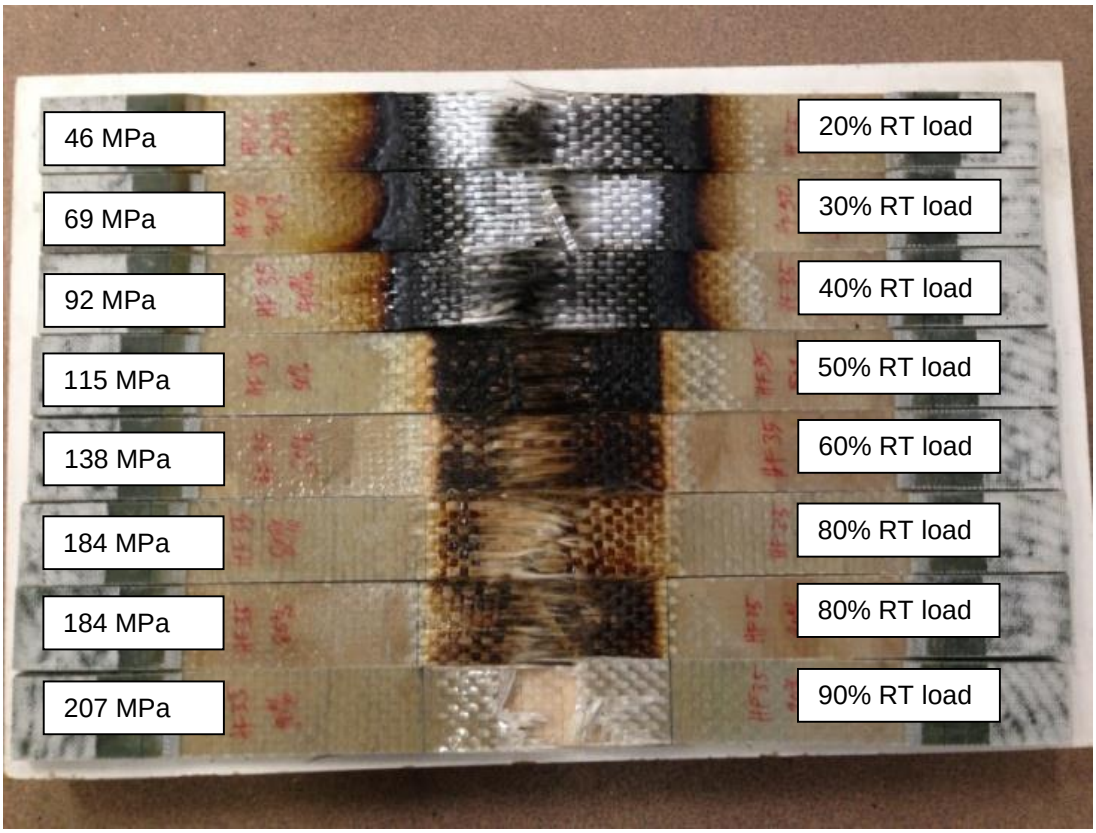
46 MPa
69 MPa
92 MPa
115 MPa
138 MPa
184 MPa
184 MPa
207 MPa
20% RT load
30% RT load
40% RT load
50% RT load
60% RT load
80% RT load
80% RT load
90% RT load

(b)

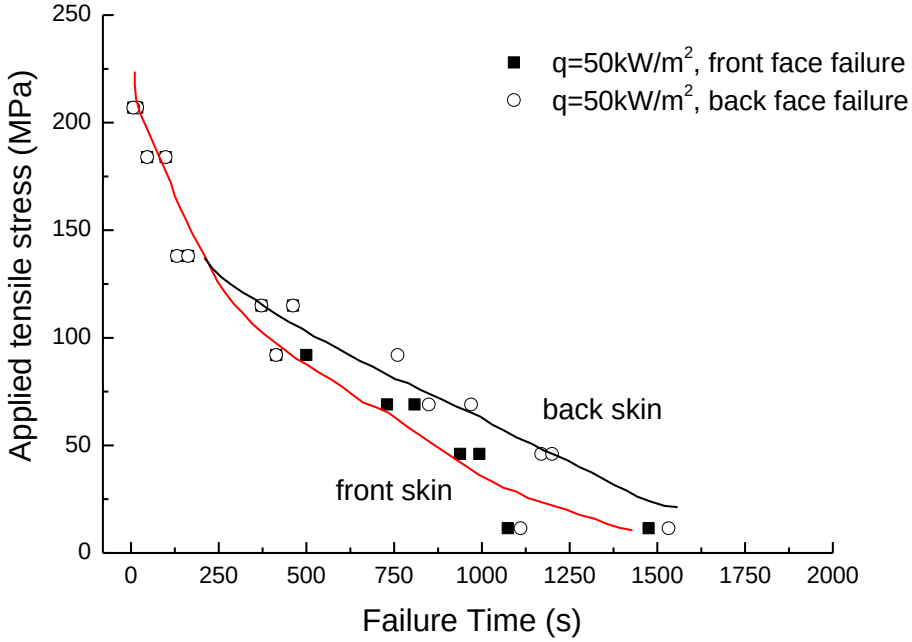

(c)

Figure 3.21: Effect of applied tensile stress on the failure times and the appearance of the failed specimens when tested at the heat fluxes of (a) 25 kW/m² (b) 35 kW/m² and (c) 50 kW/m². The curves are lines of best-fit through the experimental data.

Figure 3.22: Close up view of ruptured sandwich specimen.

The mechanical response of the sandwich composite was correlated to its decomposition response during fire structural testing. Figure 3.23 shows the change in the mass loss rate of the sandwich composite with increased heating time for the different heat fluxes. The mass loss rate was measured using a cone calorimeter with the heater aligned parallel and placed 25 mm away from the sandwich composite. In this way, the mass loss rate was measured under identical heat flux conditions to the fire structural test. The mass loss rate is a direct measure of the decomposition rate of the sandwich composite. (The cone calorimetry tests were performed by Virginia Tech by A/Prof B.Y. Lattimer). Figure 3.23 shows that the mass loss rate increased rapidly with the heat flux, and this was due to the faster heating rate and higher temperatures experienced by the sandwich composite which accelerated the decomposition rates to the polymer matrix in the face skins and to the balsa core. Included in figure 3.23 are the measured failure times of the sandwich composite. It is interesting to find that the thermal decomposition process slowed significantly after about 1000 seconds or less (depending on the heat flux); however the composite does not fail until much longer times when the applied stress was below ~50-100 MPa. This reveals that the sandwich composite failed at high tensile stress levels while the skin and core are still undergoing decomposition and pyrolysis. At low stresses, however, the sandwich composite could continue to carry load after the decomposition process has stopped (i.e. the polymer matrix to the skins and core were fully decomposed). Only the glass fibre reinforcement remains after decomposition, and it was able to provide the sandwich composite with significant residual tensile strength.

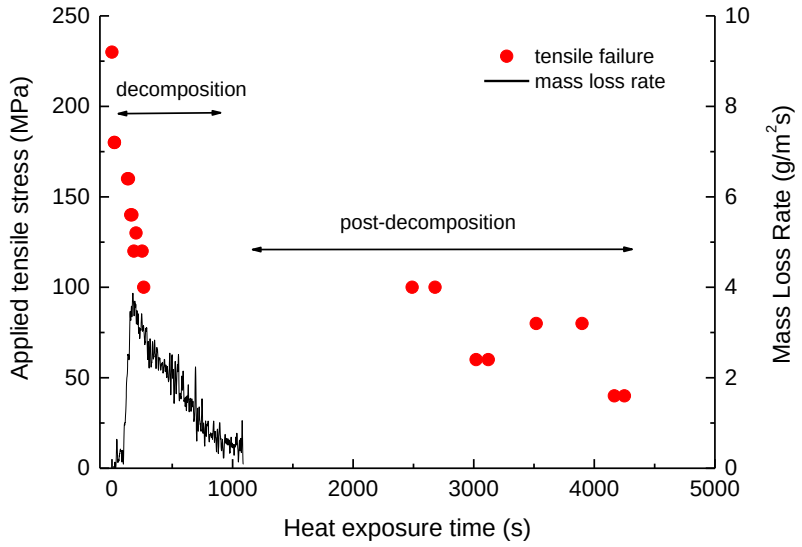
Applied tensile stress (MPa)
Mass Loss Rate (g/m²s)
Heat exposure time (s)
tensile failure
mass loss rate
decomposition
post-decomposition
0
50
100
150
200
250
0
2
4
6
8
10
0
1000
2000
3000
4000
5000

(a)

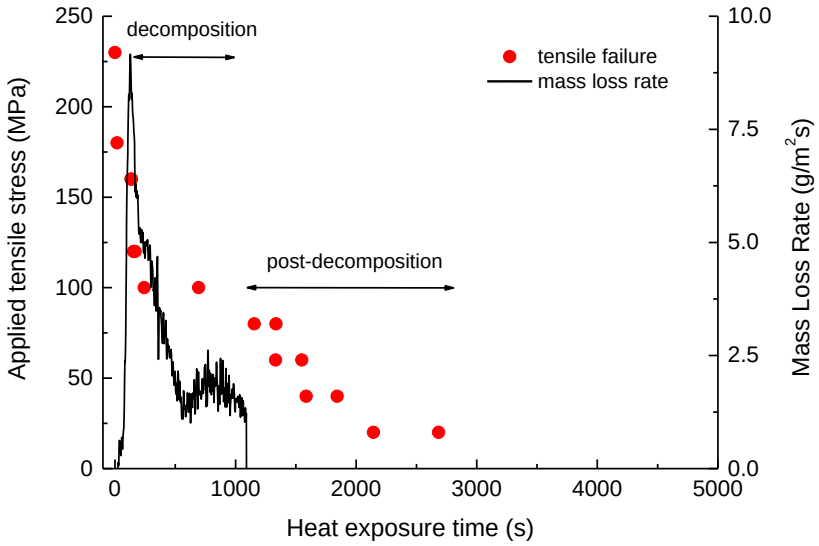
Applied tensile stress (MPa)
Mass Loss Rate (g/m²s)
Heat exposure time (s)
tensile failure
mass loss rate
decomposition
post-decomposition
0
50
100
150
200
250
0.0
2.5
5.0
7.5
10.0
0
1000
2000
3000
4000
5000

(b)

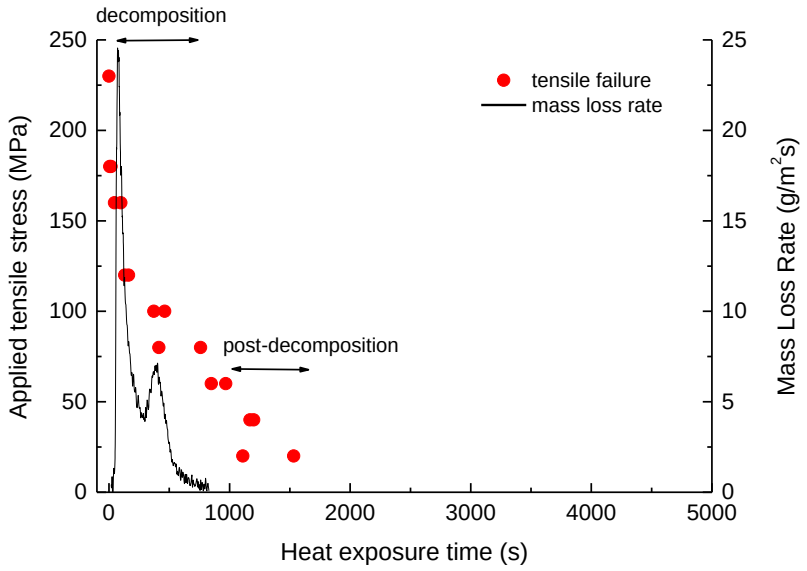

(c)

Figure 3.23: Effect of heating time on the measured failure stress (data points) and mass loss rate (line) of the sandwich composite tested at the heat fluxes of (a) 25, (b) 35 and (c) 50 kW/m^2.

The measured and calculated failure times for the sandwich composite are compared in Figure 3.24. The calculated times were determined using the thermal-mechanical model described in Section 3.2.3. (The mechanical model was solved using the data given in Tables 3.2 and 3.3). The calculated time is defined by the heating time required for the residual tensile strength of the sandwich composite to decrease to the applied tensile stress, at which point failure must occur. Agreement between the measured and calculated times is good over the range of tension stress and heat flux conditions. The residual resin content at any given point was chosen to determine the use of fibre bundle or single fibre strength data: for a residual resin content of R_{rc}>0.1, single fibre data was applied to capture the separation of fibres when the resin decomposed. The exposure to environmental air was assumed to be restricted due to the surrounding resin. For a residual resin content of R_{rc}<0.1, fibre bundle data is applied as fibres are now in contact with each other and friction between fibres leads to increased strength reduction [78]. The model accurately predicts the trend of increasing failure time with decreasing stress or

heat flux. Agreement between the measured and calculated failure times is within 10% in many cases. In some cases, however, there is significant discrepancy between the times.

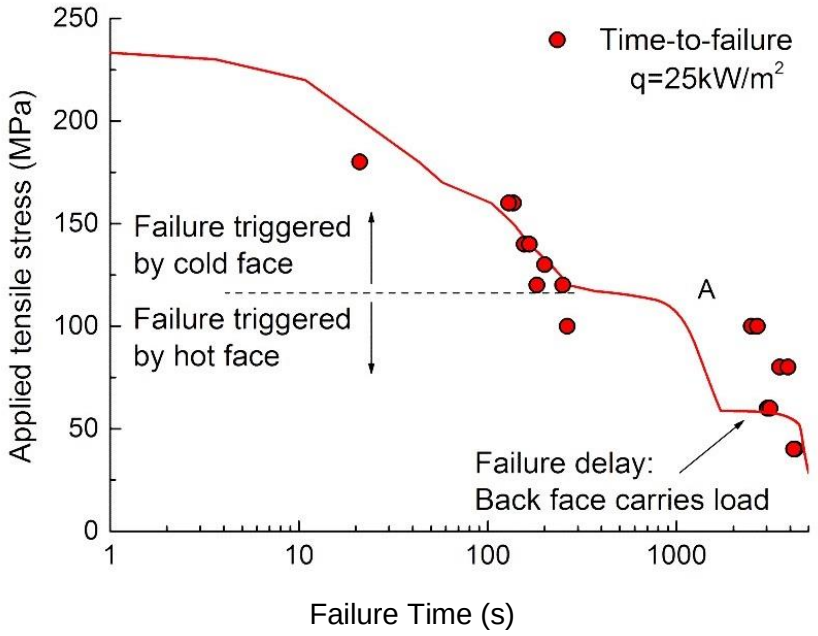

(a)

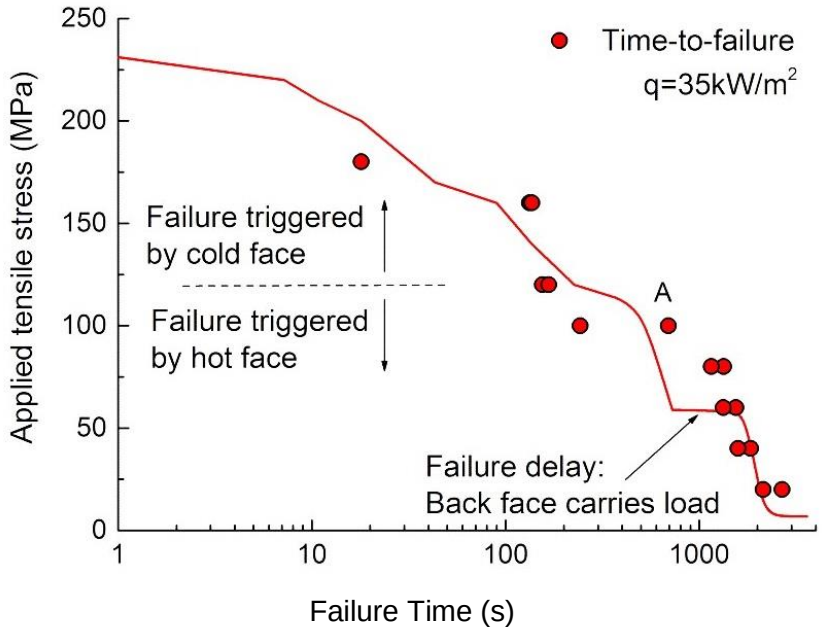

(b)

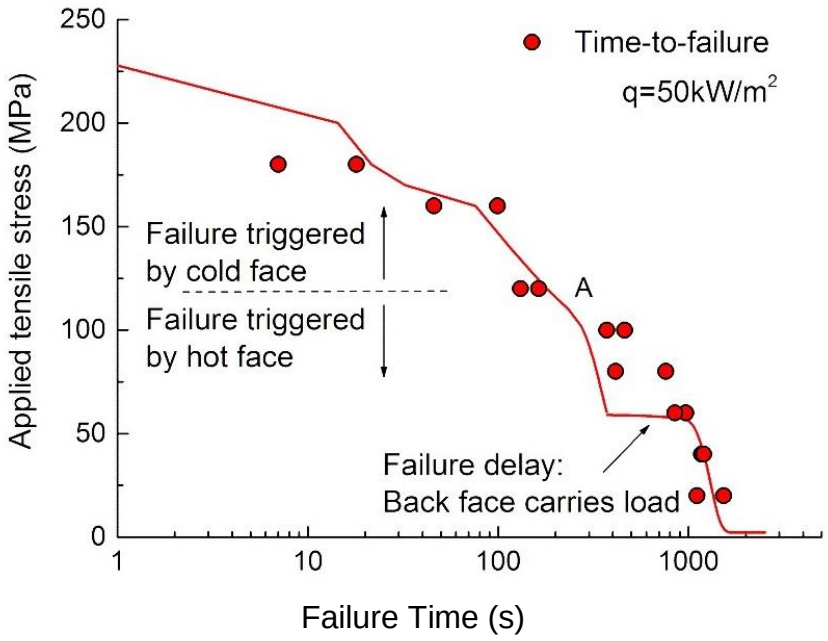

(c)

Figure 3.24: Effect of applied tensile stress on the failure time of the sandwich composite exposed to the heat fluxes of (a) 25, (b) 35 and (c) 50kW/m^2. The data points and solid lines are the measured and calculated failure times, respectively.

Table 3.2: Mechanical model parameters.

Composite	P_0	P_R	T_k [ºC]	k_m
Skin modulus E [GPa] (Eq. (3.1))	22	8	100	0.02
Skin load transfer Φ(Eq. (3.14))	1.0	0.65	88	0.026
Fibre bundle strength $\sigma_{fb,0}$ [MPa] (Eq. (3.14))	900	--	--	--
Matrix strength σ_m [MPa] (Eq. (3.15))	70	1.5	88	0.026
Core (transverse loading)	P_0		ϕ [MPa/ºC]	
Modulus [MPa] (Eq. (3.12))	130.0		0.00057	
Strength [MPa] (Eq. (3.20))	0.83		0.00372	

Table 3.3: Fibre strength parameters used to solve the model.

Values	Fibre bundles Air	Single fibres N_2
$T_{50\%}$ [ºC]	347.6	403.1
p_{fb} [ºC^{-1}]	5.83 x 10^{-3}	6.60 x 10^{-3}
k_1 [s^{-1}]	1.81 x 10^{-6}	1.2 x 10^{-6}
k_2 [ºC^{-1}]	1.45 x 10^{-2}	1.17 x 10^{-2}

For the given sandwich dimensions and constituent material properties, the load-bearing capacity of the core may be neglected as its stiffness in the loading direction (i.e. transverse grain direction) is less than 1% of the stiffness of the face skins (see Table 3.2). Similarly, the core strength is much lower than that of the laminate face skins. With these conditions, the mechanical model predicts that the sandwich composite fails via one of three mechanisms depending on the applied tensile stress. In order of decreasing stress, these mechanisms are (i) tensile rupture of the back skin due solely to matrix softening within the heated front face skin; (ii) tensile failure of the front skin due the combination of matrix and fibre softening followed by immediate failure of the back skin; and (iii) two-stage tensile failure triggered by rupture of the heated skin followed by delayed fracture of the back skin. The sequence of failure events for the three mechanisms is shown in Figure 3.25. Failure was never initiated by softening or decomposition of the core because the tensile properties of the sandwich composite are dominated by thermal softening of the face skins.

Failure of the sandwich composite at applied loads above 50% of the ultimate strength occurs within a short heating period (under 100-200 seconds) (Failure Mode I in Figure 3.25). Modelling reveals that within the heated face skins there is sufficient time for the matrix to soften (T_g~120^{o}C), but insufficient time for the glass reinforcement to weaken (which begins above ~350^{o}C). Over the same short period, the temperature of the back skin rises only slightly and remains well below the glass transition temperature of the matrix (as shown in Figure 3.13). That is, the tension stiffness and strength of the back skin have not reduced before the sandwich composite fails. Under this condition the tensile modulus of the heated skin is much lower than the back skin ($E_{s1} < E_{s2}$, see Table 3.2). Because the strain induced by the applied tension load is uniform throughout the sandwich composite, then the stress carried by the stiffer back skin is much higher than that supported by the more compliant heated skin. The stress carried by the back skin rises rapidly with heating time due to rapid matrix softening of the heated front skin, and within a short period the load exceeds the ultimate strength causing the back skin to fail. The model predicts that once the back skin fails the front skin immediately ruptures.

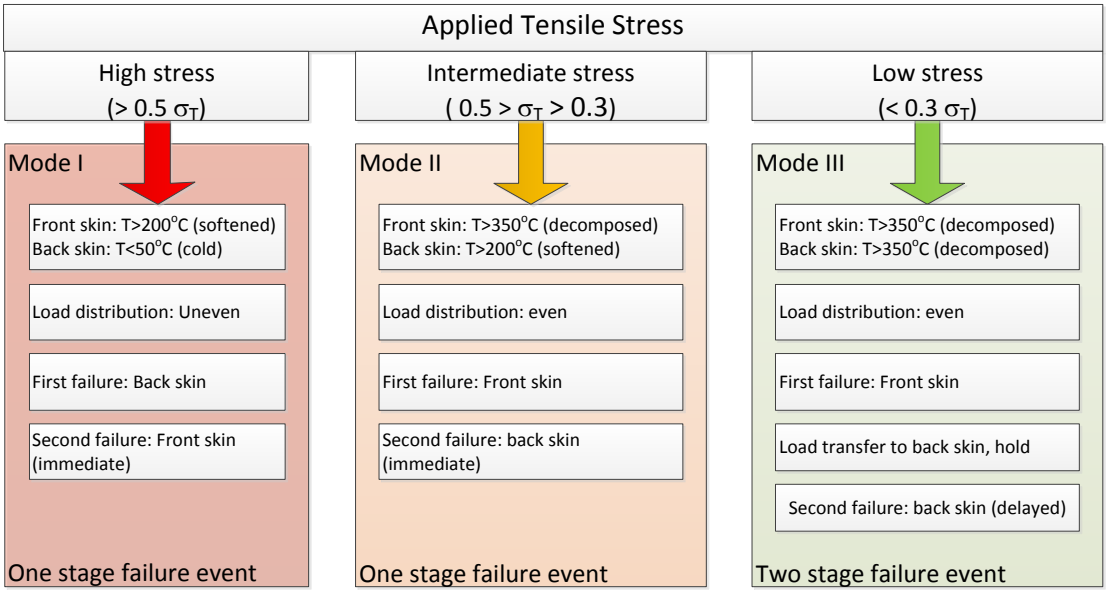

Figure 3.25: Tension failure mechanisms of the sandwich composite in fire. Mode I: Failure initiated in the back skin due to matrix softening of the heated skin. Mode II: Failure initiated in the front skin due to fibre and matrix softening of the heated skin followed by immediate failure of back skin. Mode III: Failure of the heated front skin followed by delayed fracture of the back skin.

Modelling and testing revealed that the failure mode of the sandwich composite changed when the applied stress is below 50% of the ultimate strength. A sudden increase in the failure time occurs when the applied stress is reduced below 50%, and the increase becomes larger when the heat flux is reduced (as indicated by point 'A' in Figure 3.24). As the heating time increases, the temperature of the back skin rises until its polymer matrix exceeds T_g thereby causing a loss in stiffness. When this occurs the applied stress is once again re-distributed between the front and back skins. The applied load is now carried by glass fibres within the front skin and back skin, and the matrix phase has fully softened and begun to decompose. With increasing heating time the front skin weakens due to the reduction of the glass fibre strength until eventually the front skin ruptures. When this occurs the applied stress is transferred completely on to the back skin, which then fails.

At low loads (under ~70 MPa or 30% of the ultimate stress), failure of the back skin does not occur immediately following rupture of the heated skin (Mode III in Figure 3.25). After

the front skin has broken, the mechanical model predicts that failure of the back skin is delayed because its glass fibres (within the fully softened matrix) are capable of carrying low load. Eventually, however, the back skin fails because the temperature rise and increased loading time weakens the fibres sufficiently for them to break. This failure mode of front skin fracture followed by delayed rupture of the back skin predicted by the model was confirmed by testing.

In general, the model is able to predict the failure times and failure mechanisms of the sandwich composite with good accuracy. However, in some cases there are significant differences between the calculated and measured failure times. This is attributed to several simplifying assumptions applied to the model. Firstly, the temperature profile used in the analysis assumed an average ignition time independent of load level (as shown in Table 3.4). However, it was found that the temperature increases with the tension stress due to cracking within the balsa core accelerating the egress rate of flammable gas (Figure 3.14). The model also does not consider heat-induced cracking within the skins (e.g. delaminations, matrix cracks) which reduce thermal conductivity.

Another important assumption with the model is the softening rate of the glass fibres within the skins, which is based on high temperature fibre strength tests performed in air. Feih et al. [80] have shown that the fibre softening rate is dependent on the atmosphere, with air causing a more rapid loss in strength than an inert environment. Except for the glass fibres at the surface of the skins, softening occurs within a near oxygen-free environment because the pressure of decomposition gases flowing through the skins is greater than the near ambient pressure within the fire. As a result, the model under-predicts the failure times for the sandwich composite when failure is influenced by fibre softening of the front and back skins. Despite these assumptions, the models provide a good approximation of the tension failure times and accurately determines the failure mechanisms of the sandwich composite in fire.

Table 3.4: Average core ignition time for laminates under load for various heat fluxes.

Heat flux [kW/m^2]	Core ignition time [s]
25	2000
35	1000
50	750

3.5 CONCLUSIONS

A new thermal-mechanical model for predicting the weakening and failure of sandwich composite materials under combined tension loading and one-sided heating by fire has been developed and validated. The thermal model can predict with reasonable accuracy the through-thickness temperature profile of the unloaded sandwich composite, including temperatures for the front skin, core and back skin. However, the thermal model cannot predict the increased temperature that occurs when a sandwich composite is under load. Cracks and other damage within the decomposing balsa core aid the egress of combustible gas which increases the temperature, and this cannot be analysed using the thermal model. Further development is required that incorporates damage modelling into the thermal-mechanical model.

The mechanical model can predict with reasonable accuracy the fire structural survivability and failure mode of the sandwich composite under tension loading. Both the model and experimental testing showed that the failure time increased when the applied tension stress and/or heat flux were reduced. The model predicts that the sandwich composite fails by tensile rupture of the back skin when the applied tension stress is above 50% of ultimate strength at room temperature. This failure mode occurs when thermal softening of the polymer matrix to the heated skin causes over-loading of the back skin. The failure mode changes when the applied stress is reduced below 50% of the ultimate strength. Failure is initiated by softening of both the polymer matrix and glass fibre reinforcement within the heated skin. At low applied stress, the failure times are increased because the back skin can continue to carry load after failure of the front skin. These predictions of the failure modes at different applied tensile stress levels were confirmed by fire structural testing of the sandwich composite. The model can estimate

the failure time and predict the failure mechanism of the sandwich composite for different tension stress and heat flux conditions, making it a useful analytical tool for assessing the fire structural survivability of sandwich materials.

Chapter 4 : TENSILE PROPERTIES OF SANDWICH COMPOSITES WITH OFF-AXIS FIBRES IN FIRE

ABSTRACT

This chapter extends the research into the tensile response of sandwich composites in fire by exploring the effect of fibre orientation on the softening behaviour and failure mode. The effect of changing the orientation of the warp fibres (θ) in the woven laminate face skins relative to the tensile load direction (as shown in Figure 4.1) is studied experimentally and analytically. This research is an extension of the work reported in the previous chapter where the warp fibres within the face skins were aligned parallel to the tensile load direction. The thermal-mechanical model is used in this chapter to calculate reductions to the tensile modulus and strength of the laminate face skins caused by thermal softening of both polymer matrix and fibre reinforcement and also weakening of the core. Model accuracy is evaluated with experimental data obtained from fire structural tests performed on sandwich composites in which the warp fibres were aligned at 0^o (parallel), 9^o, 15^o, 30^o or 45^o from the tensile load direction. The maximum tensile failure load and the failure time of the sandwich composite decreased rapidly with increasing warp fibre angle as the tensile properties became increasingly influenced by thermal softening and decomposition of the polymer matrix. This is predicted with good accuracy using the thermal-mechanical model. Testing also revealed that the tensile failure mode of the sandwich composite was sensitive to the warp fibre angle. The research described in this chapter provides important new insights into the contributions of fibre softening and matrix softening/decomposition on the tensile structural survivability of sandwich composites in fire.

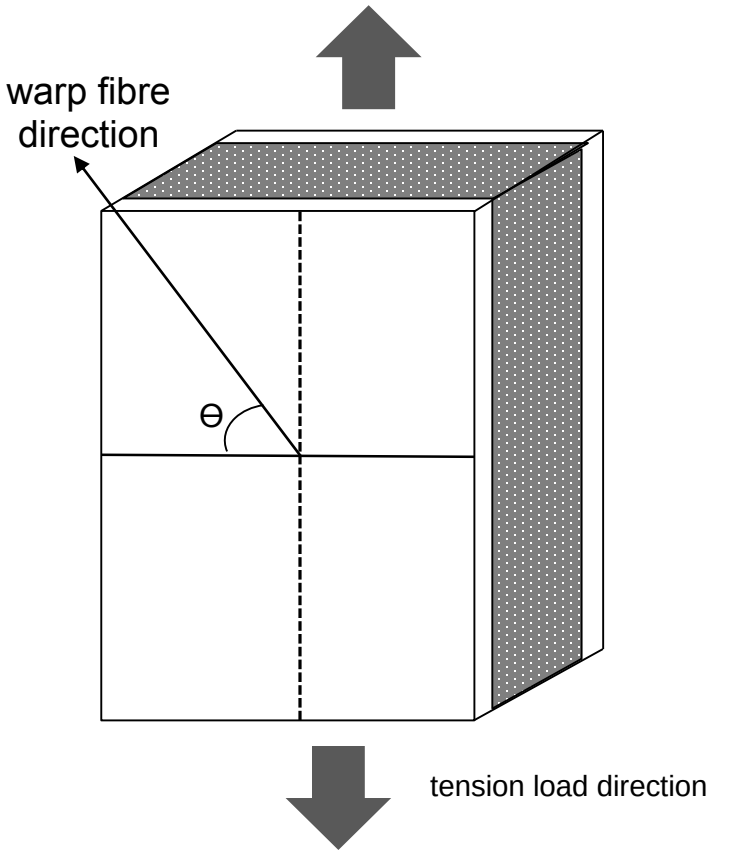

Figure 4.1: Fibre orientation angle of sandwich composites with regard to direction of tensile loading.

4.1 INTRODUCTION

Small misalignments in fibre orientation are hard to avoid during the manufacture of the laminate face skins to composite structures. During the hand lay-up of fabric plies the warp and weft tows may be misaligned due to incorrect or careless handling. When severe enough, these misalignments may influence the mechanical properties of the sandwich composites in fire. Also, sandwich composites used in naval ship and other structural applications may be inadvertently subjected to off-axis loads not aligned with the warp or weft fibres or the composite may be required to support multi-axial loads. For these reasons, it is important to understand the effect of off-axis loading on the fire

structural properties of sandwich composites. To date, there is no published research on fire tensile response of sandwich composites subject off-axis loading. In the on-axis directions (warp and weft or 0/90), woven fabric laminate skins to sandwich composites possess the highest tensile stiffness and strength properties. It is well known that the tensile properties at room temperature decrease rapidly when the composite is subjected to off-axis loading [81]. The tensile fire structural properties are also expected to decrease with increasing fibre misalignment angle, although this remains to be investigated.

This chapter is an extension of research presented in the previous chapter involving an assessment of the fire structural performance of sandwich composites under tension loading. The chapter aims to determine the effect of off-axis tensile loading on the fire structural response of sandwich composites. This chapter presents the thermal-mechanical model to predict the softening rate, failure time and failure mechanisms of sandwich composites with off-axis fibres under combined tension loading and one-sided heating by fire. In order to understand the off-axis behaviour, fire structural tests are performed on woven E-glass/vinyl ester sandwich composite which contains warp fibres aligned at 0^o (parallel), 9^o, 15^o, 30^o or 45^o from the tensile load direction. The effect of fibre angle on the tensile strength, softening rate, failure time, and failure mode of the sandwich composite is experimentally determined by elevated temperature and fire structural tests, and the results are compared with calculated predictions to validate the model.

4.2 MATERIALS AND FIRE STRUCTURAL TESTING OF SANDWICH COMPOSITES WITH OFF-AXIS FIBRES

Similar to the previous chapter, the sandwich composite used in this study is representative of a material used in naval ship structures. The laminate face skins were manufactured from E-glass plain woven fabric (830 g/m^2, Colan Industries) and vinyl ester resin (Derakane 411-350). In previous work (Chapter 3), an E-glass woven fabric with a slightly lower areal weight (800 g/m^2) was used in the skins. Different fabric is used in this

work due to the manufacturer (Colan Industries) having stopped producing the 800 g/m^2 fabric mid-way through the PhD project. The same manufacturing process as described in Section 3.3.1 was used to manufacture the sandwich composites studied in this chapter. The laminate face skins was laid-up with the warp fibres aligned at one of four different orientation which were 9^o, 15^o, 30^o and 45^o angles relative to the load direction. Skins were also made with warp fibres aligned with the load direction (0^o).

Small-scale fire structural tests were performed on the sandwich specimens to generate the experimental data in order to validate the thermal-mechanical model. The same test machines and procedures were used for the fire structural test and elevated temperature test as described in Section 3.3. In this study, the on-axis (0^o) and off-axis (9^o, 15^o, 30^o and 45^o) sandwich specimens are tested under constant tensile stress levels between 10% and 80% of the ultimate strength at room temperature while simultaneously exposed to a heat flux of 35 kW/m^2. Fire-under-load tests were performed until the specimen failed, and the heating time taken for the specimen to rupture, called the time-to-failure, was measured. The effect of fibre orientation on the softening behaviour leading up to tensile failure as well as the failure mode were recorded.

4.3 RESULTS AND DISCUSSIONS

4.3.1 Room Temperature Properties of Sandwich Composite With Off-axis Fibres

When modelling and testing the fire structural response of sandwich composites with off-axis fibres, it is important to understand the change in the stress-strain behaviour at different fibre orientations. Figure 4.2 shows typical tensile stress vs strain curves measured for the sandwich composites with different fibre angles at room temperature. Figure 4.3 shows typical samples following testing revealing differences in the fracture mode. The curves for the on-axis 0^0 and off-axis 9^0 composites show an abrupt load drop upon reaching the ultimate tensile stress, which as expected is higher for the on-axis sandwich material. Tensile failure of both materials is dominated by fracture of the load-

bearing fibres. For 15^0 off-axis sandwich composite the failure is less abrupt, with the specimen still holding about 40% of its ultimate tensile stress after first failure and then the load capacity decreased gradually with increasing strain due to the progressive failure of the skin. The sandwich composite with 15^0 off-axis fibres experienced tow rotation and interlocking under tensile loading. The curves for the 30^0 and 45^0 composite show highly non-linear deformation and large strains to failure, and these materials failed by shear-induced rupture of the skins.

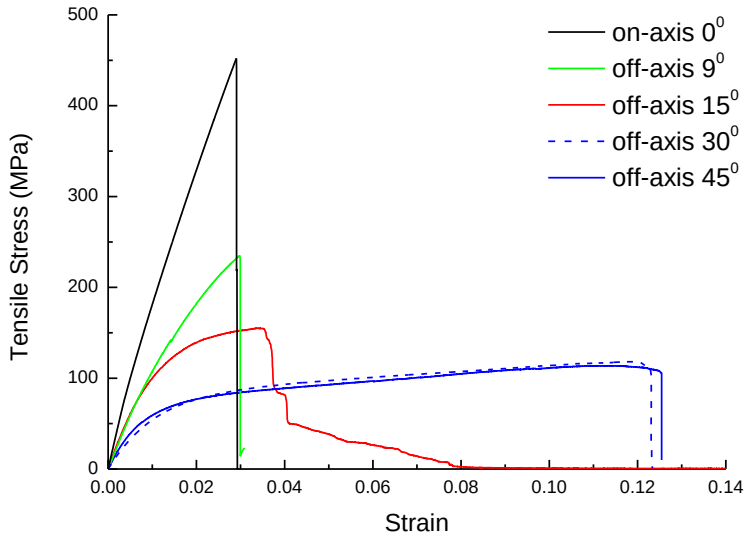

Figure 4.2: Tensile stress vs strain curves for the sandwich composite at different fibre orientation angles.

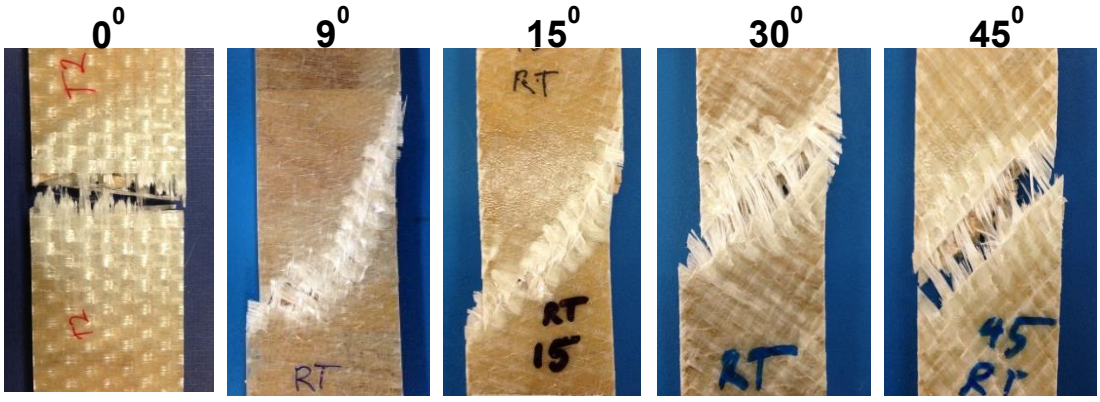

Figure 4.3: Failure modes of sandwich specimens at different fibre orientation angles.

Figure 4.4 (a) and (b) show plots of the tensile strength and modulus measured for the different fibre orientations of the sandwich composite. A total of 3 specimens were tested at each fibre orientation angle. As expected, the tensile properties decrease with increasing misalignment angle up to 45^{o}, with the strength decreasing at a more rapid rate than modulus. This is typical behaviour for composite materials subjected to off-axis loading [81].

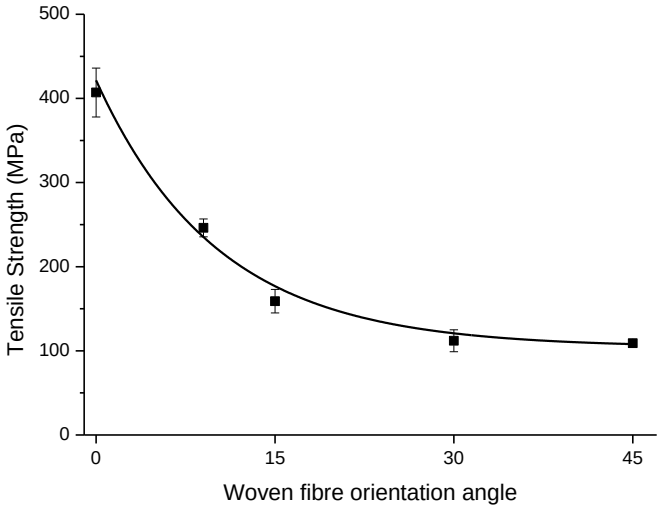

(a)

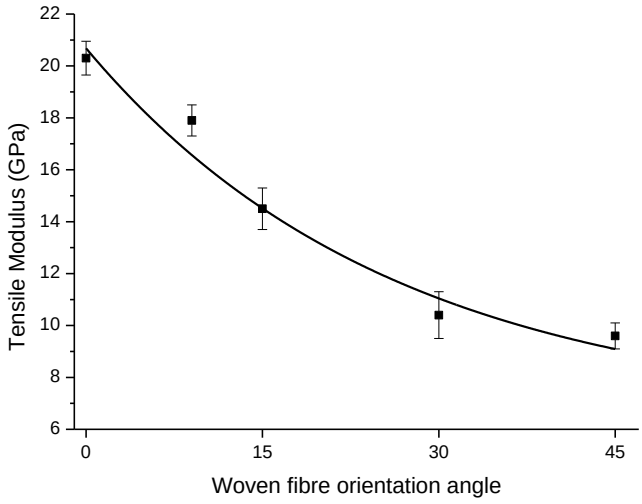

(b)

Figure 4.4: (a) Tensile strength and (b) tensile modulus vs woven fibre orientation angle. The error bars show the standard deviations.

4.3.2 High Temperature Properties of Sandwich Composite With Off-axis Fibres

The tension strength and elastic modulus of the sandwich composite as a function of temperature needs to be measured to solve the mechanical model, as described in Section 3.2.3. The tensile properties of the sandwich composites with different fibre angles were measured under isothermal conditions between 20 and 250^{o}C. The tensile properties of the vinyl ester resin to the laminate skins were also measured over this temperature range. Figure 4.5 shows the effect of temperature on the tensile strength and stiffness, and most of the softening occurs close to the glass transition temperature of the vinyl ester matrix to the laminate face skins. The solid lines are the fitted data curves using the parabolic tanh mathematical function as described in Section 3.2.3 (Equation 3.11 and 3.15). It can be observed that tensile strength decreases with increasing misalignment angle, and the neat resin gives the lowest strength. Similar trends were measured for the tensile stiffness where the loss in stiffness is attributed to the straightening of woven fibres as the matrix softens.

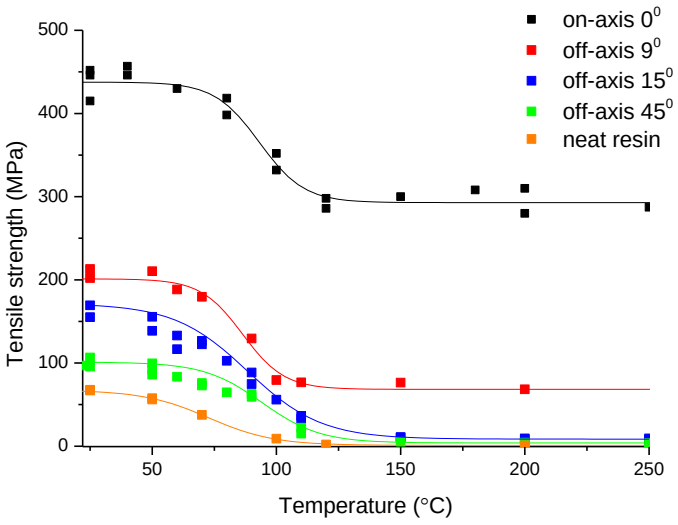

(a)

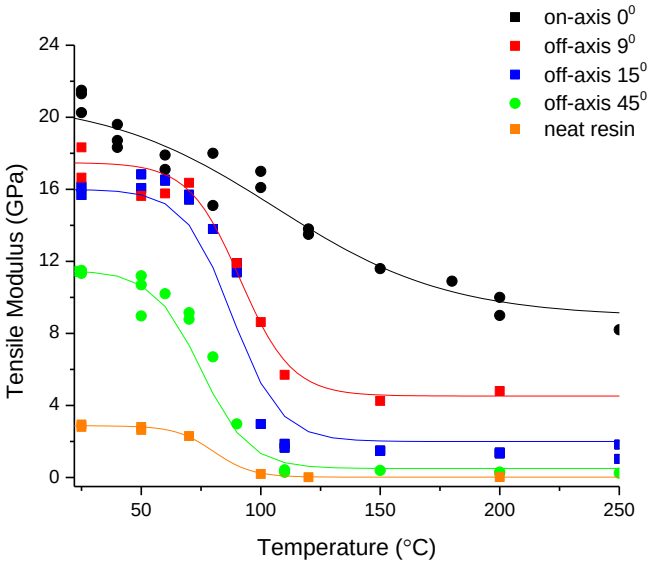

(b)

Figure 4.5: Effect by increasing temperature on the (a) tensile strength and (b) tensile modulus of the laminate used for the face skins to the sandwich composite at different fibre orientation angles.

4.3.3 Tensile Response of Sandwich Composite in Fire With Off-axis Fibres

Fire structural testing was performed on the sandwich composite containing fibres orientated at different angles from the load direction. The composite samples were tested at different applied tensile stress levels while exposed to an incident radiant heat flux of 35 kW/m^2. The effect of tension stress on the temperature-time response that is measured at the back surface of the sandwich composite is shown in Figure 4.6. As can be observed in Figure 4.6a for on-axis sandwich specimens, the back face temperature was dependent on the applied tension stress. This behaviour has been thoroughly discussed in Section 3.4.1.2. For off-axis sandwich specimens at 9^0, 15^0, 30^0 and 45^0, the back face temperature were not affected by the balsa core crack opening which dependent on the applied tension stress, as the failure times were much shorter. It is more obvious with 30^0 and 45^0 sandwich specimens as the failure times of the lowest applied tension stress (5%) were less than 300 seconds.

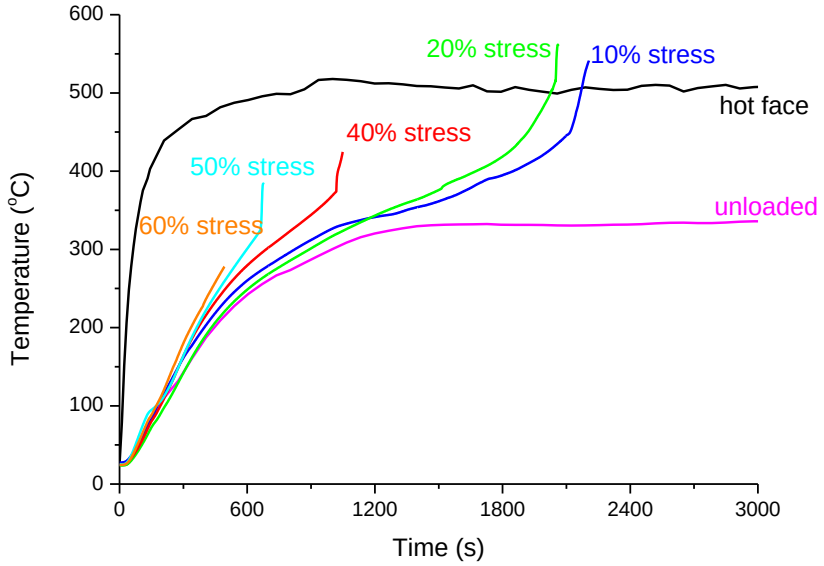
600
500
400
300
200
100
0
Temperature (°C)
0
600
1200
1800
2400
3000
Time (s)
20% stress
10% stress
hot face
40% stress
50% stress
60% stress
unloaded

(a)

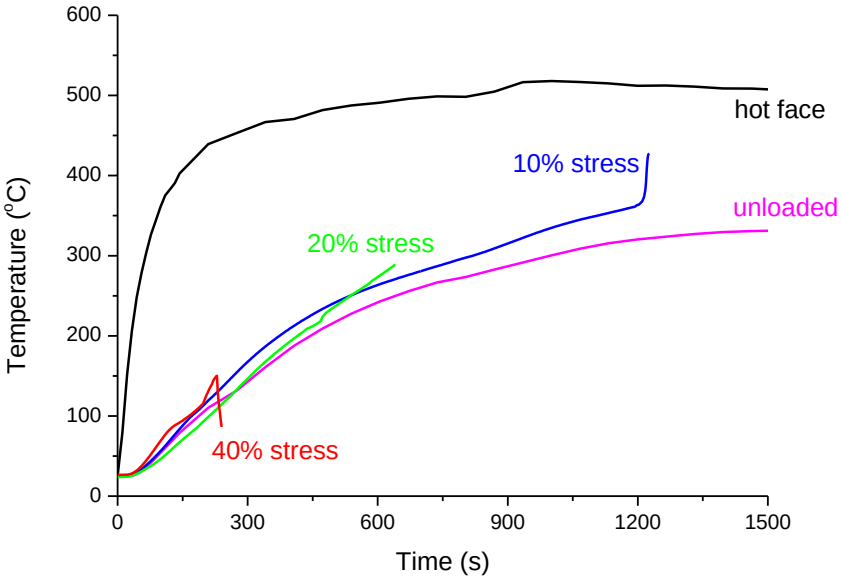
600
500
400
300
200
100
0
Temperature (°C)
0
300
600
900
1200
1500
Time (s)
hot face
10% stress
unloaded
20% stress
40% stress

(b)

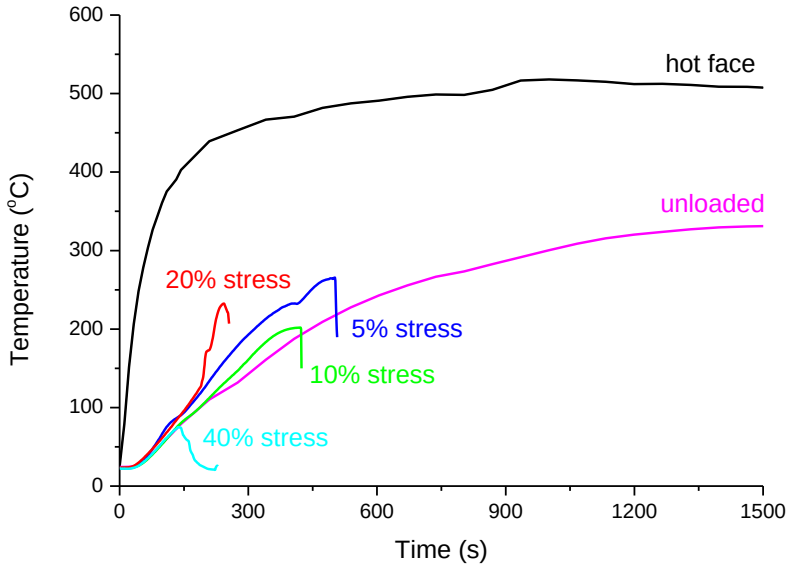
600
500
400
300
200
100
0
Temperature (°C)
0
300
600
900
1200
1500
Time (s)
hot face
unloaded
20% stress
5% stress
10% stress
40% stress

(c)

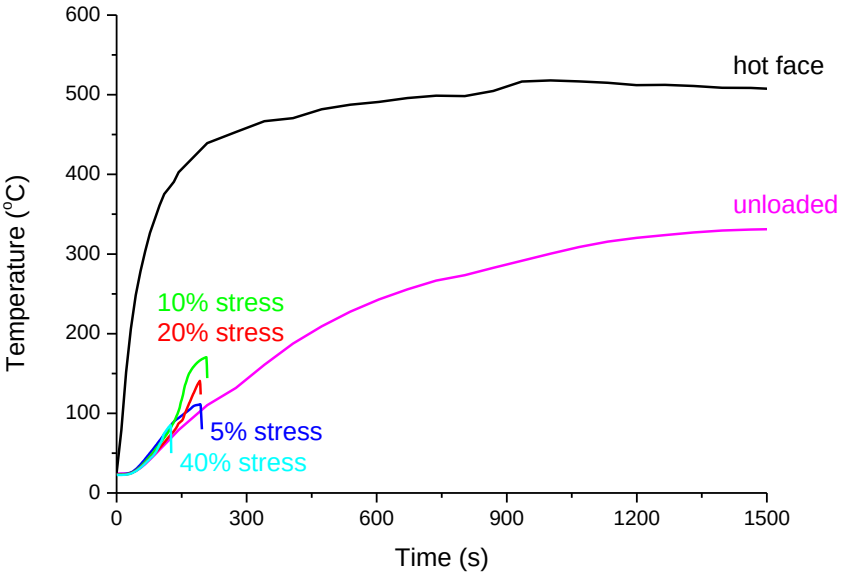
600
500
400
300
200
100
0
Temperature (°C)
0
300
600
900
1200
1500
Time (s)
hot face
unloaded
10% stress
20% stress
5% stress
40% stress

(d)

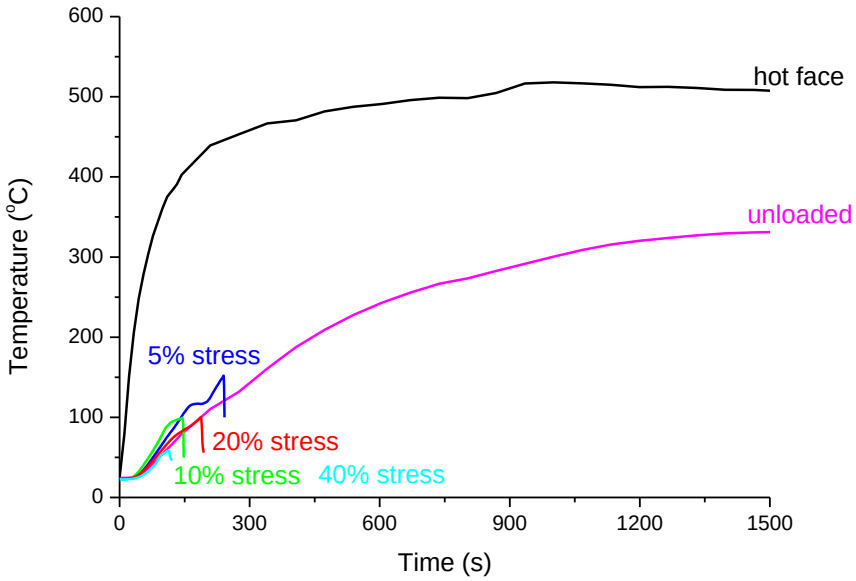

(e)

Figure 4.6: Effect of applied tensile load on the back face temperature of the sandwich composite exposed to the heat flux of 35 kW/m^2 of (a) on-axis sandwich composite, (b) off-axis 9^{o}sandwich composite, (c) off-axis 15^{o}sandwich composite, (d) off-axis 30^{o}sandwich composite and (e) off-axis 45^{o}sandwich composite. The load values are expressed as a percentage of the ultimate tensile strength of the composite.

From the fire structural testing that is performed on the sandwich composite, an axial displacement-heating times curves are measured at different load levels of both on-axis and off-axis sandwich specimens as depicted in Figure 4.7. As expected, similar to the results presented in Chapter 3, the failure times decreased with increasing applied stress. The failure times also decrease with increasing fibre angle. Similar to previous observation in Section 3.4.3, when the on-axis sandwich specimen in Figure 4.7a is subjected to a constant tension load, 3 stages of deformation were observed, where initially the displacement is rapidly deformed and then the deformation rate slowed to a quasi-steady state condition and finally the displacement rate increases rapidly until failure. For all off-axis sandwich specimens at low applied stress levels, the initial deformation rates were less rapid compared to on-axis specimens. In the second stage

where quasi-steady state condition behaviour observed with on-axis specimens was also observed with off-axis sandwich composite however in short duration of time and consequently specimens ruptured at final stage.

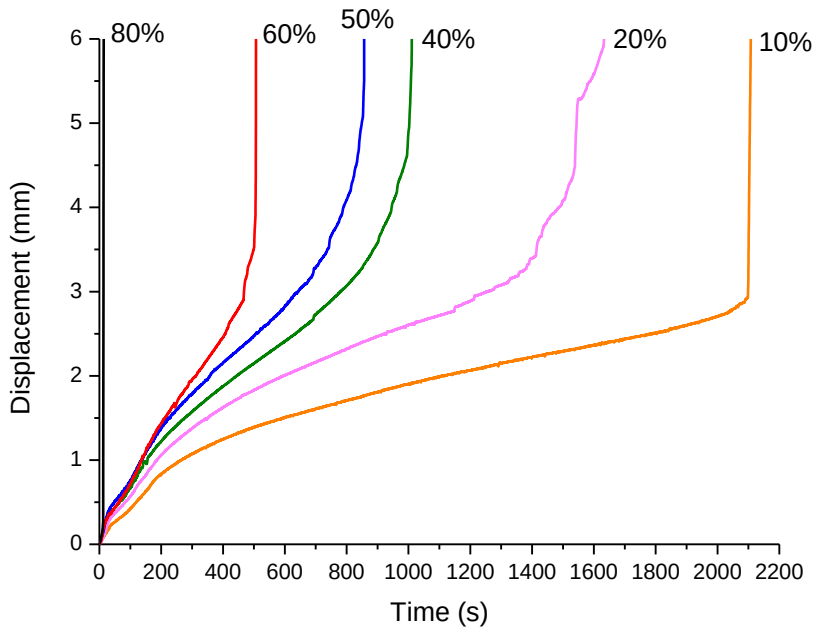

(a)

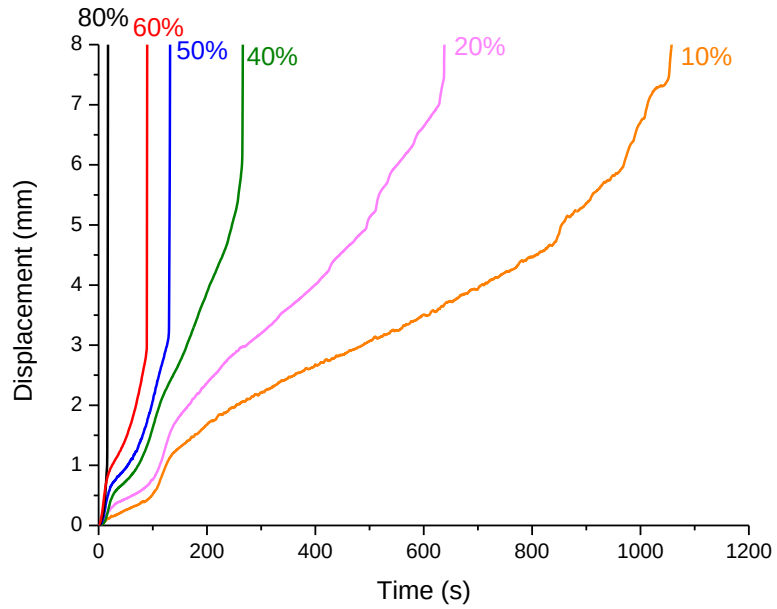
80%
60%
50%
40%
20%
10%
Displacement (mm)
Time (s)
0
1
2
3
4
5
6
7
8
0
200
400
600
800
1000
1200

(b)

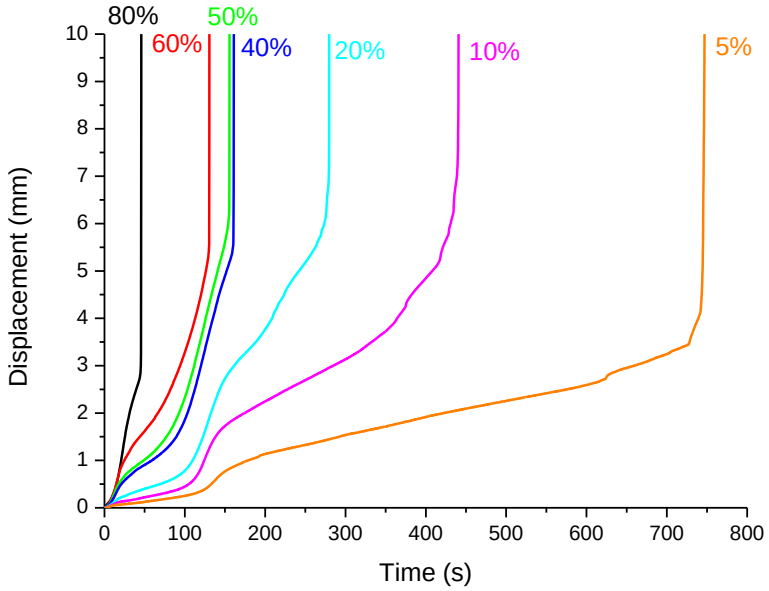
80%
60%
50%
40%
20%
10%
5%
Displacement (mm)
Time (s)
0
1
2
3
4
5
6
7
8
9
10
0
100
200
300
400
500
600
700
800

(c)

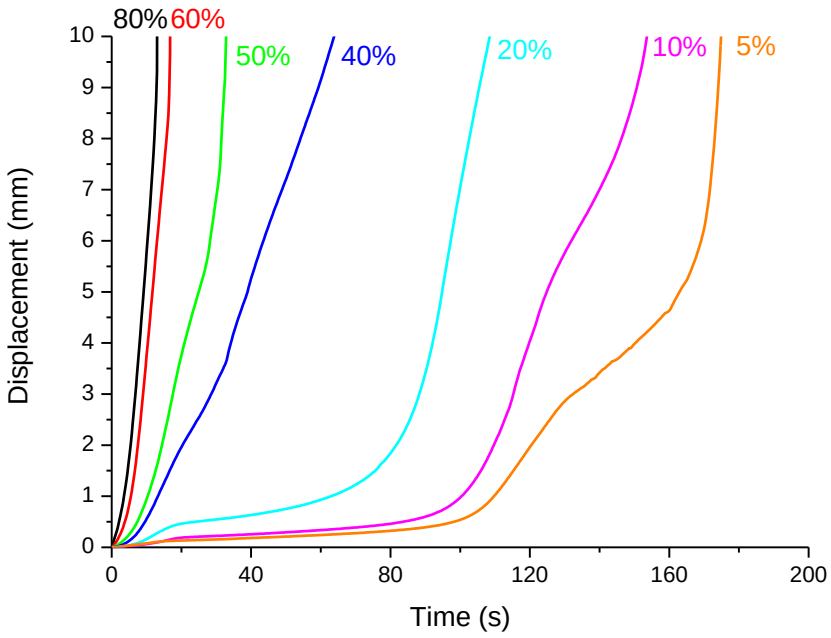

(d)

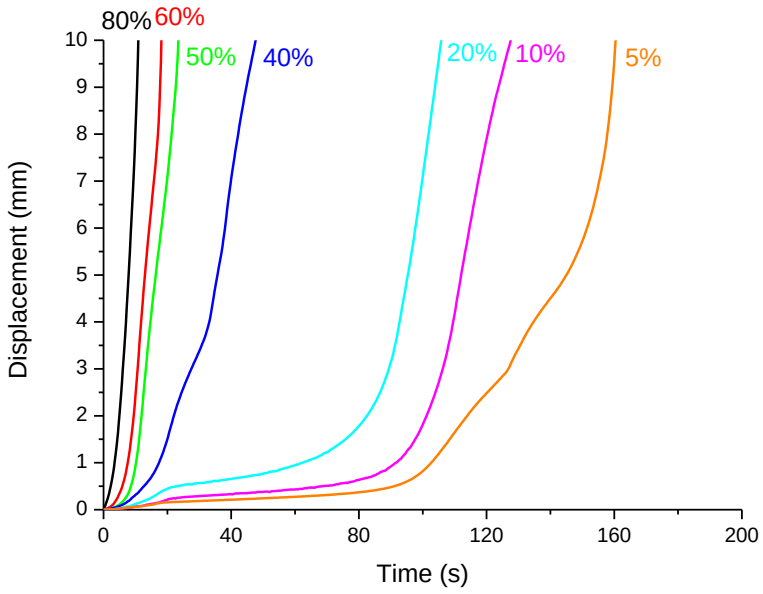

(e)

Figure 4.7: Experimental axial displacement-heating time curves for the sandwich composite at heat flux 35 kW/m^2 of (a) on-axis sandwich composite, (b) off-axis 9^0 sandwich composite, (c) off-axis 15^0 sandwich composite, (d) off-axis 30^0 sandwich composite and (e) off-axis 45^0 sandwich composite.

Plot of failure time against normalised tensile stress for the sandwich composite at different fibre orientation angle tested at heat flux 35 kW/m^2 are shown in Figure 4.8. The normalised stress is the static tensile stress applied to the sandwich composites when exposed to the heat flux divided by the tensile strength at room temperature. Figure 4.8 depicted that the failure time decreases with increasing fibre orientation angles and applied tension stress.

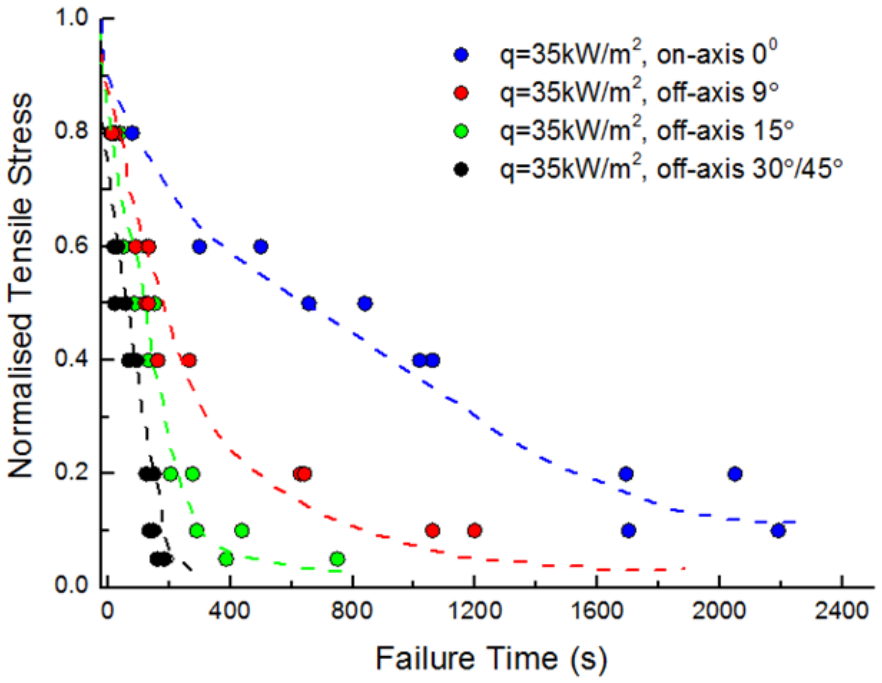

Figure 4.8: Comparison on the effect of applied tensile stress on the experimental failure time of the sandwich composite exposed to heat flux 35 kW/m^2. The curves are lines of best-fit through the experimental data.

The effect of applied tensile stress on the measured failure times for the sandwich composites with different fibre angles are shown by the data points in Figure 4.9. The curves in the figure show the calculated times that were computed using the thermal-mechanical model described in Section 3.2.3. The mechanical model was solved using the data in Table 4.1 to 4.5 for the different fibre angles. Agreement between the measured and calculated failure times is good for the different sandwich composites, with the exception for the 15^0 material where the model under predicts the failure time. For the

0^0, 9^0 and 15^0 sandwich specimens, the residual resin content at any given point was chosen to determine the use of fibre bundle or single fibre data as discussed in Section 3.4.3.

The model accurately predicts the trend of increasing failure time with decreasing tensile stress for the on-axis 0^0 and off-axis 9^0 sandwich composites as shown in Figure 4.9 (a) and (b), respectively. The off-axis 9^0 sandwich composite failed at much shorter times, and this is due to the larger strength reduction with resin softening and off-axis fibres. Failure of the 9^0 sandwich composite involved one of three modes depending on the applied stress (similar to previously discussed for the 0^0 sandwich composite in Chapter 3). Modelling and testing revealed that the failure mode of the 9^0 sandwich composite changed from cold face to hot face rupture when the applied stress dropped below ~60% of the ultimate strength. Similar to the discussion in Section 3.4.3, failure Mode II occurred at intermediate stresses between 60% and 30% of the ultimate stress where failure initiated at the front skin due to fibre and matrix softening followed by immediate failure of the back skin. In failure Mode III, failure occurred in the front skin followed by delayed failure of the back skin. The mechanical model is able to predict the delayed failure of the back skin of the 9^0 sandwich composite due to the capacity of the glass fibres to carry low load at longer heating times.

For the 15^0 sandwich composite (Figure 4.9 (c)), the time-to-failure prediction using the thermal-mechanical model is conservative (under-predicted). This discrepancy is attributed to the more gradual strength loss with increasing displacement as shown in Figure 4.2. The likely reason for the poor agreement is the complexity of the deformation and damage processes leading to failure of 15^0 sandwich composite, where there is a complex interaction between matrix softening and localised shear rotation of the tows which is not considered in the model. Figure 4.3 shows the tows do not break in tension but fail by shear rotation and rupture which is not considered by the model.

In the cases of the 30^0 and 45^0 sandwich composites, the failure times are relatively short due to larger strength reduction caused by resin softening. The stiffness and strength

properties of the skins when the load-bearing fibres are aligned at 30^0 or 45^0 is strongly influenced by the matrix properties, and less so by the fibres. Because matrix softening occurs at lower temperatures than fibre weakening, these sandwich composites softened and failed at shorter times than the sandwich materials with fibres aligned closer to the loading direction. The model used to calculate the failure times and failure mechanism for the 30^0 and 45^0 sandwich composites did not consider the fibre strength contribution, and only took into consideration the influence of matrix softening. The model was able to predict the failure times and failure mechanisms of the sandwich composite with good accuracy. Figure 4.10 shows the close-up image (front view) of the typical appearance of the sandwich composite at the highest applied stress of 80%. At low load the skins have completely charred and experience extensive burnt and ruptured at shorter failure times as depicted in Figure 4.11.

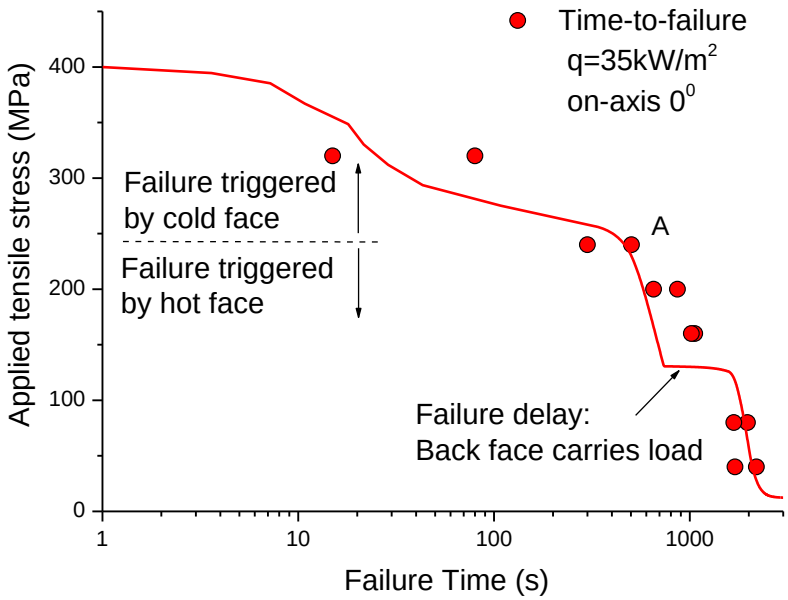

(a)

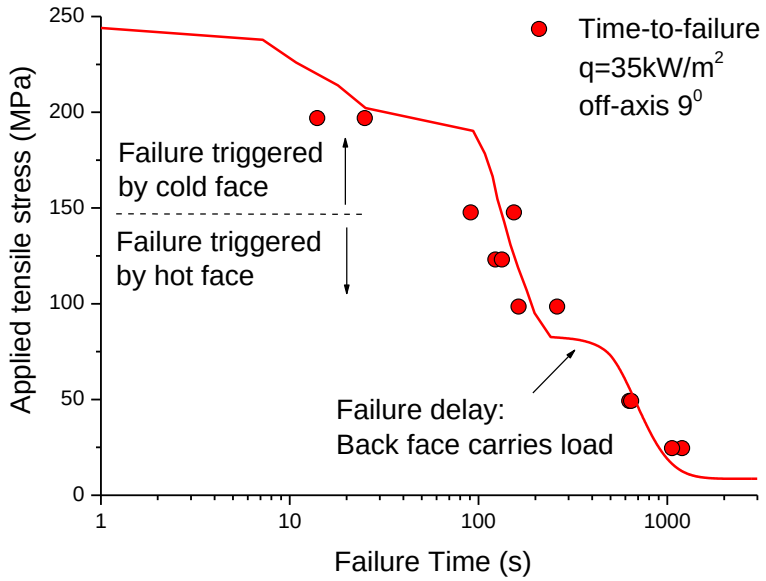
Time-to-failure
q=35kW/m2
off-axis 90
Failure triggered
by cold face
Failure triggered
by hot face
Failure delay:
Back face carries load
Applied tensile stress (MPa)
Failure Time (s)
250
200
150
100
50
0
1
10
100
1000

(b)

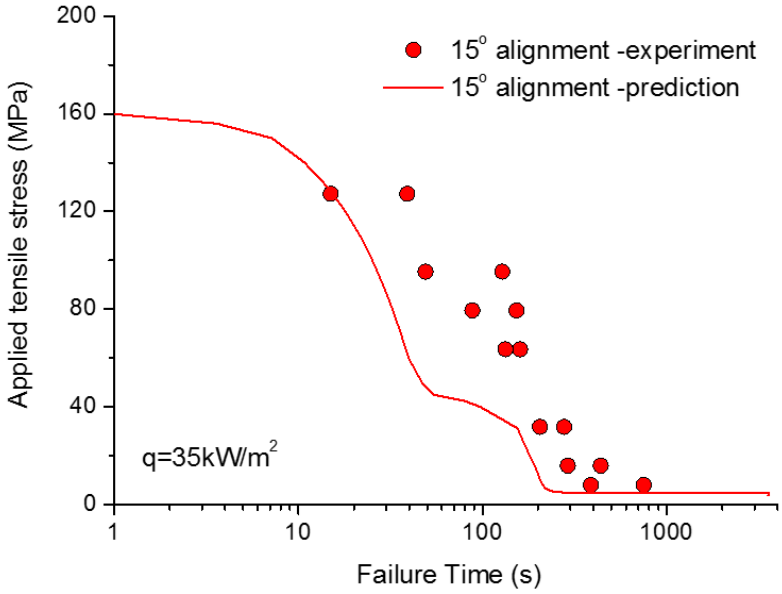
15° alignment -experiment
15° alignment -prediction
q=35kW/m2
Applied tensile stress (MPa)
Failure Time (s)
200
160
120
80
40
0
1
10
100
1000

(c)

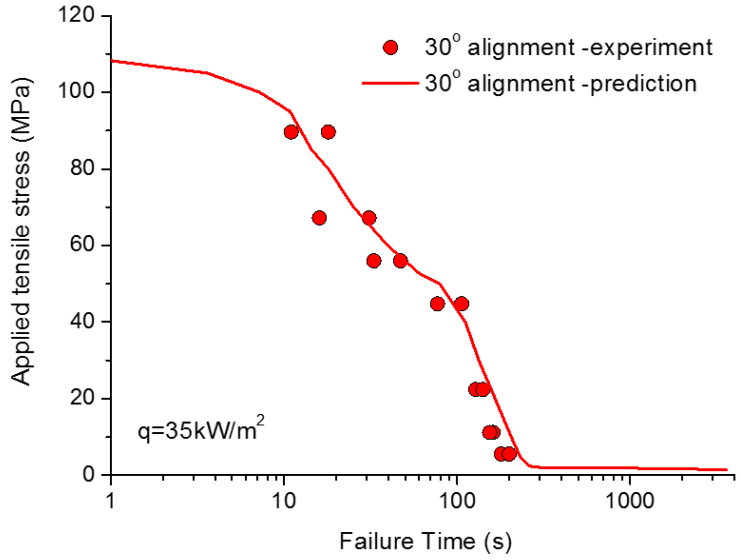

(d)

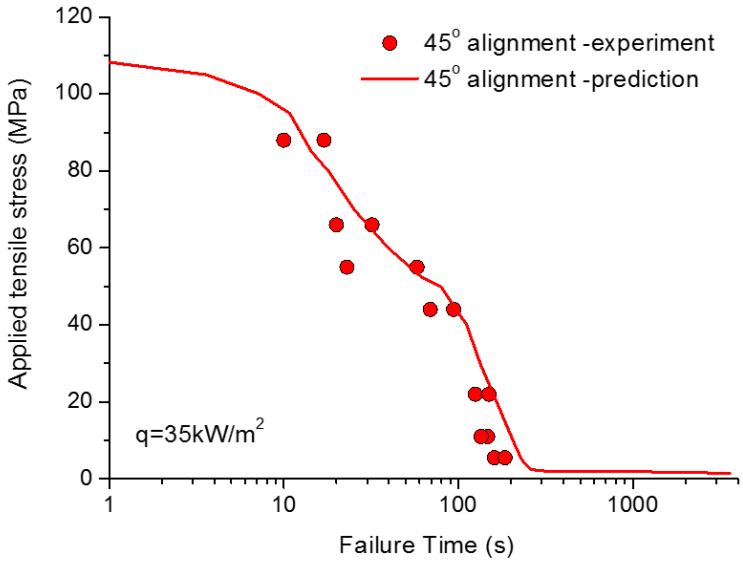

(e)

Figure 4.9: Effect of applied tensile stress on the failure time of the sandwich composite exposed to heat flux 35 kW/m^2 of (a) on-axis 0^0 specimens, (b) off-axis 9^0 specimens, (c) off-axis 15^0 specimens, (d) off-axis 30^0 specimens and (e) off-axis 45^0 specimens.

Table 4.1: Mechanical model parameters for on-axis sandwich specimens.

Composite	P_0	P_R	T_k [ºC]	k_m
Skin modulus E [GPa] (Eq. (3.1))	22	8	100	0.02
Skin load transfer Φ(Eq. (3.14))	1.0	0.65	88	0.026
Fibre bundle strength $\sigma_{fb,0}$ [MPa] (Eq. (3.14))	900	--	--	--
Matrix strength σ_m [MPa] (Eq. 3.(15))	70	1.5	88	0.026
Core (transverse loading)	P_0		ϕ [MPa/ºC]	
Modulus [MPa] (Eq. (3.12))	130.0		0.00057	
Strength [MPa] (Eq. (3.20))	0.83		0.00372	

Table 4.2: Mechanical model parameters for off-axis 9 degree sandwich specimens.

Composite	P_0	P_R	T_k [ºC]	k_m
Skin modulus E [GPa] (Eq. (3.1))	17	5	100	0.02
Skin load transfer Φ(Eq. (3.14))	1.0	0.65	88	0.026
Fibre bundle strength $\sigma_{fb,0}$ [MPa] (Eq. (3.14))	900	--	--	--
Matrix strength σ_m [MPa] (Eq. (3.15))	70	1.5	88	0.026
Core (transverse loading)	P_0		ϕ [MPa/ºC]	
Modulus [MPa] (Eq. (3.12))	130.0		0.00057	
Strength [MPa] (Eq. (3.20))	0.83		0.00372	

Table 4.3: Mechanical model parameters for off-axis 15 degree sandwich specimens.

Composite	P_0	P_R	T_k [ºC]	k_m
Skin modulus E [GPa] (Eq. (3.1))	15	1.4	100	0.02
Skin load transfer Φ(Eq. (3.14))	1.0	0.65	88	0.026
Fibre bundle strength $\sigma_{fb,0}$ [MPa] (Eq. (3.14))	900	--	--	--
Matrix strength σ_m [MPa] (Eq. (3.15))	70	1.5	88	0.026
Core (transverse loading)	P_0		ϕ [MPa/ºC]	
Modulus [MPa] (Eq. (3.12))	130.0		0.00057	
Strength [MPa] (Eq. (3.20))	0.83		0.00372	

Table 4.4: Mechanical model parameters for off-axis 45 degree sandwich specimens.

Composite	P_0	P_R	T_k [ºC]	k_m
Skin modulus E [GPa] (Eq. (3.1))	11	0.25	100	0.02
Skin load transfer Φ(Eq. (3.14))	1.0	0.65	88	0.026
Fibre bundle strength $\sigma_{fb,0}$ [MPa] (Eq. (3.14))	900	--	--	--
Matrix strength σ_m [MPa] (Eq. (3.15))	70	1.5	88	0.026
Core (transverse loading)	P_0		ϕ [MPa/ºC]	
Modulus [MPa] (Eq. (3.12))	130.0		0.00057	
Strength [MPa] (Eq. (3.20))	0.83		0.00372	

Table 4.5: Fibre strength parameters used to solve the model [5].

Values	Fibre bundles Air	Single fibres N_2
$T_{50\%}$ [ºC]	347.6	403.1
p_{fb} [ºC^{-1}]	5.83 x 10^{-3}	6.60 x 10^{-3}
k_1 [s^{-1}]	1.81 x 10^{-6}	1.2 x 10^{-6}
k_2 [ºC^{-1}]	1.45 x 10^{-2}	1.17 x 10^{-2}

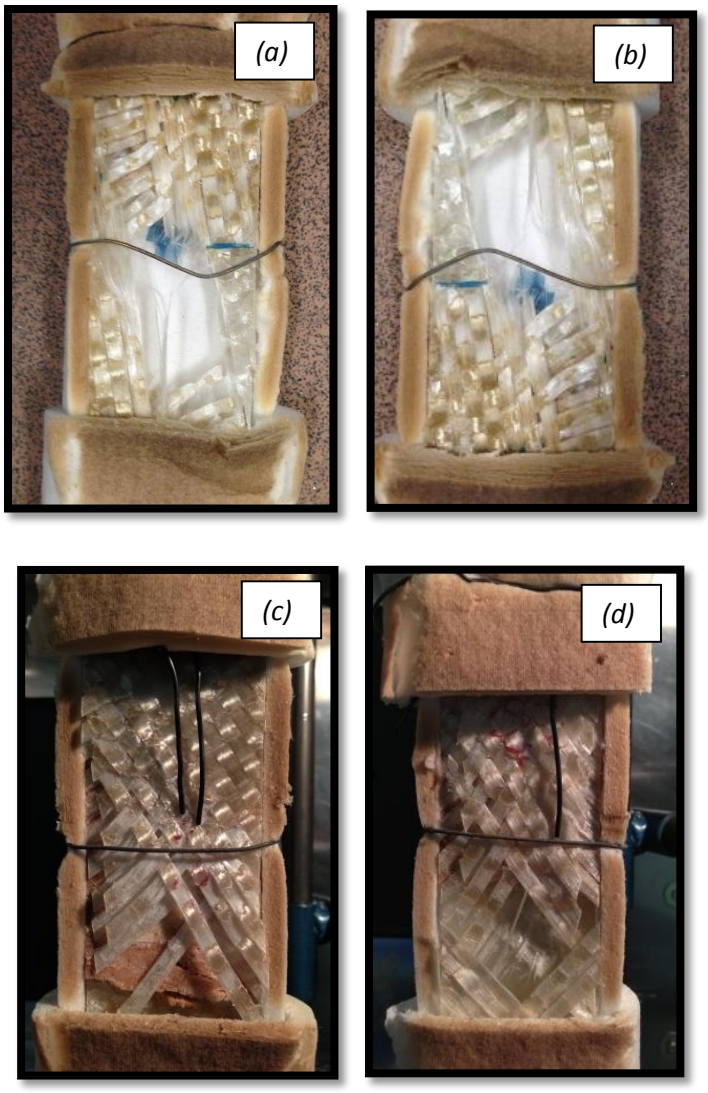

Figure 4.10: Close-up front face view of ruptured sandwich specimen at 80% applied stress of (a) 9^0, (b) 15^0, (c) 30^0 and (d) 45^0 sandwich specimens.

Figure 4.11: Close-up front view of charred and ruptured off-axis specimens tested at 5% applied stress.

4.4 CONCLUSIONS

A thermal-mechanical model for predicting the fire structural response of sandwich composites with misalignment fibre under combined tension loading and one-sided heating has been extended from Chapter. The mechanical model was able to predict the fire structural survivability and failure mode of the sandwich composite under tension loading for both on and off-axis specimens except at 15^0 misalign angle. Both the model and experimental testing showed that the failure time increased when the applied tension stress reduced and the fibre alignment was chosen to the load direction. Agreement between the measured and calculated failure times is good for the off-axis sandwich composites, with exception of 15^0 where the time-to-failure prediction the failure mode of load bearing tows is conservative. The model used to predict the failure times and mechanism for the 30^0 and 45^0 sandwich composites was able to calculate the failure times and failure mechanisms with good accuracy.

Chapter 5 : COMPRESSIVE PROPERTIES OF SANDWICH COMPOSITES IN FIRE

ABSTRACT

This chapter presents new research into the compression modelling and experimental testing of sandwich composites in fire. The research objective is to analytically and experimentally investigate the effect of axial compressive loading on the softening rate, failure time and failure mode of sandwich composites exposed to intense one-sided heating by fire. Small-scale fire structural tests are performed on long and slender sandwich composite beams with woven glass/vinyl ester skins and balsa wood core when subjected to simultaneous compression loading at different stress levels and one-sided radiant heating at a constant flux. The failure time of the sandwich composite decreased rapidly with increasing applied compressive stress due to thermal softening of the heated face skin. The experimental results are compared against a compressive failure model for sandwich composites in fire. The failure model was able to predict the compressive failure times with reasonable accuracy.

5.1 INTRODUCTION

There has been some research progress in modelling the fire structural response of sandwich composites under combined compression loading and one-sided heating, as described in Chapter 2 [3, 10, 42, 55, 59, 62, 63, 82]. Fire structural models have been developed to analyse a sandwich composite that is compressively loaded while simultaneously exposed to one-sided heating by fire. Modelling has revealed that different failure modes can occur depending on the applied compressive stress, intensity of the fire, and geometry of the sandwich composite (skin-to-core thickness ratio). Failure modes that have been modelled include front skin failure, skin wrinkling and core shear cracking. However, the validation of models using experimental data is limited. Feih et al.

[3] validated a model for compressive front skin failure of sandwich composite exposed to fire, and found good agreement between the failure times predicted by the model and measured experimentally by fire structural testing. Apart from this study, there is little published information on the experimental validation of compressive failure models for sandwich composites exposed to fire.

This chapter presents an analytical and experimental study into the fire structural survivability and failure of sandwich composites under compressive loading. The model is validated using experimental data from small-scale fire structural tests performed on a sandwich composite consisting of fibreglass/vinyl ester laminate face skins and balsa core exposed to one possible fire scenario. The study is confined to the deformation and failure mode of the sandwich composite having a long and slender geometry were failure occurs by front skin softening leading to buckling. Other potential compressive failure modes (e.g. skin wrinkling, core shear failure, skin-core debonding) are not considered in this study because they did not occur in the fire structural tests.

5.2 FIRE STRUCTURAL COMPRESSION MODEL

The axial compressive strength of sandwich materials is mostly governed by the strengths of the skins, unless failure occurs by core shear cracking. The model to calculate the time-to-failure under static compressive loading assumes that the compressive strength is dependent on the through-thickness temperature profile. Figure 5.1 shows the typical relationship between compressive strength and temperature for a fibre reinforced polymer laminate used as the skin to sandwich composites. Many laminate systems experience this type of reduction in compressive strength with increasing temperature. The strength remains at the room temperature value ($\sigma_{c(o)}$) until the laminate is heated to a critical softening temperature (T_c), above which the strength decreases with increasing temperature to a minimum value ($\sigma_{c(R)}$). In most cases the critical softening temperature is close to the glass transition temperature of the polymer matrix to the skins. Gibson et al. [39] expressed the relationship between compressive strength and temperature as:

$$\sigma_c(T) = \left(\frac{\sigma_{c(o)} + \sigma_{c(R)}}{2} - \frac{\sigma_{c(o)} - \sigma_{c(R)}}{2} \tanh(k_m(T - T'_g)) \right) R_{rc}(T)^{n'} \quad (5.1)$$

$\sigma_{c(o)}$ is measured by compression testing at room temperature. k_m is a material constant describing the temperature range over which the compressive strength is reduced during the thermal softening process. $\sigma_{c(R)}$, T_k and k_m must be fitted to the elevated temperature compression strength data for the laminate. $R_{rc}(T)$ is a scaling function to account for mass loss due to decomposition of the polymer matrix, and it is assumed that the process of resin decomposition reduces the compressive strength below $\sigma_{c(R)}$. The exponent n' is an empirical value. When $n' = 0$ it is assumed that resin decomposition has no effect on the compressive strength. When $n' = 1$ it is assumed that a linear relationship exists between mass loss and strength loss. Other values of n' can be used to describe non-linear relationships between mass loss and residual strength. The compressive strength data at elevated temperature for the woven E-glass/vinyl ester laminate used in the sandwich composite were obtained from Feih et al. [43], as shown in Figure 5.2.

After the temperature profile through a laminate has been calculated using the thermal model, the residual compressive strength is calculated at a number of locations in the through-thickness direction using Equation 5.1. The bulk compressive strength is then determined by integrating these values over the thickness of the skins using the Simpson integration technique with m intervals, where m must be an even number. t is the thickness of the skins.

$$\int_a^b \sigma(x)\,dx = \frac{b-a}{3m}\left[\sigma(x_0) + 4\sigma(x_1) + 2\sigma(x_2) + \ldots + 2\sigma(x_{k-2}) + 4\sigma(x_{k-1}) + \sigma(x_k)\right] \quad (5.2)$$

$$\sigma_{av} = \frac{1}{b-a}\int_a^b \sigma(x)\,dx \quad (5.3)$$

In the model, it is assumed that the two skins of the sandwich specimens equally support the applied compressive stress, σ_{comp}. The compressive strength of the core is assumed

to not contribute significantly to the load carrying capacity of the sandwich composite, and therefore ignored in the mechanical analysis. Compressive failure is assumed to occur once the average compressive strength (σ_{av}) is reduced to the compressive stress applied to the laminate skin. The time taken for the strength to reach the applied stress is taken to be the time-to-failure.

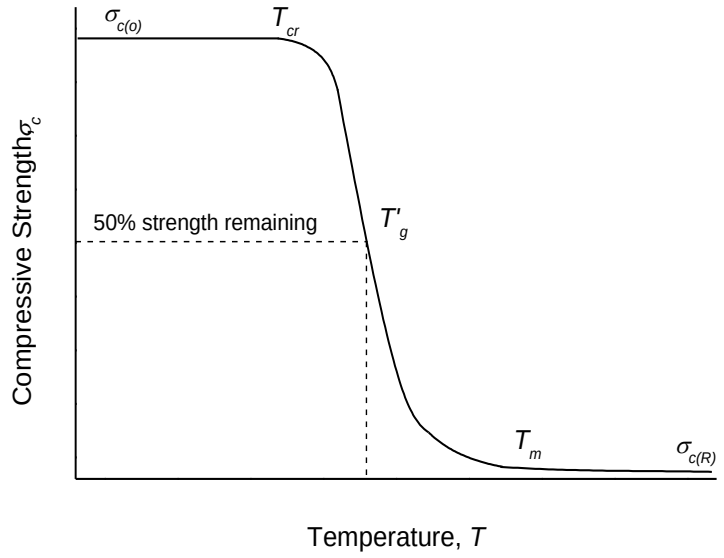

Figure 5.1: Typical effect of temperature on the compressive strength of polymer laminates [50].

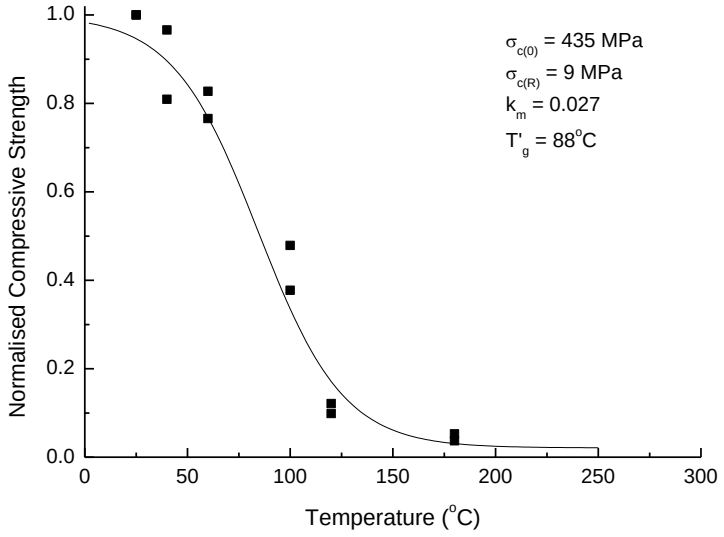

Figure 5.2: Effect of temperature on the normalised compressive strength of fibreglass/vinyl ester laminate skin used in the sandwich composite [43].

5.3 MATERIALS AND COMPRESSION FIRE STRUCTURAL TESTING

The small-scale fire structural test facility described in Chapter 3 was used to experimentally study the fire compressive response of a sandwich composite. The sandwich composite was the same material used for the studies into the fire structural behaviour under off-axis tensile loading (Chapter 4); that is, woven glass/vinyl ester face skins and balsa wood core. The warp tows in the face skins were aligned parallel with the compressive load direction during testing. The sandwich composites were tested in the form of rectangular beam-shaped samples measuring 600 mm long and 50 mm wide, and only a 100 mm long section at the centre of the sample was exposed to the heat flux. The ends of sandwich composite were clamped with the compression loading machine, as shown in Figure 5.3.

Testing involved pre-loading the sandwich specimen in compression while simultaneously heating one side using a radiant heater operated at the constant heat flux of 35 kW/m^2. A constant compressive stress between 20% and 80% of the buckling failure stress at room temperature was applied to the specimens. Duplicate tests were performed on the sandwich composite tested at the same compressive stress levels. The axial contraction and failure time of the sandwich composite was measured from the test, and the times were used to validate the model.

Figure 5.3: End clamping of the sandwich composite specimens for fire structural testing.

5.4 RESULTS AND DISCUSSIONS

The compressive stress-strain response of the sandwich composite at room temperature is shown in Figure 5.4. Stress-strain curves are shown for three sample specimens tested under compression at the end-shortening rate of 0.5 mm/min to failure. The average room temperature buckling stress of the sandwich composite was measured to be 34 MPa. Figure 5.3 shows one of failed sample following testing (three sandwich specimens are tested), and failure occurred by large-scale elastic-plastic Euler buckling due to the high specimen length-to-thickness aspect ratio (about 60-to-1). The other two sandwich specimens fail due to only buckling case, where upon the release of load, there is no visible skin or core damaged is observed. Core shear cracking and partial skin-to-core debonding damage also occurred to the samples tested at room temperature, although this is believed to follow failure by buckling.

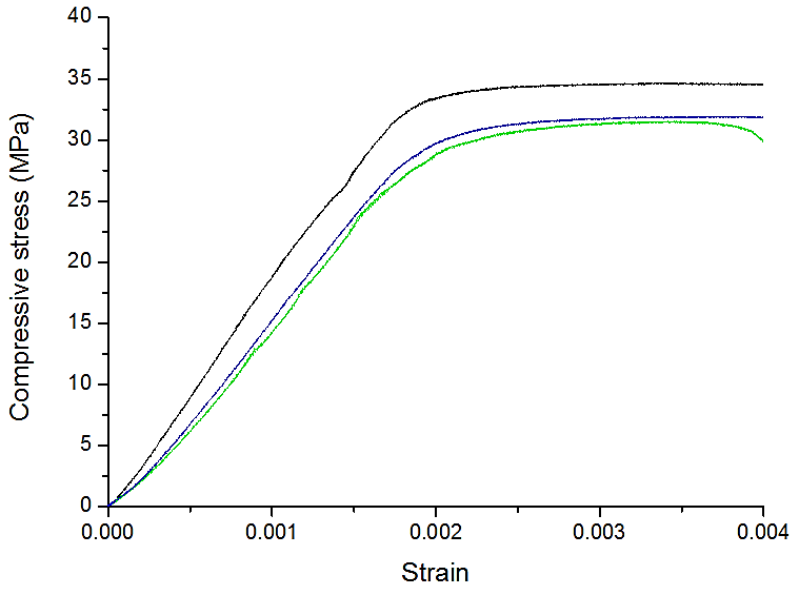

Figure 5.4: Compressive stress-strain curves for the sandwich composite at room temperature.

Typical temperature-time curves for the front and back surfaces of the sandwich composite during exposed to the heat flux of 35 kW/m^2 are shown in Figure 5.5. Curves are shown for the measured and calculated temperatures. The calculated temperatures were determined using the thermal model presented in Chapter 3. As previously reported, the model predicts the thermal response of the sandwich composite with good accuracy. Unlike tensile loading, it was found that the temperature of the sandwich composite was not affected by the applied compressive stress (as shown in Figure 5.6). For the different stress levels, there was no measurable difference between the temperatures. Under compression loading the cracks within the balsa core do not open up, and therefore the accelerated egress of flammable volatiles which causes the higher temperatures under tensile loading do not occur under compression.

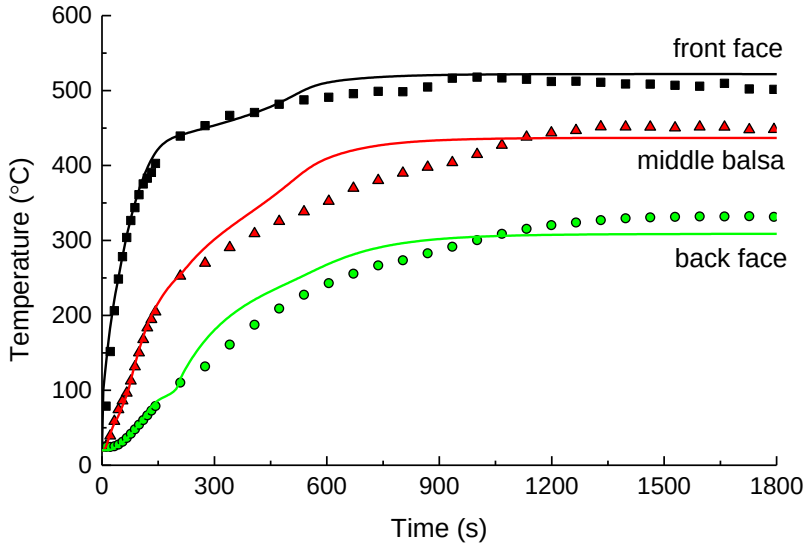

Figure 5.5: Unload temperature-time profiles of the sandwich composite.

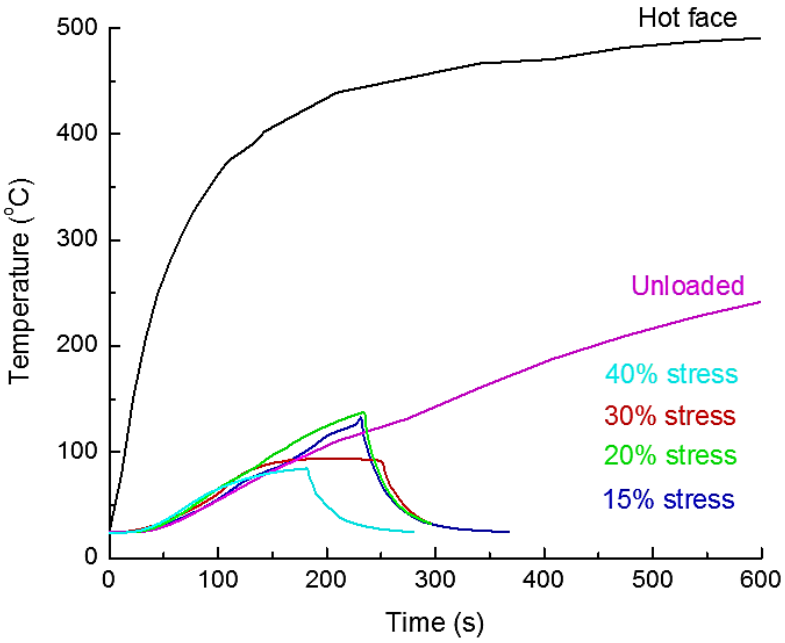

Figure 5.6: Effect of applied tensile load on the back face temperature of the sandwich composite.

Axial displacement-heating time curves were measured at different load levels (15% to 40% of the buckling stress at room temperature), and these are shown in Figure 5.7. As expected, the failure times increased with decreasing applied stress. Due to the large load cell capacity (250 kN) to the compression machine, the displacement vs time curves generated in the fire structural tests were “noisy” as the applied load was only about 1 to 5 kN. Despite this, the curves reveal that the sandwich composite experienced only a small amount of axial contraction before failing catastrophically, indicating structural stability preceding final failure.

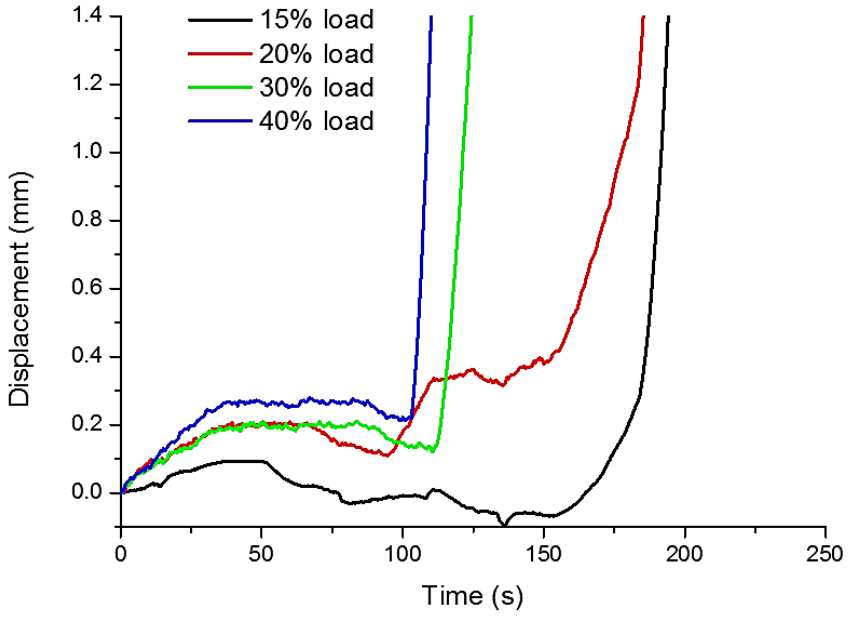

Figure 5.7: Experimental axial displacement-heating time curve for the sandwich composite.

Figure 5.8 shows the effect of applied compressive stress on the failure time of the sandwich composite measured by fire structural testing at the heat flux of 35 kW/m^2. As expected, the failure times increased with decreasing applied stress. The curves in the figure show the calculated times that were computed using the thermal-mechanical model described in Section 5.2. The model is solved using temperature profile through the sandwich composite and the compressive strength properties at elevated temperature. The relationship between strength and temperature is described in previous section in this chapter. The model predicts that the failure time increases when the applied stress

is reduced, and this agrees with the experimental data. A similar trends has been measured for laminated composites where the time-to-failure increases with decreasing applied compressive stress [43]. The model slightly under-predicted the experimental data due to no consideration being made for progressive ply failure as the model is purely strength-based. However, the model is able to predict the overall trend of failure times and progressive failure is suspected to have only minor influence on the time-to-failure. Figure 5.7 shows the failure modes of the sandwich specimens tested at different compression load levels. In this study, all sandwich specimens subjected to the heat flux failed by compressive failure of the front (heated) skin, irrespective of the applied stress. There was no appreciable damage to the back skin.

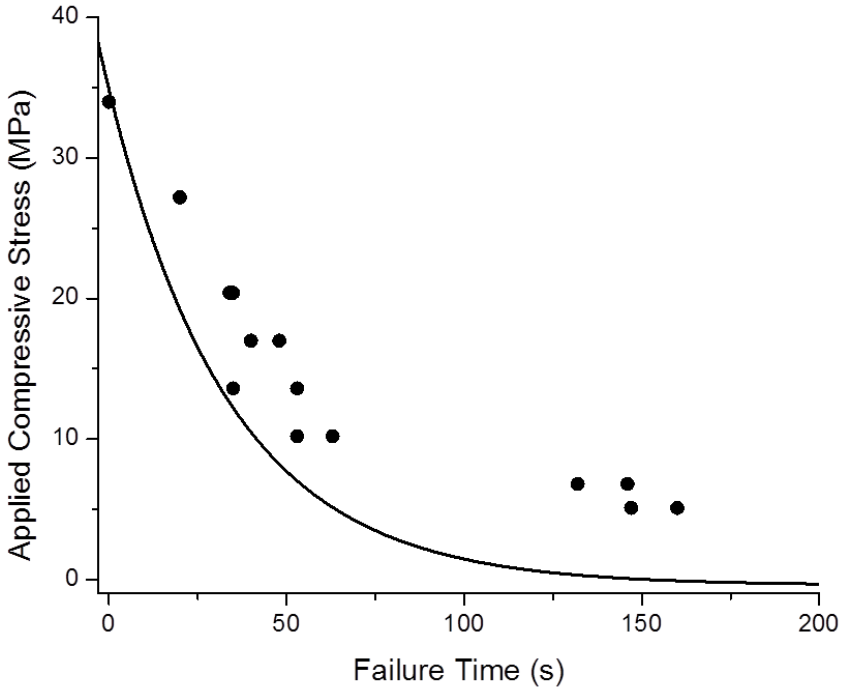

Figure 5.8: Effect of applied stress on the failure times of the sandwich composite. The curve was calculated using the thermal-mechanical model.

Figure 5.9: Failure modes of sandwich specimens tested at different compressive load levels as a percentage of the failure load at room temperature.

5.5 CONCLUSIONS

The thermal-mechanical model presented in this chapter to estimate the residual compressive strength of sandwich composite materials and the time-to-failure has been developed and validated. However, the model needs to be further developed to account for progressive failure. The model predicts that the failure times decrease by reducing the applied stress. It is envisaged that the model can be used in the design of sandwich composite materials with improved fire structural compression properties.

Chapter 6 : POST-FIRE MECHANICAL PROPERTIES OF SANDWICH COMPOSITES

ABSTRACT

This chapter presents original research into the post-fire experimental testing and modelling of sandwich composites materials. The effects of increasing heat flux exposure time and heat flux level on the residual tensile and compressive properties of the sandwich composite are experimentally determined. The residual properties are compared to the types and amounts of fire-induced damage. A new model for calculating the post-fire mechanical properties of the sandwich composite is formulated, and predictions are compared against experimental results. Experimental testing reveals that the residual tensile and compressive properties decrease rapidly due to thermal decomposition to the fire-exposed face skin. The model can accurately predict the post-fire stiffness and strength properties. The research described in this chapter provides important new insights into the residual structural integrity of burnt sandwich composite structures following fire exposure.

The work presented in this chapter has been submitted for publication:
A. Anjang, V.S. Chevali, B.Y. Lattimer, S. Feih and A.P. Mouritz, 'Modelling the post-fire mechanical properties of sandwich composites', Composites Part A.

6.1 INTRODUCTION

A factor restricting the wider use of polymer composites by the marine industry is the reduction in strength and stiffness experienced by the structure following fire [1]. The polymer matrix used in the sandwich structure will decompose, ignite and burn when exposed to high temperature fire. Similar to polymer matrix, most core materials used in sandwich composites (e.g. polymer foam, syntactic foam, balsa wood) are flammable. Fire is a major threat to the application of sandwich composites used in aircraft, ship, civil infrastructure, offshore platform and other uses. Inadequate fire protection will result in

rapid ignition of sandwich composite structures that release large amounts of heat (which adds to the fuel load), smoke and potentially toxic fumes [6, 15, 16]. After a fire is extinguished, it is very important to analyse the post-fire properties in order to assess the residual integrity and safety of the structure.

Fire structural performance and survivability of sandwich composites rely on both modelling and experimental testing, as described in Chapter 3. A large amount of experimental data reveals that the post-fire properties of laminates are mainly determined by the temperature, heating time, loading condition, and decomposition properties of the polymer matrix [8, 66-71, 73, 74, 83]. Less experimental data is available on the post-fire properties of sandwich composite materials [15]. For the scope of post-fire analytical modelling, the two-layer model is the most established method used in calculating the post-fire properties of laminates, as presented in Section 2.5 [66].

Similar to laminates, there is also a need to calculate the residual mechanical properties of sandwich composites after the fire has been extinguished. Determining the post-fire properties is important in order to evaluate the structural integrity and safety of heat-affected and burnt sandwich structures. Mouritz and Gardiner [40] developed a model to calculate the post-fire compressive stiffness and strength of polymer core sandwich composites which failed by core shear cracking or front skin buckling. The work by Gardiner and Mouritz revealed that the extent of decomposition (char) through the sandwich composite is a major factor controlling the post-fire compressive properties. Ulven and Vaidya [84] experimentally assessed the effect of fire on the impact response of sandwich composite materials. Apart from these two studies, the post-fire mechanical properties of sandwich composites have not been studied.

This chapter presents a thermal-mechanical model for calculating the post-fire mechanical properties of sandwich composite materials. The thermal component of the model computes the heat conduction through the sandwich composite and the resultant decomposition to the face skins and core. The mechanical component calculates the residual stiffness and strength properties of the fire-damaged sandwich composite based

on the extent of decomposition. The accuracy of the model is assessed using post-fire tensile and compressive property data for a sandwich composite material consisting of woven glass/vinyl ester laminate face skins and balsa wood core.

6.2 POST-FIRE MODEL

The model to calculate the post-fire mechanical properties involves thermal, decomposition and mechanical analysis of sandwich composites with organic face skins and core. The model involves three main analytical steps: (1) thermal analysis, (2) decomposition analysis and (3) post-fire property analysis. The first step involves thermal analysis to calculate the through-thickness temperatures of the sandwich composite when heated from one-side by fire. The second step involves computing the amount of through-thickness decomposition (char formation) to the sandwich composite, which is based on the thermal analysis. The final step involves the use of mechanical models to calculate the post-fire tensile and compressive properties of the sandwich composite at room temperature, which is based on the decomposition analysis. It is assumed with the model that the reduction to the post-fire properties is caused solely by char formation, and that other types of heat-induced damage (e.g. skin-core debonding, delaminations in the skins) have no effect on the properties.

Step 1: Thermal Analysis

Thermal analysis of the sandwich composite exposed to one-sided radiant heating representative of a possible fire scenario is based on the model developed by Feih et al. [3] as described in Chapter 3. The thermal analysis assumes that the sandwich composite is uniformly heated over one face skin, and heat transfer only occurs in the through-thickness direction (and not in the lateral or transverse directions). The thermal model described in Chapter 3 (section 3.2.2) is used to calculate the temperature of the sandwich composite exposed to fire. h_{solid} and h_{gas} are the enthalpies of the solid material and decomposition gas, respectively, and respectively are defined as:

$$h_{solid} = \int_{T_\infty}^{T} C_{p(solid)} dT \tag{6.1}$$

$$h_{gas} = \int_{T_\infty}^{T} C_{p(gas)} dT \tag{6.2}$$

k_x, $C_{p(solid)}$, $C_{p(gas)}$ and E_a must be experimentally determined for the skins and core.

The thermal model is validated in this study using a sandwich composite consisting of woven E-glass/vinyl ester laminate skins and balsa wood core. Lattimer et al. [77] experimentally determined the thermal conductivity of these materials up to about 600°C, and are defined as a function of temperature using:

skin
$$k_{x(s)} = 4.405x10^{-5}T + 0.312 \quad \text{below the matrix decomposition temperature} \tag{6.3a}$$
$$k_{x(s)} = 2.83x10^{-4}T + 0.095 \quad \text{above the matrix decomposition temperature} \tag{6.3b}$$

core
$$k_{x(c)} = 9.211x10^{8}T^{2.503} + 0.06 \quad \text{below the balsa decomposition temperature} \tag{6.4a}$$
$$k_{x(c)} = 2.223x10^{6}T^{2.503} + 0.0008 \quad \text{above the balsa decomposition temperature} \tag{6.4b}$$

Lattimer et al. [77] also determined the empirical relationship between specific heat capacity and temperature for the skins and core:

skin
$$C_{p(s)} = 0.0452T + 1080 \quad \text{below the matrix decomposition temperature} \tag{6.5a}$$
$$C_{p(s)} = 0.259T + 1041 \quad \text{above the matrix decomposition temperature} \tag{6.5b}$$

core
$$C_{p(c)} = 0.68T + 1420 \quad \text{below the balsa decomposition temperature} \tag{6.6a}$$
$$C_{p(c)} = 1.33T + 3194 \quad \text{above the balsa decomposition temperature} \tag{6.6b}$$

The specific heat capacities of the gases evolved from the polymer matrix to the skins and the balsa core are dependent on the temperature according to [77]:

skin
$$C_{pg(s)} = -91.151 + 4.400T - 1.7279x10^{-3}T^2 \tag{6.7a}$$

core $C_{pg(c)} = 299.8 + 5.4037T - 1.60x10^{-3}T^2$ (6.7b)

Step 2: Decomposition Analysis

Decomposition of the polymer matrix to the face skins and to the organic core is assumed to occur via a single-stage reaction process. The decomposition reaction rate can be defined by the density change to the skins or core ($d\rho/dt$) due to mass loss caused by the conversion of solid material to volatiles. When the skins and core decompose via a single-stage decomposition process then the density change can be expressed using the Arrhenius relationship:

Skins $$\frac{d\rho_{(s)}}{dt} = -(\rho_{v(s)} - \rho_{d(s)})\left[\frac{\rho - \rho_{d(s)}}{\rho_{v(s)} - \rho_{d(s)}}\right]^n A_{(s)} e^{-(E_a/RT)} \quad (6.8)$$

Core $$\frac{d\rho_{(c)}}{dt} = -(\rho_{v(c)} - \rho_{d(c)})\left[\frac{\rho - \rho_{d(c)}}{\rho_{v(c)} - \rho_{d(c)}}\right]^n A_{(c)} e^{-(E_a/RT)} \quad (6.9)$$

n and *A* are the reaction order constant and pre-exponential factor, respectively. *R* is the universal gas constant. ρ_t, ρ_v and ρ_d are the instantaneous density, original (virgin material) density and density of the decomposed material, respectively.

Gibson et al. [74] found that for thermoset matrix laminates the onset of char formation occurs when the instantaneous density reached 0.8 (i.e. 20% of the original density of the polymer matrix had thermally decomposed to volatiles). Gibson and colleagues found that when this occurs, the polymer matrix assumes the visible blackness characteristic of char formation, even though it has not completely decomposed. During this approach, the thermal model (Eq. 6.8) is used to compute the temperatures at many points through-the-thickness of the sandwich composite for increasing increments of heating time. When the local temperature at any point is sufficiently high to cause a 20% reduction to the density of the polymer matrix to the skins using Eq. 6.8 or to the core with Eq. 6.9 then charring had occurred. By solving these equations for increasing heating times it is possible to

calculate the initiation and growth of the char region from the front skin surface exposed directly to the fire through the core and towards the back skin (which is coolest).

Step 3: Post-Fire Mechanical Property Analysis

As mentioned in Chapter 2, models have been formulated by Mouritz and colleagues [66, 68] to calculate the post-fire stiffness and strength of fibre-polymer laminates. The models treat the fire-damaged composite as a two-layered material: one layer consisting of thermally decomposed (char) material and the other layer being pristine laminate. It is assumed in the model that the polymer matrix within the decomposed layer is degraded into a brittle and weak solid char and volatile gases, and therefore has negligible stiffness and strength. The pristine layer is assumed to be unaffected by fire exposure and therefore its mechanical properties are taken to be the same as the virgin (original) laminate. The pristine layer can exceed the glass transition temperature during fire exposure, but does not reach the temperature to cause decomposition and charring of the polymer matrix. When the material within the pristine layer cools to room temperature following fire exposure the properties of the polymer are assumed to revert back to the original values with no residual softening or heat-induced damage. The post-fire properties are calculated by assuming a reduction in the net load-bearing section of the laminate due to the decomposition (char) layer.

The modelling framework developed by Mouritz et al. [66, 68] for laminates is applied here to calculate the post-fire mechanical properties of sandwich composites. That is, the mechanical properties of the face skins and core are assumed to be negligible when thermally degraded to char. Char formation is assumed to occur when the temperature is sufficiently high to cause a 20% density loss to the polymer matrix of the skins or to the core, as mentioned earlier. The mechanical properties of the skins (calculated using Eqs. 3.1a and 3.1b as described in Chapter 3) and core (using Eqs. 6.8 and 6.9) without char damage are assumed to be the same as their original properties. This is supported by work which shows that the post-fire properties of laminates similar to the face skins recover their original properties when matrix decomposition does not occur [8, 66, 67, 70].

Similarly, core materials such as balsa wood recover most of their mechanical properties following heating to temperatures up to the decomposition temperature [78].

Post-Fire Modulus

The axial tensile and compressive modulus (E) of a sandwich composite is determined using:

$$E = \frac{E_{s,1}t_{s,1} + E_{s,2}t_{s,2} + E_c t_c}{t} \tag{6.10}$$

The subscripts 1 and 2 refer to the front and back skins, respectively. E_s and E_c is the original Young's modulus of the skin or core, respectively. t_s, t_c and t are the thickness of the skin, core and sandwich composite, respectively.

When it is assumed that the elastic modulus of any portion of the skins and core are reduced to zero (i.e. $E_s = 0$, $E_c = 0$) when decomposed to char and that the strain across the load-bearing section of the sandwich composite is uniform, then the post-fire modulus is determined using:

$$E_{pf} = E_{s,1}\frac{(t_{s,1} - t_{char,1})}{t_{s,1}} + E_{s,2}\frac{(t_{s,2} - t_{char,2})}{t_{s,2}} + E_c\frac{(t_c - t_{char,c})}{t_c} \tag{6.11}$$

where $t_{char,1}$, $t_{char,2}$ and $t_{char,c}$ are the thicknesses of the char region in the front skin, back skin and core, respectively. Knowing the original elastic modulus and the thickness values for the skins and core together with computing the char depth using the procedure described above, then the post-fire tensile or compressive modulus of the sandwich composite can be determined.

Post-Fire Tensile Strength

When a sandwich composite without fire damage is axially loaded in tension and it is assumed that the face skins and the core have the same strain, then the stress distributions for the material constituents are calculated using:

$$\sigma_{s1} = \frac{E_{s1}F}{A_s(E_{s1} + E_{s2}) + A_c E_c} \tag{6.12a}$$

$$\sigma_{s2} = \frac{E_{s2}F}{A_s(E_{s1} + E_{s2}) + A_c E_c} \tag{6.12b}$$

$$\sigma_c = \frac{E_c F}{A_s(E_{s1} + E_{s2}) + A_c E_c} \tag{6.12c}$$

where A_s and A_c are the load-bearing areas of a single skin and core, respectively. F is the applied tension load.

Following fire exposure and when it is assumed that the tensile strength of any portion of the skins or core is reduced to zero when the material decomposes to char, then the residual tensile failure stress of the sandwich composite (σ_{pf}) can approximated using:

$$\sigma_{T,pf} = \sigma_{t,s,1}\frac{(t_{s,1} - t_{char,1})}{t_{s,1}} + \sigma_{t,s,2}\frac{(t_{s,2} - t_{char,2})}{t_{s,2}} + \sigma_{t,c}\frac{(t_c - t_{char,c})}{t_c} \tag{6.13}$$

where the subscript T refers to tension.

Post-Fire Compressive Strength

The post-fire compressive strength of a sandwich composite is dependent on the failure mode, which can involve global buckling, core shear failure, skin failure or skin wrinkling. The model used to compute the post-fire compressive stress is dependent on the failure mode. In this study, only one failure mode is considered: global buckling. This occurs when the face skins are thin and the core is thick and when the length of the sandwich composite is much greater than its thickness. When it is assumed that any portion of the

skins or core which have decomposed to char have no residual compressive stiffness, then the post-fire buckling load (P_{pf}) can be determined using:

$$P_{C,pf} = 4\pi^2 E_C b(t - t_c)\left[\frac{0.2887\,(t - t_c)}{L}\right]^2 \tag{6.14}$$

E_c is the original compressive modulus of the sandwich composite without fire damage. b and L are the width and unsupported length of the sandwich composite, respectively. From this equation, the post-fire compressive buckling stress is simply calculated:

$$\sigma_{C,pf} = \frac{P_{C,pf}}{bt} \tag{6.15}$$

6.3 MATERIALS AND POST-FIRE STRUCTURAL TESTING

Similar to the previous research chapters, the sandwich composite used in this post-fire study is representative of the material used in naval ship structures. The laminate face skins to the sandwich composite were manufactured from E-glass plain woven fabric (830 g/m^2, Colan Industries) and vinyl ester resin (Derakane 411-350). The same manufacturing process as described in Section 3.3.1 is performed to manufacture the sandwich composites studied in this chapter.

Small-scale post-fire structural tests were performed on sandwich specimens to generate the experimental data in order to validate the model. In order to simulate fire exposure, the sandwich composite was exposed to one-sided radiant heating that is representative of one possible fire scenario. A 100 mm long section of the front skin was exposed directly to an electric heater that radiated a constant heat flux of 35 kW/m^2 for different times up to a maximum of 20 minutes, at which point the sandwich composite was completely decomposed. The surface temperatures of the two face skins were recorded continuously using thermocouples during exposure to the heat flux.

Following heating, the sandwich composite samples were cooled to room temperature and the extent of decomposition and post-fire mechanical properties were measured. The post-fire tensile stiffness and strength was measured by axially loading the sandwich composite at an extension rate of 2 mm/min to failure. The geometry and dimensions of the tensile specimen is shown in Figure 6.1a. Tensile failure always occurred within the heat-affected region of the sandwich specimen. The post-fire compressive properties were determined using the specimen illustrated in Figure 6.1b. For post-fire compression, testing involved axially compressing the sandwich specimen at an end shortening rate of 0.5 mm/min to failure. The ends of sandwich composite were clamped (Figure 6.2) and the relatively large unsupported length-to-thickness ratio (approximately 50-to-1) caused the sample to deform and fail by Euler buckling with the largest lateral deflection at the mid-point. The post-fire modulus was determined using a 25 mm long extensometer attached to the fire-damaged region of the sandwich composite.

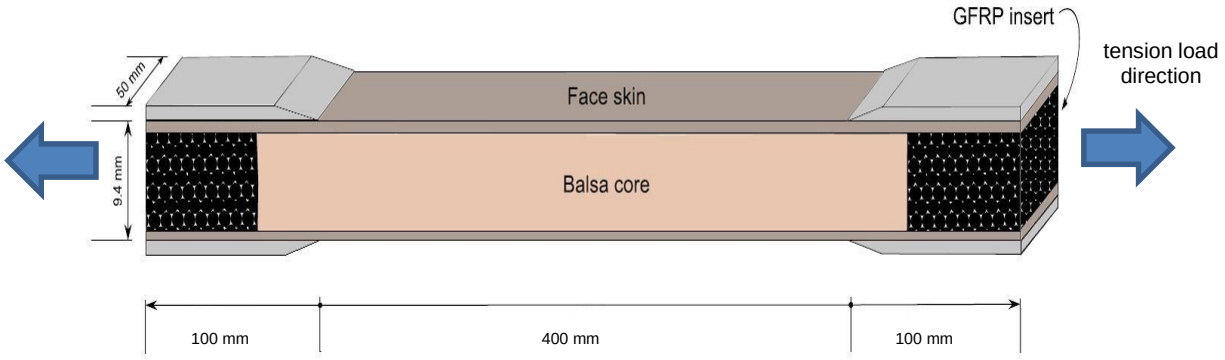

(a)

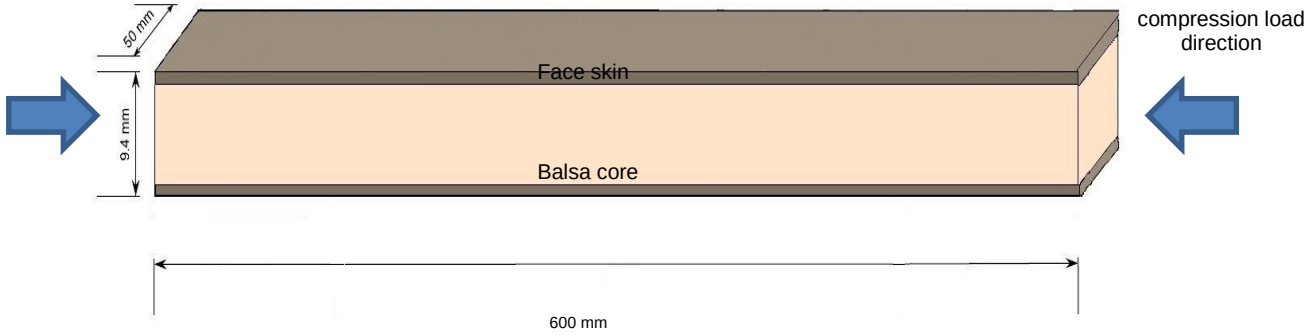

(b)

Figure 6.1: Geometry and dimensions of the test specimens for (a) post-fire tension and (b) post-fire compression testing.

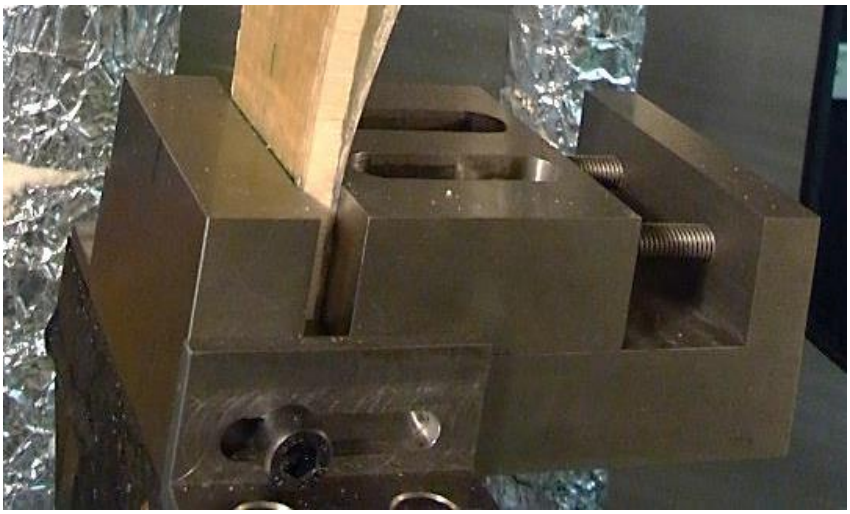

Figure 6.2: End clamped of the specimen for post-fire compression testing.

6.4 RESULTS AND DISCUSSIONS

6.4.1 Thermal and Decomposition Response of Sandwich Composite

Figure 6.3 shows the effect of heating time on the temperature of the sandwich composite exposed to the radiant incident heat flux of 35 kW/m^2. The data points and solid lines show respectively the measured and calculated temperature-time profiles at the heated

(front) face skin, middle of the balsa core, and unheated (back) skin. The temperature profiles were calculated with the thermal model described in Chapter 3.

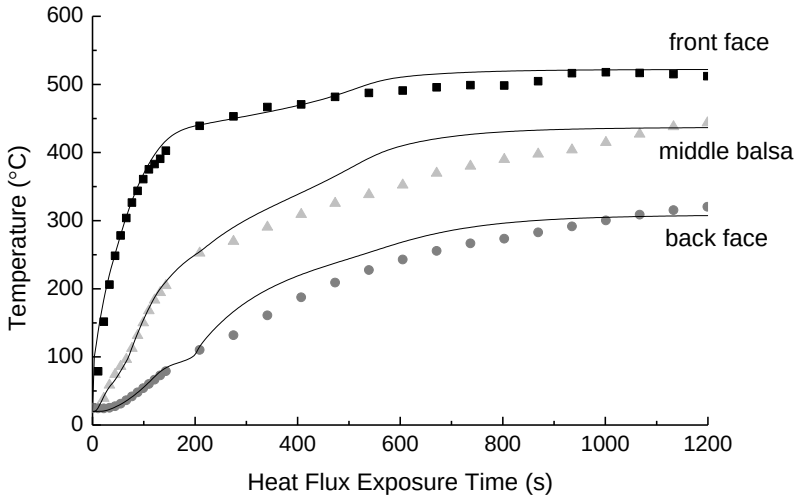

Figure 6.3: Temperature-time profiles at the front (heated) skin, middle of the balsa core and back skin of the sandwich composite exposed to the heat flux of 35 kW/m^2. The curves and data points are the calculated and measured temperatures, respectively.

The organic materials within the sandwich composite thermally degrade when heated above a critical decomposition temperature. The temperature range over which the sandwich composite (vinyl ester resin and balsa wood core) decomposed has been determined using thermogravimetric analysis (TGA) on the vinyl ester resin used in the laminate face skins and on the balsa wood core [78, 85]. The TGA of the vinyl ester and balsa was performed by Feih et al. [4] and Goodrich et al. [85], respectively. TGA was performed on the vinyl ester and balsa at 20^{o}C/min in nitrogen atmosphere using a Netzsch STA 449 F1 Jupiter instrument. Due to the relatively high moisture content within the balsa, the wood was dried at 110°C before TGA testing. Mass loss-temperature curves measured using TGA for the vinyl ester resin used in the laminate face skins and the balsa wood core are shown in Figure 6.4. The polymer matrix within the skins decomposes over the temperature range of about ~350 and 450^{o}C into a highly porous carbonaceous char. The temperature of the front skin exposed directly to the heat flux reached the decomposition temperature very rapidly (in less than 100 seconds), as shown

in Figure 6.3. Decomposition of the polymer matrix and the vapourisation of the low molecular weight gases created by the decomposition reaction transformed the laminate face skin into a highly porous material consisting mostly of the glass fibre reinforcement and a small amount of char, as shown in Figure 6.5 [70]. The TGA curve for the balsa shows that decomposition started at about 250^{o}C and was largely complete by ~350-400^{o}C, with about 80% of the original mass transformed into volatiles and the remaining 20% transformed into charred wood. Figure 6.6 shows the original microstructure micrographs (SEM) of the balsa at room temperature and following heating within the decomposition temperature range [78]. During decomposition the balsa become highly porous due to the break-down of the organic constituents such as cellulose, hemicellulose and lignin [78].

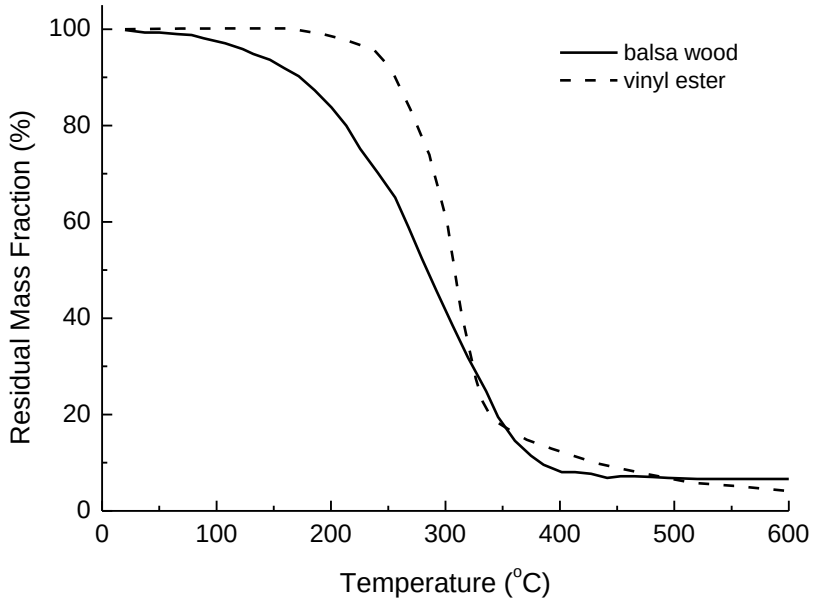

Figure 6.4: TGA mass loss-temperature curves for the vinyl ester resin and balsa wood. The TGA curves for the vinyl ester and balsa were taken from Feih et al. [4] and Goodrich et al. [78].

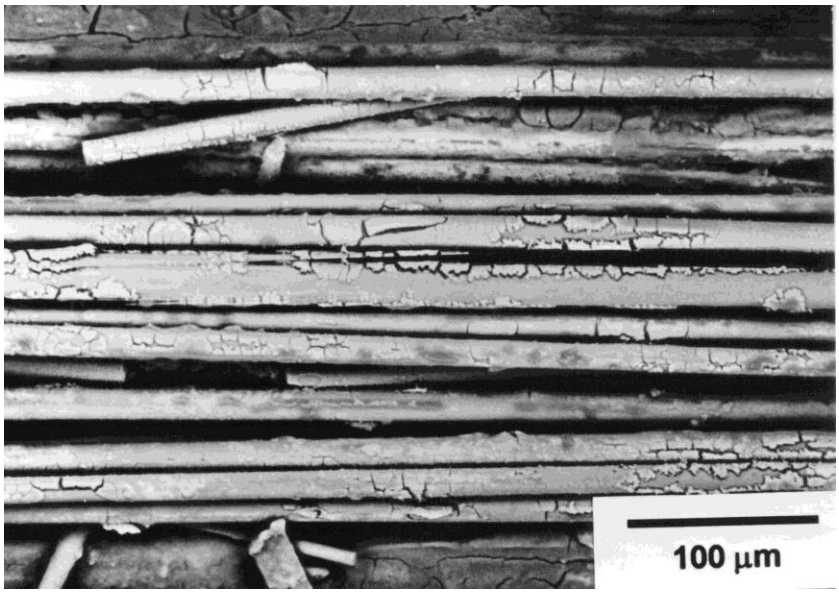

Figure 6.5: Microstructure of the laminate after thermal decomposition of the polymer matrix. The decomposed laminate consists of exposed glass fibres and a small amount of residual char [70].

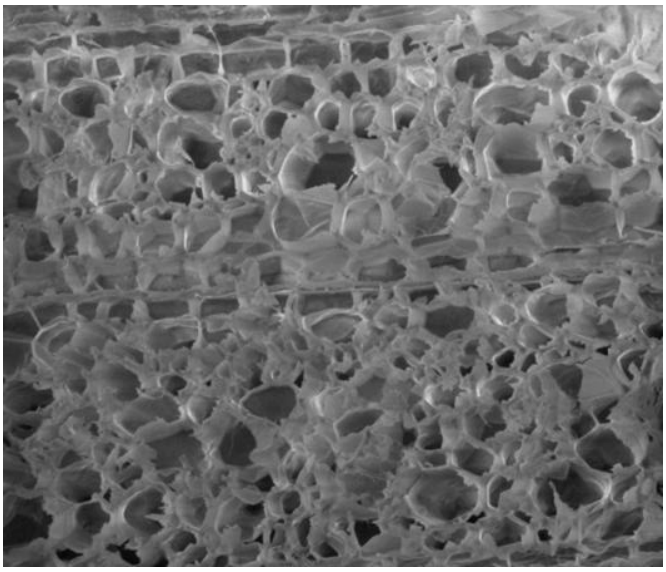

(a)

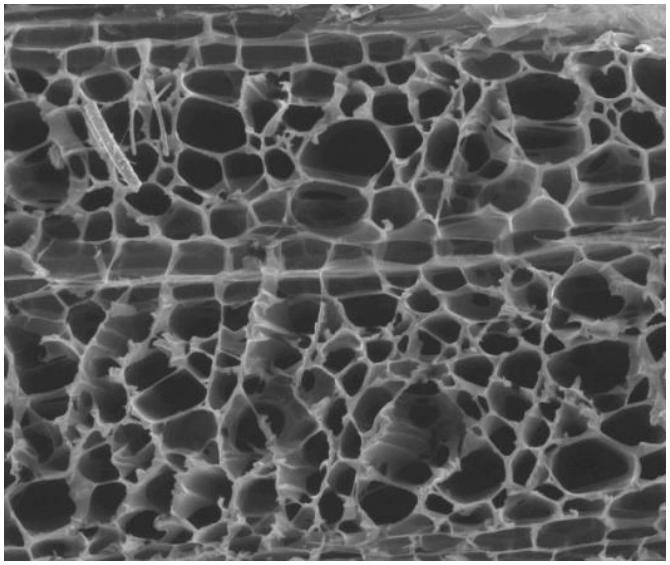

(b)

Figure 6.6: Microstructure of the balsa (a) before and (b) after thermal decomposition. The balsa in (b) was heated to 307^{o}C. Images from Goodrich et al. [78].

Figure 6.7 shows the effect of increasing exposure time to the radiant heat flux on the physical condition of the sandwich composite in the through-thickness direction. The decomposed material appears dark due to char formation, and as expected this began thicker with longer exposure time to the heat flux. A plot of the effect of heat flux exposure time on the percentage thickness of the sandwich composite which has thermally decomposed to char is shown in Figure 6.8. The char thickness increased rapidly with time up to ~10 mins, beyond which both face skins and the entire core had completely decomposed to char (see Fig. 6.7c). The data points are the measured percent char thickness values and the curve was calculated using the thermal decomposition model. The agreement between the measured and calculated char thickness values is good, although the model slightly over-predicts the extent of charring for shorter times (under ~10 mins) and under-predicts at longer times. The char predictions are sensitive to the calculated temperatures through-the-thickness of the sandwich composite. The thermal model (Eqns. 6.1 and 6.2) gave a good, but not precise, prediction of the temperatures (Fig. 6.4) and this would account for the small discrepancy between the measured and calculated char thickness values.

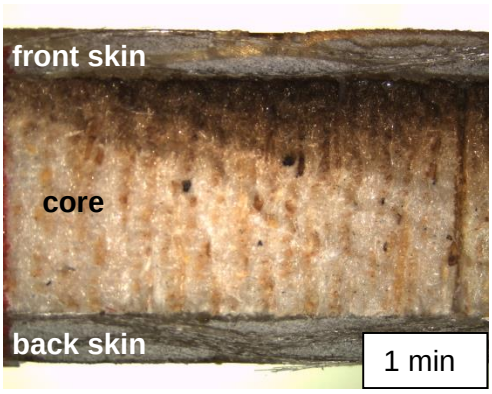

(a)

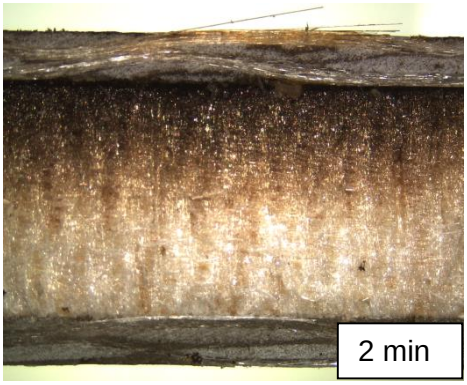

(b)

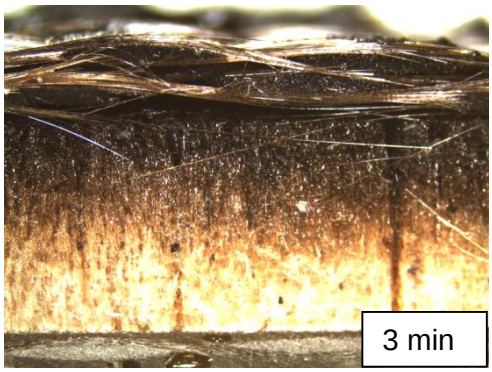

(c)

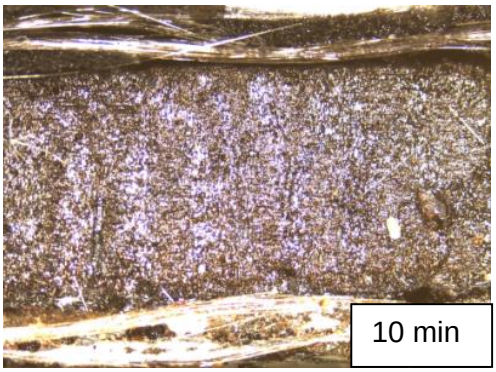

(d)

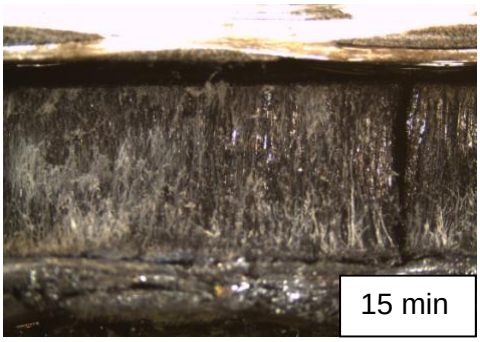

(e)

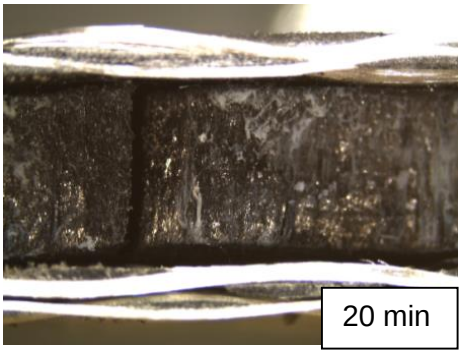

(f)

Figure 6.7: Cross-sectional digital views of the sandwich composite following exposure to the heat flux for different times. The top face skin was directly exposed to the heat flux (35 kW/m^2).

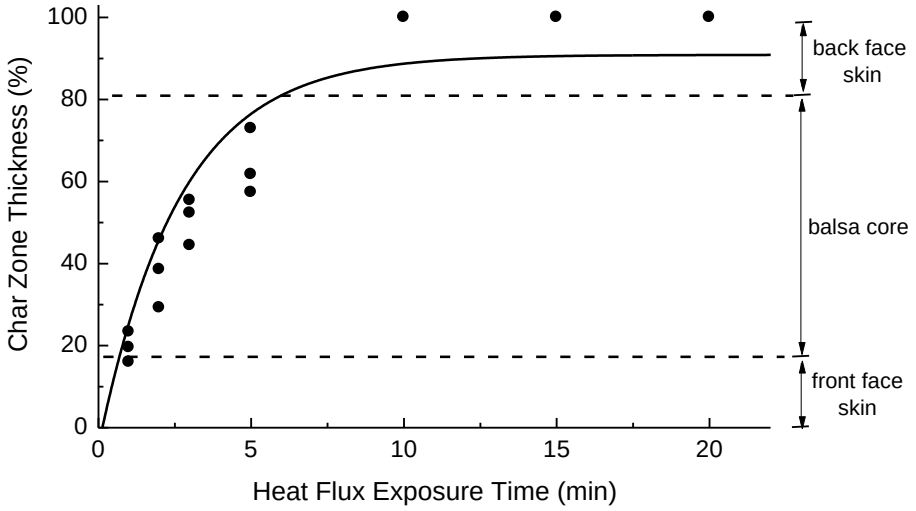

Figure 6.8: Effect of heat flux (35 kW/m^2) exposure time on the percentage thickness of the sandwich composite which has thermally decomposed to char. The data points and curve show the measured and calculated char thickness values, respectively. The relative thicknesses of the face skins and core are indicated.

6.4.2 Post-fire Tensile Properties

Figure 6.9 presents measured tension stress-strain curves for the sandwich composite in the original (as-received) condition and following exposure to the heat flux for different times. The curves were measured at room temperature. There is rapid reduction to the tensile modulus and strength when heated for longer than about 2-3 mins, which is the time taken to thermally decompose the front face skin exposed directly to the heat flux. Mouritz and Mathys [66] have shown that the post-fire tensile properties of glass fibre laminates similar to the face skin of the sandwich composite are severely reduced (more than 90%) once the polymer matrix has decomposed to char. Decomposition of the polymer results in the loss in stress transfer between the glass fibres, resulting in a large reduction to the tensile stiffness and strength of the front face skin. Also, Feih and colleagues [80] have shown that E-glass tows rapidly loss strength when heated above ~300-350^{o}C due to thermally-activated growth of submicron-sized cracks at the fibre

surface. This contributes to the weakening of the front face skin which contributes to the large reduction in the post-fire tensile strength. The balsa core is much more compliant and weaker than the face skins, and therefore when it decomposes it does not have a significant effect of the post-fire tensile properties. Therefore, once the post-fire tensile properties of the heated face skin has been greatly reduced due to matrix decomposition and fibre weakening, the post-fire stiffness and strength of the sandwich composite is determined mostly by the back skin. This skin decomposes when the sandwich composite is heated for longer than ~10 mins, and this accounts for the very low post-fire tensile properties at longer heat exposure times.

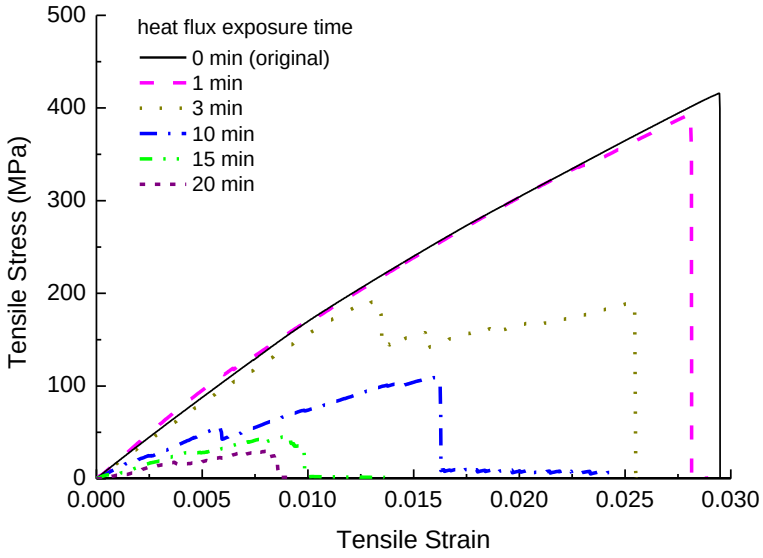

Figure 6.9: Tensile stress-strain curves measured for the sandwich composite in the original condition and following exposure to the heat flux for different times.

The effect of increasing exposure time to the heat flux on the post-fire tensile modulus and strength properties of the sandwich composite is shown in Figure 6.10. The data points show the measured post-fire property values and the curves show the calculated post-fire properties. There is good agreement between the measured and calculated properties; however the residual stiffness and strength were under-predicted using the model at intermediate heating times (typically between 5-10 mins). This difference is

attributed in part to differences between the measured and calculated depths of the char zone (Fig. 6.8). The calculated char depth was used to compute the post-fire tensile properties (using Eqns. 6.13 and 6.15). Any discrepancy between the measured and calculated char depths will cause differences between the measured and calculated post-fire tensile properties. Another reason for the under-prediction of the post-fire properties is the assumption with the model that the tensile stiffness and strength are negligible when the material decomposes to char. However, laminates similar to the face skins [66, 68] and the balsa core [78] retain a low amount of residual stiffness and strength (typically under 10%) following decomposition. Therefore, the char region contributes (albeit slightly) to the post-fire properties of the sandwich composite, which is not considered with the model.

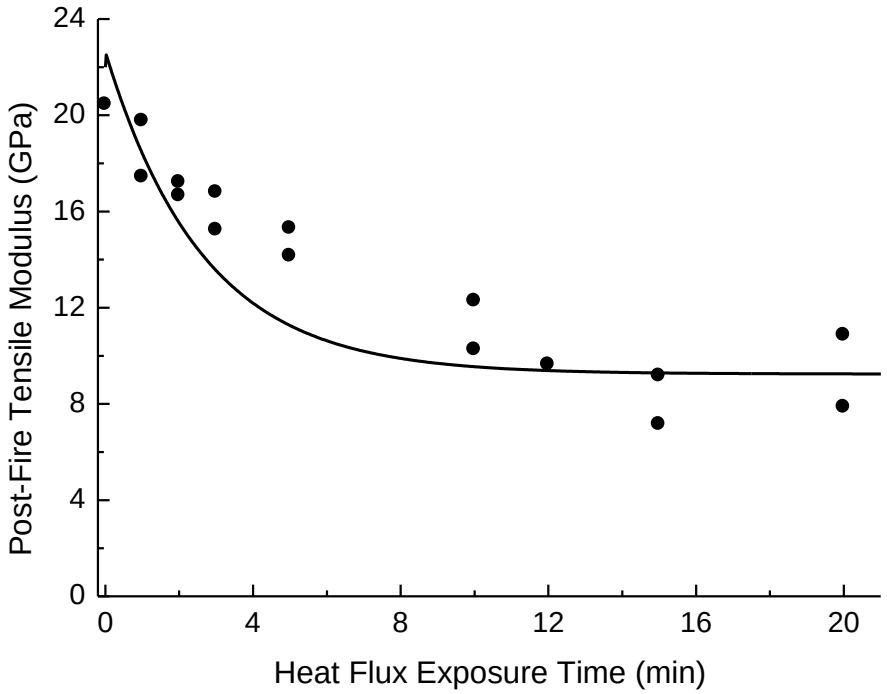

(a)

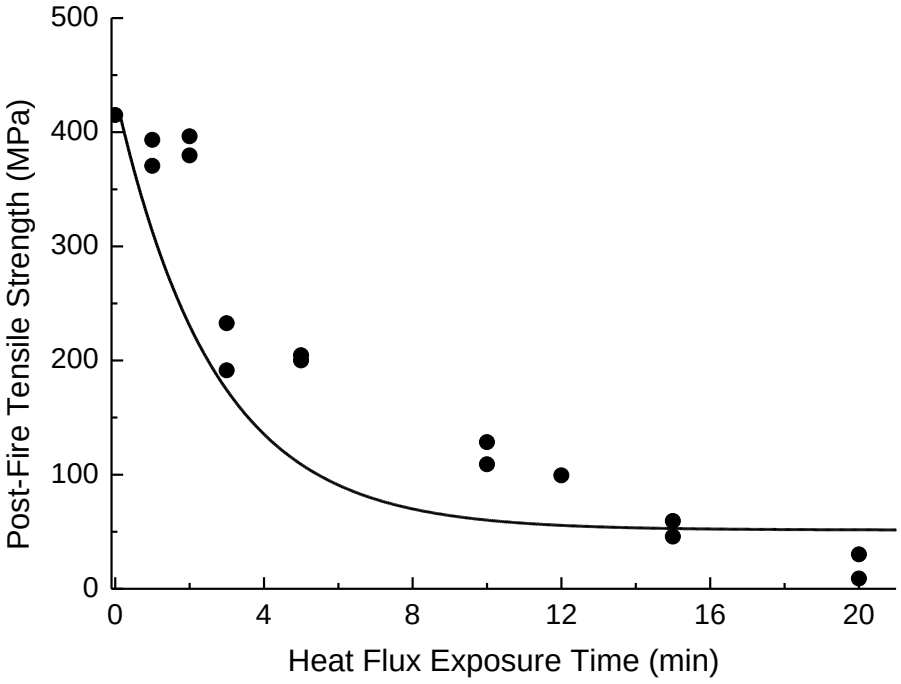

(b)

Figure 6.10: Effect of heat flux exposure time on the post-fire (a) tensile modulus and (b) tensile failure stress. The data points and curves show the measured and calculated post-fire properties, respectively.

6.4.3 Post-fire Compressive Properties

Post-fire compressive stress-strain curves for the sandwich composite for different heat flux exposure times are shown in Figure 6.11. The sandwich composite before heating failed by global buckling due to the large sample length-to-thickness ratio, and therefore the peak stress in the curve is the Euler buckling stress. There is a large reduction to the compressive stiffness and strength following exposure to the heat flux, even for short times (e.g. 1 min). The fire-damaged sandwich composites at different heat exposure times also failed by buckling as shown in Figure 6.12. The rapid reduction to the post-fire compressive properties is attributed to asymmetry in the load-bearing capacity across the net section area of the sandwich composite. A relatively small amount of decomposition to the heated face skin makes it more compliant and weaker than the unheated skin.

Under compressive loading this asymmetry in the post-fire properties between the two skins causes the sandwich composite to fail by buckling, even for short heating times when the back skin has not been degraded.

Figure 6.13 shows the effect of increasing heat flux exposure time on the post-fire compressive modulus and strength. The data points and curves show the measured and calculated properties, respectively. The model can accurately predict the post-fire compressive properties when deformation and failure occurs by buckling. The post-fire strength values were over-predicted using the model, and this discrepancy is attributed to the small error in the depth of the char zone. Small errors in char depth result in much larger error in post-fire buckling stress because $\sigma_{C,pf}\ \alpha(t-t_c)^2$, as defined in equation 6.16.

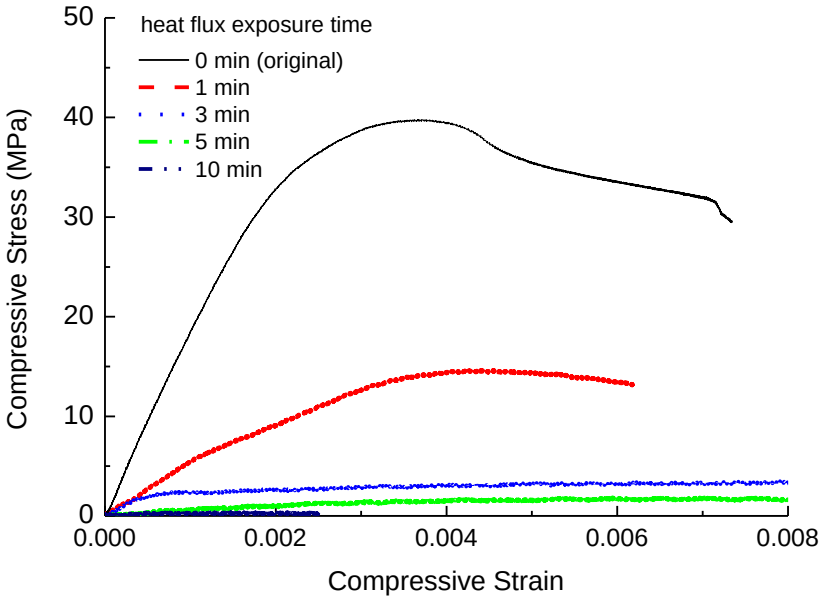

Figure 6.11: Compressive stress-strain curves measured for the sandwich composite in the original condition and following exposure to the heat flux for different times.

Figure 6.12: Failure modes of sandwich composites from 0 to 10 minutes heat exposure times. 0 min is a sandwich composite specimen at original condition.

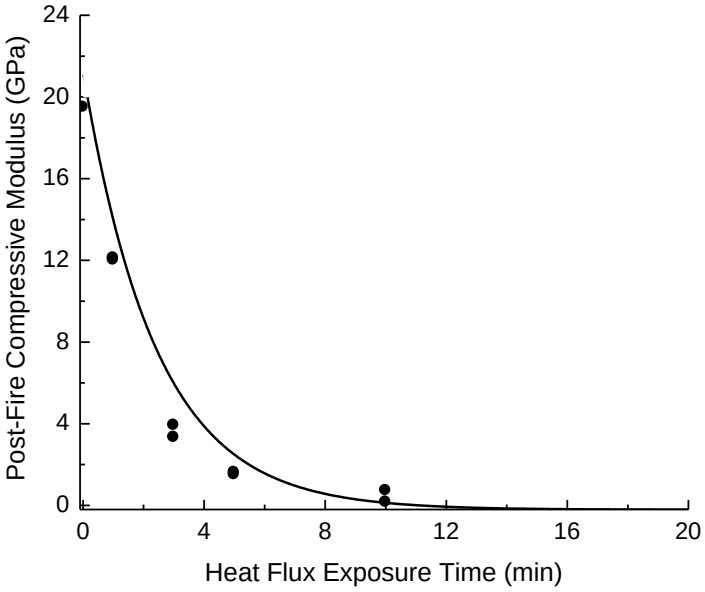

(a)

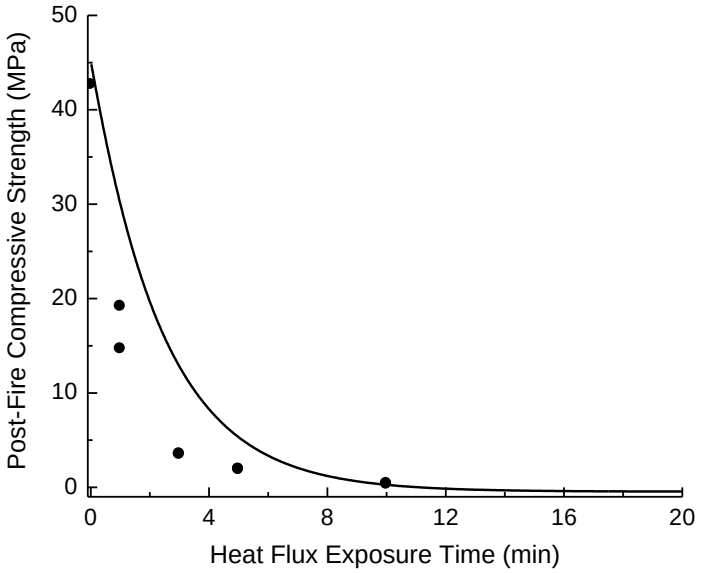

(b)

Figure 6.13: Effect of heat flux (35 kW/m^2) exposure time on the post-fire (a) compressive modulus and (b) compressive failure stress. The data points and curves show the measured and calculated post-fire properties, respectively.

6.4.4 Effect of Heat Flux on Post-Fire Properties

Research into the effect of heat flux on the post-fire properties has been performed on sandwich specimens to further assess their sensivity to the intensity of a fire. Figure 6.14 shows that the post-fire tensile load decreases with increasing heat flux from 25 to 50 kW/m^2. At highest heat flux (50 kW/m^2), the tension load decreases very rapidly. Similar to post-fire tension, the post-fire buckling load also decreases with increasing heat flux and heat exposure time as shown in Figure 6.15. At increasing heat flux exposure times the model predicts large reductions to the buckling load in less than a few minutes.

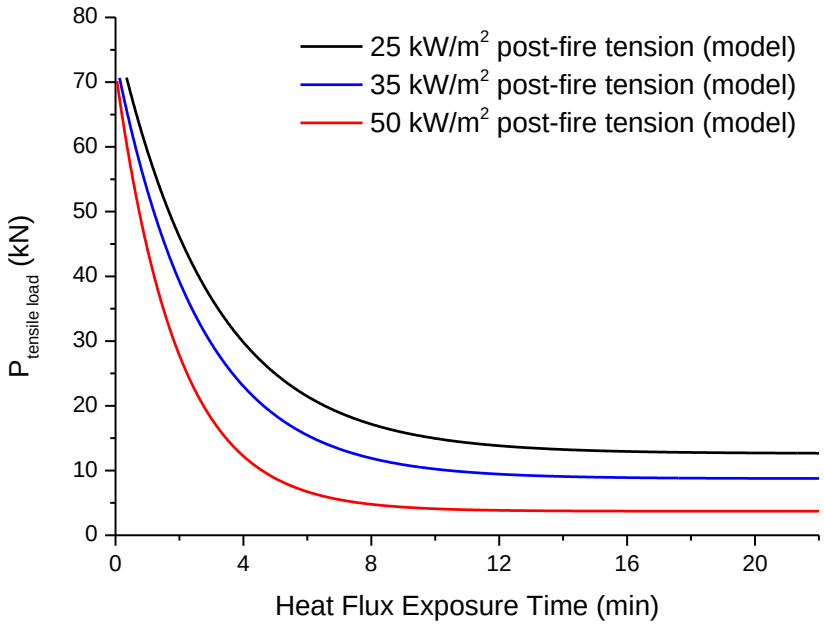

Figure 6.14: The prediction on the effect of heat flux and heat exposure time on the post-fire tension failure load.

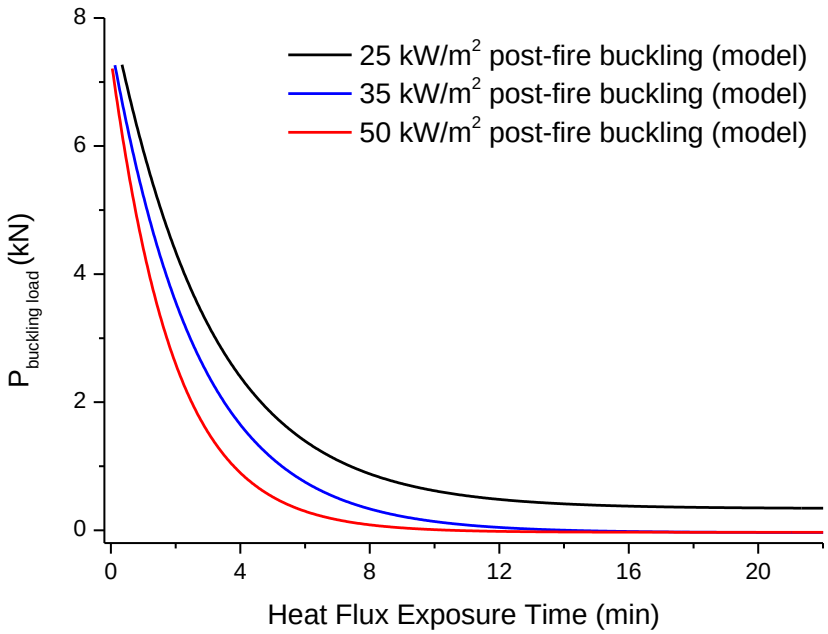

Figure 6.15: The prediction on the effect of heat flux and heat flux exposure time on the post-fire compression buckling load.

6.5 CONCLUSIONS

A model for calculating the post-fire mechanical properties of sandwich composites at room temperature has been developed and validated. The model computes the thermal history in the through-thickness direction of the composite when exposed to radiant heat flux generated by a possible fire scenario. Based on the temperatures, the initiation and growth of the decomposition (char) zone through the composite can be calculated. Mechanical models are then used to compute the residual stiffness and strength properties based on the amount of decomposition to the face skins and core. The numerical accuracy of the model was assessed using a sandwich composite material consisting of woven E-glass/vinyl ester laminate face skins and balsa wood core. The thermal model can predict the temperatures, the decomposition model can estimate the extent of char formation, and the mechanical model can compute the post-fire tensile and compressive properties with good accuracy. Further investigations using the model have shown that the post-fire mechanical properties is very sensitive to the radiant heat flux.

Chapter 7 : FIRE PROPERTIES OF SANDWICH COMPOSITES CONTAINING WATER

ABSTRACT

This chapter presents preliminary new research into the effect of water absorption on the fire structural response of sandwich composites. The aim of the research is to determine whether the thermal response, softening rate and failure mode of sandwich materials in fire is altered by the absorption of water. The sandwich composite studied consisted of woven E-glass/vinyl ester skins and a balsa wood core, and is the same material used in the previously reported research. The effect of exposure to hot-wet environmental conditions on the water absorption behaviour of the skin laminates, balsa core and sandwich composite were investigated. Mechanical testing of the face skins following exposure to the hot-wet environment for increasing periods of time up to and beyond saturation showed a reduction to the tensile strength, but not the modulus. The elevated temperature tensile properties of the face skins were determined for different amounts of absorbed water. Fire structural testing of the sandwich composite which was fully saturated with water showed a substantial reduction to the fire resistance, particularly at relatively high applied tensile stress levels. The reduction to the fire structural performance due to water absorption was predicted using the thermal-mechanical model described in Chapter 3. The reduced fire performance is attributed to tensile weakening of the face skins caused by the absorbed water.

7.1 INTRODUCTION

The moisture absorption of a sandwich composite material is a major concern in naval sandwich structures. Numerous studies have reported that absorbed water can reduce the mechanical properties of composite materials, usually by plasticisation of the polymer matrix and weakening of the fibre-matrix interface [86]. Very little research has been reported on the effect of water absorption on the mechanical properties of sandwich

composites used in naval ships, although based on the work on laminates it may be expected that the load-carrying capability can be significantly reduced by the presence of water in the face skins and core that is absorbed during operational service. Moisture absorption may accelerate the evolution of damage in sandwich composite structures [87-92]. Water may weaken interfacial bonding and cause delamination and matrix cracking as well as plasticising the polymer matrix, and thus will affect the mechanical performance and long-term durability of sandwich composite structures.

This research chapter presents a preliminary investigation into the effect of water absorption on the fire structural properties of a sandwich composite material under tension loading. To date, there is no published research on the fire response of sandwich composites that contain water. The balsa core, laminate skins and the sandwich composite were exposed to hot (70^0C) and humid (85% relative humidity) conditions for increasing times up to and beyond saturation. Room and elevated temperature tests are performed on the laminate skins to determine whether absorbed water affected their tensile properties. In addition, fire structural tests are performed on the sandwich composite in a fully saturated condition and compared with a water-free material to determine whether the thermal and structural properties are affected by water. The model described in Chapter 3 is used to predict the fire structural response of the sandwich composite containing water.

7.2 MATERIALS AND EXPERIMENTAL TECHNIQUES

The sandwich composite material used in this study is representative of the material used in naval ship structures. Similar materials and experimental techniques were used in this study to those reported in Chapter 3.

The balsa core, glass-vinyl ester laminate skins, and sandwich composite material were conditioned in an environmental chamber (Sunrise SU600, Angelantoni Industries) at elevated temperature (70^0C) and humidity (85%) for increasing periods of time up to about 26 days. The specimens were prepared according to ASTM Standard D 5229

specifications for the purpose of studying the effect of moisture absorption. The size of the specimens was 55 mm by 55 mm, with a thickness of 6 mm, 4 mm and 9.4 mm for the balsa core, laminate skin and sandwich composite, respectively (see Figure 7.1). Water absorption was monitored by weighing the specimens using a microbalance with an accuracy of 100 mg at different times up to 26 days. Three samples of each material were conditioned to determine the variability in the water absorption properties.

The laminate skin specimens were removed from the environmental chamber at different conditioning times to measure their tensile properties at room and elevated temperatures (up to 300^{o}C). Two specimens were tested at each temperature and at different conditioning times. The tensile properties were measured using the same test procedure that has been described in Chapter 3 (Section 3.3.3).

The sandwich composites specimens for fire structural testing were conditioned in the chamber until fully saturated, as determined by weight change measurements. After the sandwich specimens had saturated they were removed from the chamber and sealed in a plastic bag and stored at 4^{0}C prior to fire structural testing to minimise any loss of absorbed water. Small-scale fire structural tests were performed on the sandwich composite under combined tension loading and one-sided exposure to a radiant heat flux of 35 kW/m^{2}. Tests were performed on the saturated sandwich material following conditioning for 26 days as well as before conditioning (i.e. near water-free).

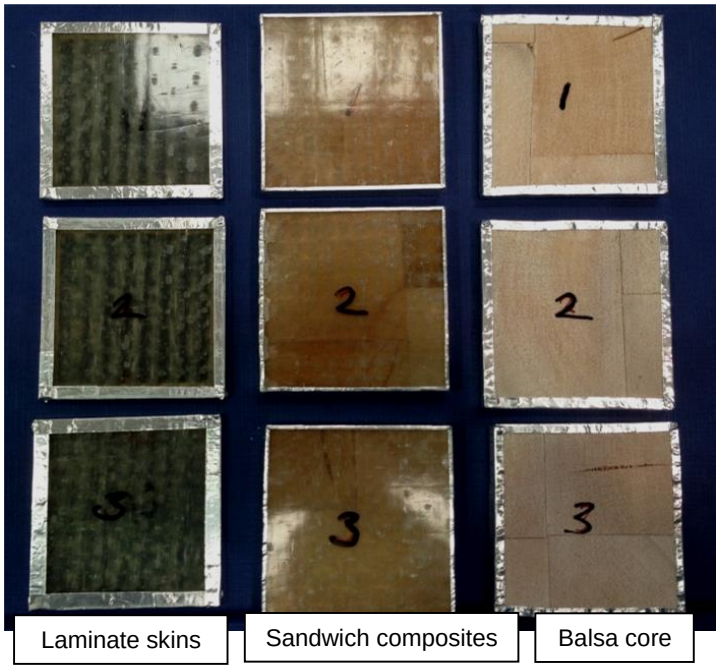

Figure 7.1: Specimens for moisture absorption study.

7.3 RESULTS AND DISCUSSIONS

7.3.1 Effect of Hot-wet Environment on The Moisture Absorption Behaviour

The moisture absorption behaviour of the balsa core, laminate skin and sandwich composite specimens is shown in Figure 7.2. This figure shows the measured change in the percentage weight gain plotted against the square root of hot-wet conditioning time (i.e. $t^{0.5}$). All three materials exhibited a weight gain due to water absorption during the initial exposure period to the hot-wet environment, with the balsa core specimens having the highest moisture uptake (up to 2.3%) followed by sandwich composite (0.9%) and then the laminate skin (0.2%). The curves show that the time to maximum weight gain was also different for the materials; being approximately 7 $hr^{0.5}$, 10 $hr^{0.5}$ and 22 $hr^{0.5}$ for the balsa core, sandwich composite and laminate skin, respectively.

The balsa showed non-Fickian diffusion behaviour with the weight gain decreasing steady with increasing conditioning time above ~7 $hr^{0.5}$. Such behaviour is usually indicative of irreversible degradation of the material, possibly due to the dissolution and release of low

molecular weight compounds from the wood into the environment. The moisture uptake curve for the laminate skin shows classic Fickian behaviour, with the material appearing to become saturated after ~16 hours$^{0.5}$, beyond which the weight did not change significantly. The curve for the sandwich composite was intermediate of the curves for balsa core and laminate skin, with the weight decreasing gradually with increasing time beyond the point of maximum mass gain. This slight reduction is attributed to the mass loss of the balsa core.

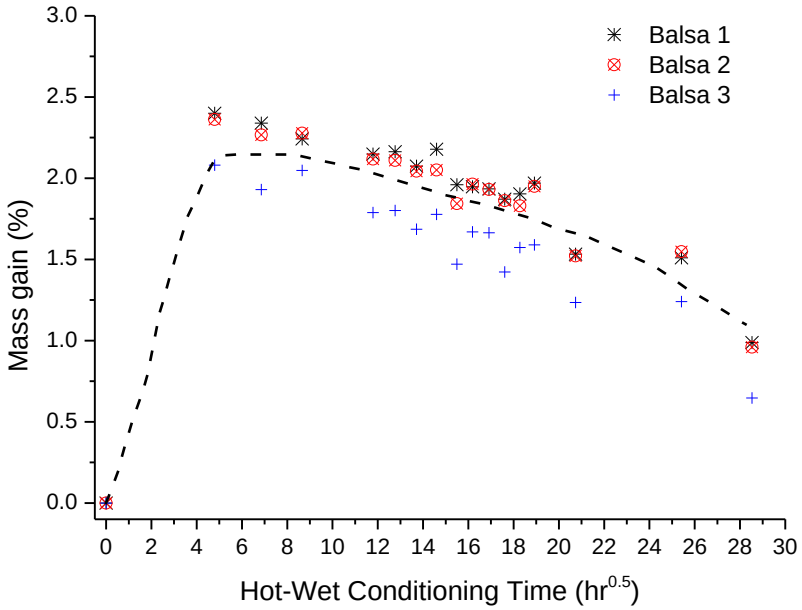

(a)

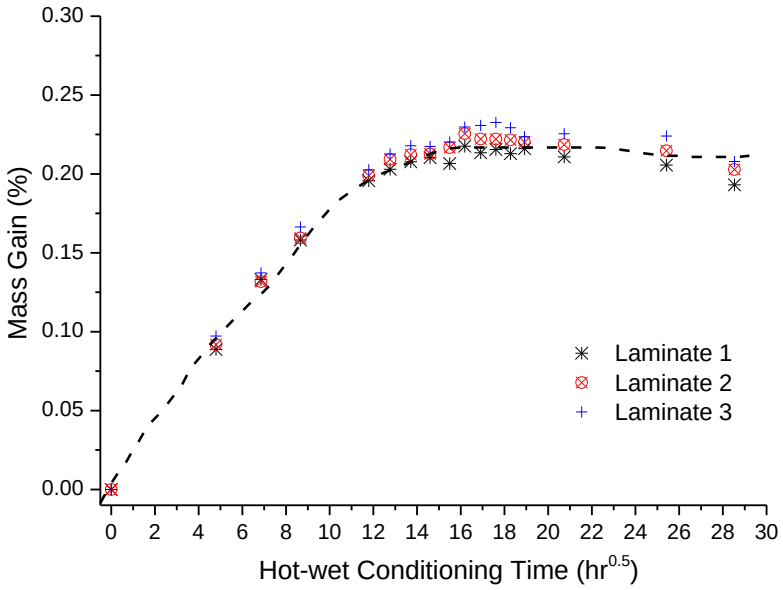

(b)

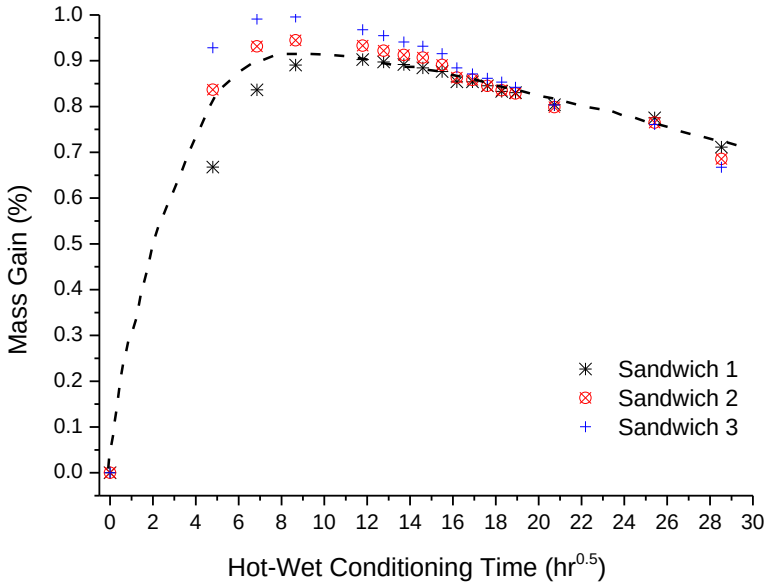

(c)

Figure 7.2: Effect of hot-wet exposure time on the percentage moisture gain of the (a) balsa core, (b) composite laminates and (c) sandwich composites. The dotted curves are the lines of best fit with the experimental data.

7.3.2 Effect of Hot-wet Environment on Elevated Temperature Tension Test

Figure 7.3 shows the measured loss in the tensile properties of the laminate skin with increasing temperature following exposure to the hot-wet environment for different conditioning times. The tensile strength at room temperature decreased with increasing conditioning time, and at the longest time (625 hours) when the laminate was fully saturated the failure stress was reduced by 30-35%. However, contrarily to the strength, the stiffness values were not affected significantly by water absorption. The tensile strength of the laminate before and after conditioning decreased over the temperature range of 75-125^{o}C due to glass transition softening of the vinyl ester matrix (T_g = 120^{0}C). Above the glass transition temperature the difference in strength values between the laminate in the original and saturated conditions is less than below T_g, although the failure stress remained lower due to water absorption. The solid lines in both tensile strength and stiffness vs temperature curves were fitted as described previously in Section 3.4.2 for the mechanical model used in validation.

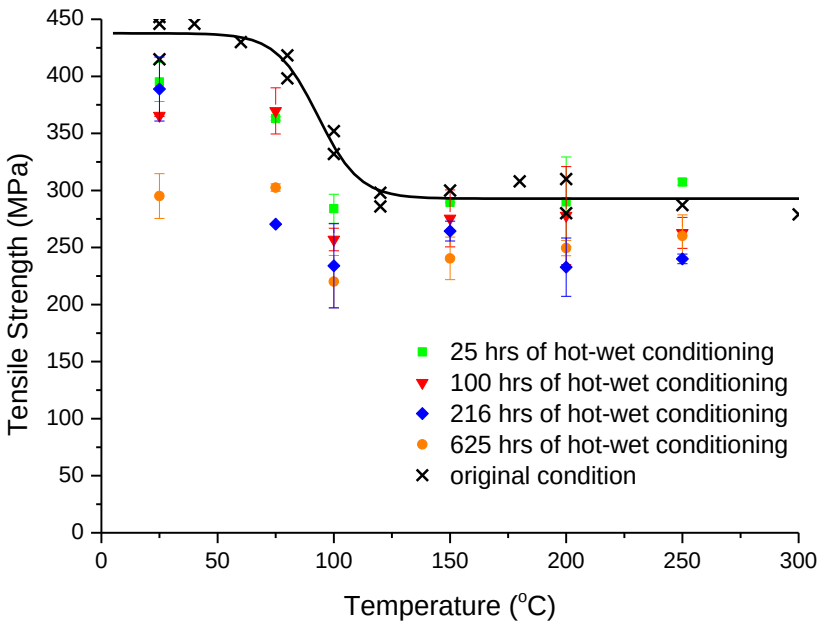

(a)

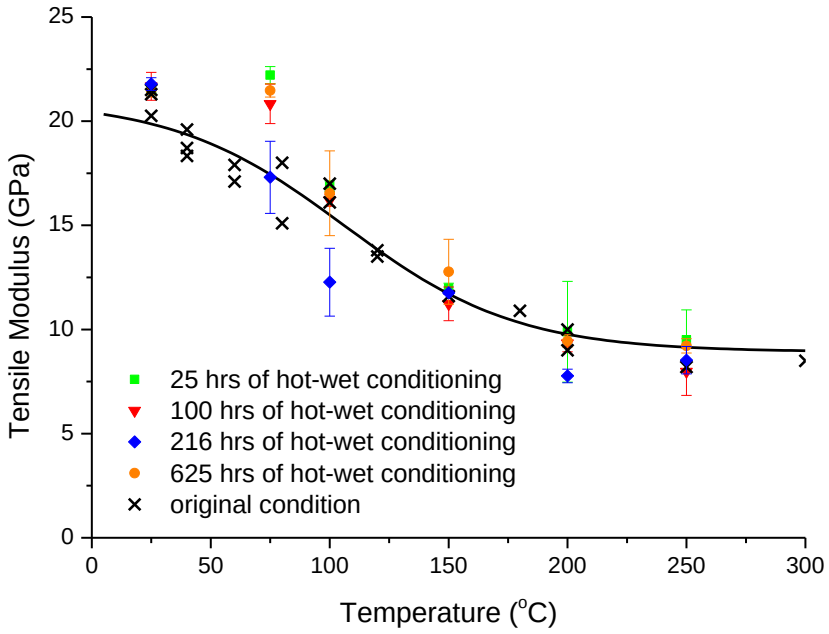

(b)

Figure 7.3: Effect of increasing temperature on the (a) tensile strength and (b) tensile modulus of the laminate used for the face skin to the sandwich composite at different hot-wet conditioning time.

7.3.3 Effect of Hot-wet Environment on Fire Structural Properties of Saturated Sandwich Composite

Fire structural tests were performed on the sandwich composite in the original and saturated conditions. Saturation occurred by exposing the composite to the hot-wet environment for 625 hours. Thermocouples attached to the hot and back faces of the sandwich composite revealed that the temperatures when exposed to the incident radiant heat flux (of 35 kW/m^2) did not change significantly. For example, Figure 7.4 compares the front and back face temperatures of the original and saturated sandwich materials under a tensile load of 240 MPa, and there is no significant difference.

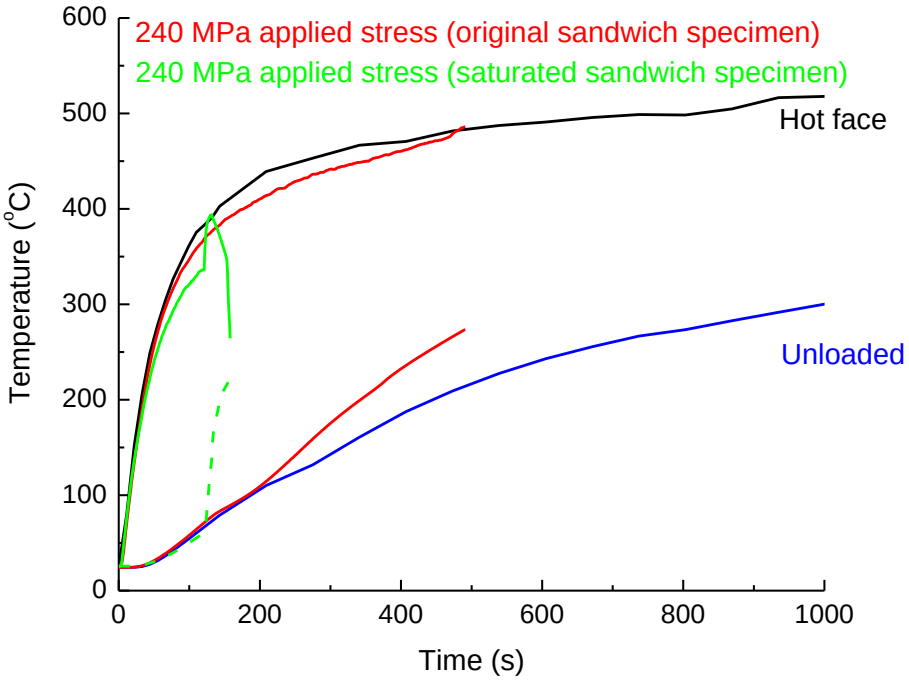

Figure 7.4: Front skin and back face temperature profile of the original and saturated sandwich specimens at the same applied stress.

The effect of applied tension stress on the failure time of the original and saturated sandwich composite when exposed to the heat flux of 35 kW/m^2 is shown in Figure 7.5. Separate failure times are given for the front and back face skins. Both materials show a rapid increase to the failure time with decreasing applied stress. Also, both materials displayed different failure modes depending on the stress level (as explained in Chapter 3 for the sandwich composite without absorbed water). The only significant difference between the composites was that water absorption reduced the fire structural resistance, with the saturated material failing within shorter times (particularly at relatively high applied stress levels). This reduction is attributed mostly to tensile weakening of the laminate skins caused by the absorbed water, as shown in Figure 7.3. The solid curves in figure 7.5 show the calculated failure times that were computed using the thermal-mechanical model described in Chapter 3. The failure times of the saturated composite were determined using the measured tensile strength values for the saturated skin

laminate (Fig 7.3). Using these values the model predicts with good accuracy the fire structural resistance of the sandwich composite. This further supports the findings that the reduction to the fire structural performance caused by water absorption is due mainly to the reduction to the tensile strength of the laminate skins.

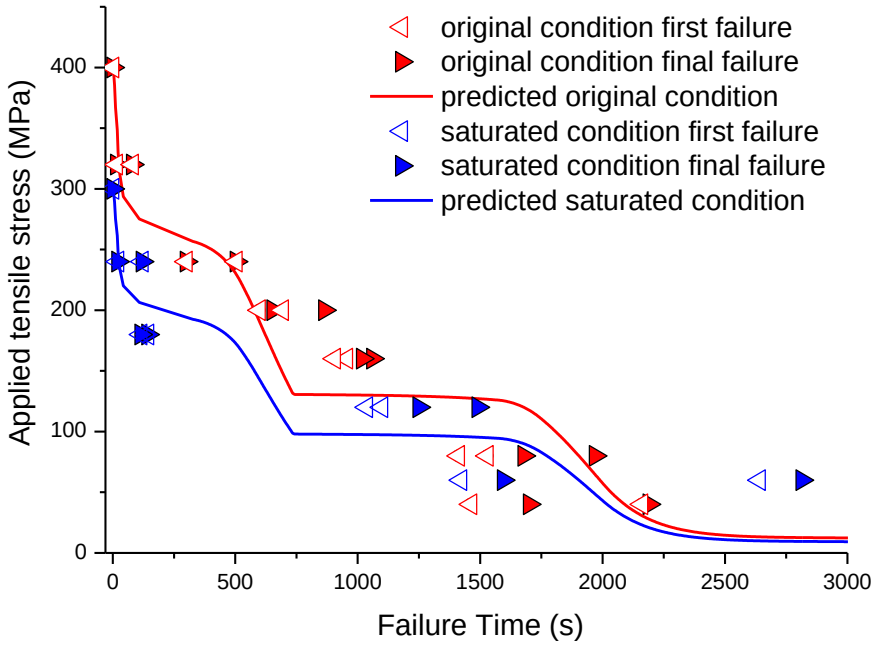

Figure 7.5: Effect of applied tensile stress on the failure time of original and hot-wet sandwich composites exposed to heat flux 35 kW/m².

7.4 CONCLUSIONS

Water absorption reduced the structural performance of the sandwich composite under combined tensile loading and one-sided radiant heating representative of a fire scenario. The skins displayed classical Fickian behaviour in the absorption of water from a hot-wet environment whereas the balsa core show a progressive reduction to the weight gain due presumably to chemical break-down and/or dissolution of compounds within the wood. The absorption of water reduced significantly the tensile strength (but not the modulus) of the laminate skins, and this was primarily responsible for the saturated sandwich composite having inferior fire structural resistance under tensile loading compared to the

original material. The thermal-mechanical model described in Chapter 3 was able to compute the failure times and failure modes of the saturated composite by accounting for the knock-down in the tensile failure stress of the skins caused by the absorbed water. This research provides a preliminary indication that the fire structural resistance of sandwich composites may be degraded over time due to the absorption of water as part of the natural ageing process.

Chapter 8 : CONCLUSIONS AND FUTURE RESEARCH

8.1 CONCLUSIONS

The fire structural properties of a sandwich composite representative of one of the main structural materials used in naval ships have been thoroughly evaluated in this PhD project. Using both experimental techniques and analytical modelling, the structural properties during fire and post-fire were investigated, and this has contributed significantly to important new insights into the fire response of sandwich composites.

A new thermal-mechanical model has been formulated to calculate the temperature rise, softening rate, failure time and failure mechanisms of sandwich composites under combined tension loading and one-sided heating representative of a fire. The accuracy of the model was assessed using experimental data obtained from small-scale fire structural tests performed on a sandwich composite made from fibreglass-vinyl ester laminate skins and balsa core. The thermal component of the model predicted with reasonable accuracy the through-thickness temperature profile of the unloaded sandwich composite. However, the thermal response under tensile loading was stress-dependent due to the accelerated egress of flammable volatiles from the damaged core, which increased considerably the temperature. The dependence of the internal temperature on the applied tensile stress is a complex phenomenon in the thermal modelling of sandwich composites. Despite this stress-dependence and other simplified assumptions (e.g. not considering heat-induced damage within the skins); the thermal-mechanical model was capable of accurately predicting the failure times and failure mechanisms of the sandwich composite. Both the model and experimental testing showed that the failure time increased with reduced applied tension stress and/or heat flux. The model also predicted that the sandwich composite can fail by one of three mechanisms depending on the applied tensile stress: Mode I failure which was initiated in the back skin due to matrix softening of the heated skin; Mode II failure where failure initiated in the front skin due to fibre and matrix softening followed by immediate failure of the back skin; and Mode III where failure of the heated skin was followed by delayed rupture of the back skin.

The fire structural response of sandwich composites was further investigated by exploring the effect of fibre orientation on the softening behaviour and failure mode. The effect of changing the orientation of the warp (load-bearing) fibres in the skins relative to tensile load direction was determined experimentally and analytically. Testing indicated that the internal temperature of the off-axis sandwich composite specimens was not dependent on the applied tensile stress, although this is due to short failure times which limited the amount of core damage and decomposition before the material ruptured. From the fire structural testing, it was found that the failure times decreased rapidly with increasing fibre misorientation angle, and this is because the tensile response was increasingly dominated by matrix softening rather than fibre weakening. The thermal-mechanical model predicted the failure times for the sandwich composites containing warp fibres misaligned at different angles, except for 150 off-axis specimen which was a conservative prediction due to the complexity of the skin failure process.

The compressive structural response of sandwich composite in fire was also investigated experimentally and analytically. The internal temperature of the sandwich composite was not affected by the applied compressive stress. The failure times under compressive loading were much shorter than for tensile loading, and this was due to the failure process being controlled by rapid softening of the polymer matrix to the heated skin. The thermal-mechanical model (buckling) predicted the compressive failure times of the sandwich composite with reasonable accuracy.

Research on post-fire experimental testing and modelling of sandwich composite materials has contributed new insights into the residual structural integrity of burnt sandwich structures following fire exposure. A new post-fire model for sandwich composites was developed to calculate the residual tensile and compressive properties, and the predictions were compared against experimental property data. The model developed to calculate the post-fire properties involved thermal, decomposition and mechanical analysis. The model assumed that the reduction to the post-fire properties is due solely to char formation, and other types of fire-induced damage have no effect.

Despite the assumption, the post-fire model predicted the post-fire tensile and compressive properties (strength and modulus) with reasonable accuracy.

The effect of water absorption on the fire structural properties of composite materials was studied for the first time. At room temperature, it was found that the absorption of water reduced the tensile properties of the sandwich composite, due presumably to plasticisation of the polymer matrix and fibre-matrix interface to the skins and possibly weakening of the core (although this was not measured). However, the tensile stiffness of the sandwich composite was not affected by water absorption. The fire structural response of the sandwich composite under tensile loading was reduced significantly by absorbed water when compared to a water-free material. The deterioration to the fire structural performance is attributed to weakening of the skins caused by the absorbed water. These results have practical significance for the fire structural safety of naval sandwich composites after many years of operation when a significant amount of water absorption has occurred.

8.2 FUTURE WORK

Although major progress has been achieved in the fire structural modelling and testing of sandwich composite materials, further analysis and experimental research is required to achieve a complete understanding. The PhD project has examined the fire structural response of sandwich composite with on-axis and off-axis fibres under tensile loading; the fire structural survivability of sandwich composite under compressive loading; the post-fire tension and compression properties of sandwich composites; and the effect of water absorption on the fire structural response. Below are suggestions for further research to deepen the understanding of the fire structural behaviour of sandwich composite materials.

1. The thermal model developed to calculate the temperature distribution in sandwich composites exposed to fire cannot accurately predict the temperature rise for tensile loads. As reported in Chapter 3, damage such as cracks within the

decomposed balsa core accelerates the egress of flammable volatiles and therefore causes a temperature rise that cannot be accurately calculated using the thermal model. Further development is required that incorporates damage analysis into the model.

2. The extended thermal-mechanical model for sandwich composites with misaligned load-bearing fibre under combined tension loading and one-sided heating has been developed and validated, as reported in Chapter 4. The model was able to predict the fire structural survivability and failure mode of the sandwich composite under tension loading for both on and off-axis load-bearing fibres. Good agreement was found between the calculated and measured failure times for off-axis sandwich specimens, except for the off-axis 15^0 specimens where the model under-predicted the failure times. This discrepancy is attributed to more gradual strength loss with increasing displacement that has been observed at room and elevated temperatures. For future work, it is very interesting to investigate the gradual strength loss phenomena in order to obtain better predictions with the experimental data. In addition, the model needs to be more rigorously validated for the fire tensile response of other types of sandwich composites, in addition to the material studied in this PhD project.

3. The thermal-mechanical model was used to predict the residual compressive strength and time-to-failure of the sandwich composite when exposed to fire (Chapter 5). The thermal model was able to predict the temperature profile and amount of decomposition through-the-thickness of the sandwich composite and the mechanical component of the model able to calculate the compression failure times with reasonable accuracy. However, further validation is suggested using other composite materials and fire scenarios. The model also needs to be further developed to analyse other compressive failure modes such as skin wrinkling and core shear cracking.

4. A model for calculating the post-fire mechanical properties of sandwich composites at room temperature was been developed and validated using experimental data (Chapter 6). The two-layer model was successfully validated for the sandwich composite with E-glass/vinyl ester skins and balsa core for post-fire tension and compression loading. Further validation is suggested for other sandwich composite materials with different core materials such as polymer foam. It is also interesting to validate the model for the post-fire bending properties of sandwich materials.

5. The effect of water absorption on the fire structural response of sandwich composites has been assessed, as reported in Chapter 7. The thermal-mechanical model was able to predict with good accuracy the time-to-failure of saturated sandwich composites loaded in tension and exposed to fire. In the future it would be interesting to further develop the model by exploring the effect of changing core materials and thickness as well as different laminate system and thickness. Also, the water degradation mechanisms that cause the deterioration to the fire structural properties need to be studied in greater detail. Lastly, the effect of water absorption on the fire structural response of sandwich composites under other load cases, such as compression and bending, is worthy of investigation.

REFERENCES

1. Mouritz, A.P., S. Feih, E. Kandare, Z. Mathys, A.G. Gibson, P.E. Des Jardin, S.W. Case, and B.Y. Lattimer, *Review of fire structural modelling of polymer composites.* Composites Part A: Applied Science and Manufacturing, 2009. **40**(12): p. 1800-1814.
2. Mouritz, A.P., E. Gellert, P. Burchill, and K. Challis, *Review of advanced composite structures for naval ships and submarines.* Composite Structures, 2001. **53**(1): p. 21-42.
3. Feih, S., Z. Mathys, A.G. Gibson, and A.P. Mouritz, *Modeling Compressive Skin Failure of Sandwich Composites in Fire.* Journal of Sandwich Structures and Materials, 2008. **10**(3): p. 217-245.
4. Feih, S., Z. Mathys, A.G. Gibson, and A.P. Mouritz, *Modelling the tension and compression strengths of polymer laminates in fire.* Composites Science and Technology, 2007. **67**(3–4): p. 551-564.
5. Feih, S., A.P. Mouritz, Z. Mathys, and A.G. Gibson, *Tensile Strength Modeling of Glass Fiber—Polymer Composites in Fire.* Journal of Composite Materials, 2007. **41**(19): p. 2387-2410.
6. Mouritz, A.P. and A.G. Gibson, *Fire Properties of Polymer Composite Materials*. 2006: Springer.
7. Egglestone, G.T. and D.M. Turley, *Flammability of GRP for use in ship superstructures.* Fire and Materials, 1994. **18**(4): p. 255-260.
8. Mouritz, A.P., *Post-fire flexural properties of fibre-reinforced polyester, epoxy and phenolic composites.* Journal of Materials Science, 2002. **37**(7): p. 1377-1386.
9. Mouritz, A.P., *Review of Smoke Toxicity of Fiber-Polymer Composites Used in Aircraft.* Journal of Aircraft, 2009. **46**(3): p. 737-745.
10. Gu, P. and R.J. Asaro, *Designing sandwich polymer matrix composite panels for structural integrity in fire.* Composite Structures, 2009. **88**(3): p. 461-467.
11. Lattimer, B.Y., Ouellette J, Sorathia U, *Large scale fire resistance tests on sandwich composite materials.* In: Proceedings of SAMPE 04, 2004(Long Beach, CA, May 16-20).
12. Looyeh MRE, R.K., Bettess P., *Thermomechanical response of sandwich panels to fire.* Finite Element Anal. & Design, 2001. **37**: p. 913-927.
13. Krysl, P., Ramroth W, Asaro RJ, *FE modeling of FRP sandwich panels exposed to heta: uncertainty analysis.* In: Proceedings of the SAMPE Technical Conference & Exhibition. **16-20 May 2004**(Long Beach, CA).
14. Birman, V., G.A. Kardomateas, G.J. Simitses, and R. Li, *Response of a sandwich panel subject to fire or elevated temperature on one of the surfaces.* Composites Part A: Applied Science and Manufacturing, 2006. **37**(7): p. 981-988.
15. Mouritz AP, G.C., *Post-fire properties of sandwich polymer composites.* Composites A, 2002. **33**: p. 609-620.
16. Giancaspro, J., P. Balaguru, and R. Lyon, *Use of Inorganic Polymer to Improve the Fire Response of Balsa Sandwich Structures.* Journal of Materials in Civil Engineering, 2006. **18**(3): p. 390-397.
17. Tewarson, A. and D.P. Macaione, *Polymers and Composites- An Examination of Fire Spread and Generation of Heat and Fire Products.* Journal of Fire Sciences, 1993. **11**(5): p. 421-441.
18. Scudamore, M.J., *Fire performance studies on glass-reinforced plastic laminates.* Fire and Materials, 1994. **18**(5): p. 313-325.
19. Grenier, A.T., N.A. Dembsey, and J.R. Barnett, *Fire characteristics of cored composite materials for marine use.* Fire Safety Journal, 1998. **30**(2): p. 137-159.

20. Mouritz, A.P., Z. Mathys, and A.G. Gibson, *Heat release of polymer composites in fire.* Composites Part A: Applied Science and Manufacturing, 2006. **37**(7): p. 1040-1054.
21. Allison, D.M., A.J. Marchand, and R.M. Morchat, *Fire performance of composite materials in ships and offshore structures.* Marine Structures, 1991. **4**(2): p. 129-140.
22. Feih, S. and A.P. Mouritz, *Tensile properties of carbon fibres and carbon fibre–polymer composites in fire.* Composites Part A: Applied Science and Manufacturing, 2012. **43**(5): p. 765-772.
23. Tinney, E.R., *The combustion of wooden dowels in heated air.* Tenth Symposium (International) on Combustion, 1965.
24. Kung, H.C., *A mathematical model of wood pyrolysis.* Combustion and Flame, 1972. **18**(2): p. 185-195.
25. Shi, L. and M.Y.L. Chew, *A review of fire processes modeling of combustible materials under external heat flux.* Fuel, 2013. **106**(0): p. 30-50.
26. Kansa, E.J., H.E. Perlee, and R.F. Chaiken, *Mathematical model of wood pyrolysis including internal forced convection.* Combustion and Flame, 1977. **29**(0): p. 311-324.
27. Henderson, J.B., J.A. Wiebelt, and M.R. Tant, *A Model for the Thermal Response of Polymer Composite Materials with Experimental Verification.* Journal of Composite Materials, 1985. **19**(6): p. 579-595.
28. Tant, M.R., J.B. Henderson, and C.T. Boyer, *Measurement and modelling of the thermochemical expansion of polymer composites.* Composites, 1985. **16**(2): p. 121-126.
29. Henderson, J.B. and T.E. Wiecek, *A Mathematical Model to Predict the Thermal Response of Decomposing, Expanding Polymer Composites.* Journal of Composite Materials, 1987. **21**(4): p. 373-393.
30. Florio Jr, J., J.B. Henderson, F.L. Test, and R. Hariharan, *A study of the effects of the assumption of local-thermal equilibrium on the overall thermally-induced response of a decomposing, glass-filled polymer composite.* International Journal of Heat and Mass Transfer, 1991. **34**(1): p. 135-147.
31. Sullivan, R.M. and N.J. Salamon, *A finite element method for the thermochemical decomposition of polymeric materials—I. Theory.* International Journal of Engineering Science, 1992. **30**(4): p. 431-441.
32. Sullivan, R.M. and N.J. Salamon, *A finite element method for the thermochemical decomposition of polymeric materials—II. Carbon phenolic composites.* International Journal of Engineering Science, 1992. **30**(7): p. 939-951.
33. Sullivan, R.M., *A Coupled Solution Method for Predicting the Thermostructural Response of Decomposing, Expanding Polymeric Composites.* Journal of Composite Materials, 1993. **27**(4): p. 408-434.
34. G. A. Pering, P.V.F., G. S. Springer, *Degradation of tensile and shear properties of composites exposed to fire or high temperature.* J Compos Mater, 1985(14): p. 54-66.
35. Mcmanus, H.L.N. and G.S. Springer, *High Temperature Thermomechanical Behavior of Carbon-Phenolic and Carbon-Carbon Composites, I. Analysis.* Journal of Composite Materials, 1992. **26**(2): p. 206-229.
36. Mcmanus, H.L.N. and G.S. Springer, *High Temperature Thermomechanical Behavior of Carbon-Phenolic and Carbon-Carbon Composites, II. Results.* Journal of Composite Materials, 1992. **26**(2): p. 230-255.
37. Dimitrienko, Y.I., *Thermal stresses and heat-mass transfer in ablating composite materials.* International Journal of Heat and Mass Transfer, 1995. **38**(1): p. 139-146.
38. Dimitrienko, Y.I., *Thermomechanical behaviour of composite materials and structures under high temperatures: 1. Materials.* Composites Part A: Applied Science and Manufacturing, 1997. **28**(5): p. 453-461.

39. A. G. Gibson, Y.S.W., H. W. Chandler, J. A. D. Wilcox, P. Bettess, *A Model for the Thermal Performance of Thick Composite Laminates in Hydrocarbon Fires.* Oil & Gas Science and Technology-revue De L Institut Francais Du Petrole - OIL GAS SCI TECHNOL, 1995. **50**(1): p. 69-74.
40. Mouritz, A.P. and C.P. Gardiner, *Compression properties of fire-damaged polymer sandwich composites.* Composites Part A: Applied Science and Manufacturing, 2002. **33**(5): p. 609-620.
41. Dodds, N., A.G. Gibson, D. Dewhurst, and J.M. Davies, *Fire behaviour of composite laminates.* Composites Part A: Applied Science and Manufacturing, 2000. **31**(7): p. 689-702.
42. Krysl, P., W.T. Ramroth, L.K. Stewart, and R.J. Asaro, *Finite element modelling of fibre reinforced polymer sandwich panels exposed to heat.* International Journal for Numerical Methods in Engineering, 2004. **61**(1): p. 49-68.
43. Feih, S., Z. Mathys, A.G. Gibson, and A.P. Mouritz, *Modelling the compression strength of polymer laminates in fire.* Composites Part A: Applied Science and Manufacturing, 2007. **38**(11): p. 2354-2365.
44. Dao, M. and R.J. Asaro, *A study on failure prediction and design criteria for fiber composites under fire degradation.* Composites Part A: Applied Science and Manufacturing, 1999. **30**(2): p. 123-131.
45. Bai, Y., T. Vallée, and T. Keller, *Modeling of thermal responses for FRP composites under elevated and high temperatures.* Composites Science and Technology, 2008. **68**(1): p. 47-56.
46. Bai, Y. and T. Keller, *Modeling of mechanical response of FRP composites in fire.* Composites Part A: Applied Science and Manufacturing, 2009. **40**(6-7): p. 731-738.
47. Keller, T., C. Tracy, and E. Hugi, *Fire endurance of loaded and liquid-cooled GFRP slabs for construction.* Composites Part A: Applied Science and Manufacturing, 2006. **37**(7): p. 1055-1067.
48. Luo, C., J. Lua, and P.E. DesJardin, *Thermo-mechanical damage modeling of polymer matrix sandwich composites in fire.* Composites Part A: Applied Science and Manufacturing, 2012. **43**(5): p. 814-821.
49. Elmughrabi, A.E., M. Robinson, and A.G. Gibson, *Effect of stress on the fire reaction properties of polymer composite laminates.* Polymer Degradation and Stability, 2008. **93**(10): p. 1877-1883.
50. Gibson, A.G., Y.-S. Wu, J.T. Evans, and A.P. Mouritz, *Laminate Theory Analysis of Composites under Load in Fire.* Journal of Composite Materials, 2006. **40**(7): p. 639-658.
51. *Modeling of naval composite structures in fire / edited by L. Couchman and A.P. Mouritz*, ed. L.S. Couchman, A.P. Mouritz, and S. Cooperative Research Centre for Advanced Composite. 2006, [Fishermans Bend, Vic.] :: Cooperative Research Centre for Advanced Composite Structures.
52. Gu, P. and R.J. Asaro, *Designing polymer matrix composite panels for structural integrity in fire.* Composite Structures, 2008. **84**(4): p. 300-309.
53. Lua, J., J. O'Brien, C.T. Key, Y. Wu, and B.Y. Lattimer, *A temperature and mass dependent thermal model for fire response prediction of marine composites.* Composites Part A: Applied Science and Manufacturing, 2006. **37**(7): p. 1024-1039.
54. Boyd, S.E., S.W. Case, and J.J. Lesko, *Compression creep rupture behavior of a glass/vinyl ester composite subject to isothermal and one-sided heat flux conditions.* Composites Part A: Applied Science and Manufacturing, 2007. **38**(6): p. 1462-1472.
55. Gu, P. and R.J. Asaro, *Skin wrinkling of sandwich polymer matrix composite panels subjected to fire exposure.* Thin-Walled Structures, 2012. **51**(0): p. 139-146.

56. Gibson, A.G., M.E.O. Torres, T.N.A. Browne, S. Feih, and A.P. Mouritz, *High temperature and fire behaviour of continuous glass fibre/polypropylene laminates.* Composites Part A: Applied Science and Manufacturing, 2010. **41**(9): p. 1219-1231.
57. Gu, P., M. Dao, and R.J. Asaro, *Structural stability of polymer matrix composite panels in fire.* Marine Structures, 2009. **22**(3): p. 354-372.
58. Bausano, J.V., J.J. Lesko, and S.W. Case, *Composite life under sustained compression and one sided simulated fire exposure: Characterization and prediction.* Composites Part A: Applied Science and Manufacturing, 2006. **37**(7): p. 1092-1100.
59. Liu, L., J. Holmes, G. Kardomateas, and V. Birman, *Compressive Response of Composites Under Combined Fire and Compression Loading.* Fire Technology, 2011. **47**(4): p. 985-1016.
60. Asaro, R.J., B. Lattimer, and W. Ramroth, *Structural response of FRP composites during fire.* Composite Structures, 2009. **87**(4): p. 382-393.
61. Summers, P.T., B.Y. Lattimer, S. Case, and S. Feih, *Predicting compression failure of composite laminates in fire.* Composites Part A: Applied Science and Manufacturing, 2012. **43**(5): p. 773-782.
62. Gu, P. and R.J. Asaro, *Structural buckling of polymer matrix composites due to reduced stiffness from fire damage.* Composite Structures, 2005. **69**(1): p. 65-75.
63. Gu, P. and R.J. Asaro, *Wrinkling of sandwich polymer matrix composite panels under transverse thermal gradients.* Fire Safety Journal, 2008. **43**(2): p. 151-160.
64. Sorathia, U., C. Beck, and T. Dapp, *Residual Strength of Composites during and after Fire Exposure.* Journal of Fire Sciences, 1993. **11**(3): p. 255-270.
65. Mouritz, A.P. and Z. Mathys, *Mechanical properties of fire-damaged glass-reinforced phenolic composites.* Fire and Materials, 2000. **24**(2): p. 67-75.
66. Mouritz, A.P. and Z. Mathys, *Post-fire mechanical properties of marine polymer composites.* Composite Structures, 1999. **47**(1–4): p. 643-653.
67. Mouritz, A.P. and Z. Mathys, *Post-fire mechanical properties of glass-reinforced polyester composites.* Composites Science and Technology, 2001. **61**(4): p. 475-490.
68. Mouritz, A.P., *Simple models for determining the mechanical properties of burnt FRP composites.* Materials Science and Engineering: A, 2003. **359**(1–2): p. 237-246.
69. Gardiner, C.P., Z. Mathys, and A.P. Mouritz, *Post-fire structural properties of burnt GRP plates.* Marine Structures, 2004. **17**(1): p. 53-73.
70. Gibson, A.G., P.N.H. Wright, Y.S. Wu, A.P. Mouritz, Z. Mathys, and C.P. Gardiner, *The integrity of polymer composites during and after fire.* Journal of Composite Materials, 2004. **38**(15): p. 1283-1307.
71. Mouritz, A.P., Z. Mathys, and C.P. Gardiner, *Thermomechanical modelling the fire properties of fibre–polymer composites.* Composites Part B: Engineering, 2004. **35**(6–8): p. 467-474.
72. Gardiner, C.P., Z. Mathys, and A.P. Mouritz, *Tensile and Compressive Properties of FRP Composites with Localised Fire Damage.* Applied Composite Materials, 2002. **9**(6): p. 353-367.
73. Z. Mathys, C.P.G., A.P. Mouritz, C.R. Townsend, *Mechanical properties of GRP composites with localised thermal damage.* Int. J. of Materials and Product Technology, 2002. **17**(1/2): p. 134-142.
74. Gibson, A.G., Wright P.H.N., Wu Y.S., Mouritz A.P., Mathys Z., Gardiner C.P., *Modelling residual mechanical properties of polymer composites after fire.* Plastics, Rubber and Composites, 2003. **32**(2): p. 81-90.
75. Lattimer, B.Y., Ouellette J, Sorathia U, *Fire resistance of composite bulkheads and overheads.* 2003(Presented at NPFA 03 Annual Meeting, Dallas, TX).

76. Gibson, A., T. Browne, S. Feih, and A. Mouritz, *Modeling composite high temperature behavior and fire response under load.* Journal of Composite Materials, 2012. **46**(16): p. 2005-2022.
77. Lattimer, B.Y., Ouellette J, Trelles J, *Thermal response of composite materials to elevated temperatures.* In: Modeling of Naval Composite Structures in Fire, 2011(Ed. L. Couchman and A.P. Mouritz. Acclaim, Melbourne): p. 1-49.
78. Goodrich, T., N. Nawaz, S. Feih, B. Lattimer, and A. Mouritz, *High-temperature mechanical properties and thermal recovery of balsa wood.* Journal of Wood Science, 2010. **56**(6): p. 437-443.
79. Da Silva, A. and S. Kyriakides, *Compressive response and failure of balsa wood.* International Journal of Solids and Structures, 2007. **44**(25–26): p. 8685-8717.
80. Feih, S., E. Boiocchi, G. Mathys, Z. Mathys, A.G. Gibson, and A.P. Mouritz, *Mechanical properties of thermally-treated and recycled glass fibres.* Composites Part B: Engineering, 2011. **42**(3): p. 350-358.
81. Hull, D. and T.W. Clyne., *An Introduction to Composite Materials*. 1996: Cambridge University Press.
82. Kim, J., S.W. Lee, and S. Kwon, *Time-to-failure of Compressively Loaded Composite Structures Exposed to Fire.* Journal of Composite Materials, 2007. **41**(22): p. 2715-2735.
83. Mouritz, A.P., *Fire resistance of aircraft composite laminates.* Journal of Materials Science Letters, 2003. **22**(21): p. 1507-1509.
84. Ulven, C.A. and U.K. Vaidya, *Post-fire low velocity impact response of marine grade sandwich composites.* Composites Part A: Applied Science and Manufacturing, 2006. **37**(7): p. 997-1004.
85. Goodrich, T.W. and B.Y. Lattimer, *Fire decomposition effects on sandwich composite materials.* Composites Part A: Applied Science and Manufacturing, 2012. **43**(5): p. 803-813.
86. Ishida, H. and J.L. Koenig, *The reinforcement mechanism of fiber-glass reinforced plastics under wet conditions: A review.* Polymer Engineering & Science, 1978. **18**(2): p. 128-145.
87. Buck, S.E., D.W. Lischer, and S. Nemat-Nasser, *The Durability of E-Glass/Vinyl Ester Composite Materials Subjected to Environmental Conditioning and Sustained Loading.* Journal of Composite Materials, 1998. **32**(9): p. 874-892.
88. Ray, B.C., *Temperature effect during humid ageing on interfaces of glass and carbon fibers reinforced epoxy composites.* Journal of Colloid and Interface Science, 2006. **298**(1): p. 111-117.
89. Kootsookos, A. and A.P. Mouritz, *Seawater durability of glass- and carbon-polymer composites.* Composites Science and Technology, 2004. **64**(10–11): p. 1503-1511.
90. Hossain, M.K., K.A. Imran, M.V. Hosur, and S. Jeelani, *Degradation of Mechanical Properties of Conventional and Nanophased Carbon/Epoxy Composites in Seawater.* Journal of Engineering Materials and Technology, 2011. **133**(4): p. 041004-041004.
91. Zafar, A., F. Bertocco, J. Schjødt-Thomsen, and J.C. Rauhe, *Investigation of the long term effects of moisture on carbon fibre and epoxy matrix composites.* Composites Science and Technology, 2012. **72**(6): p. 656-666.
92. Strait, L.H., M.L. Karasek, and M.F. Amateau, *Effects of Seawater Immersion on the Impact Resistance of Glass Fiber Reinforced Epoxy Composites.* Journal of Composite Materials, 1992. **26**(14): p. 2118-2133.